Titre: Title:	Detection of Hidden Corrosion by Pulsed Eddy Current Using Time Frequency Analysis
Auteur: Author:	Seid Mohammad Saleh Hosseini
Date:	2012
Type:	Mémoire ou thèse / Dissertation or Thesis
Référence: Citation:	Hosseini, S. M. S. (2012). Detection of Hidden Corrosion by Pulsed Eddy Current Using Time Frequency Analysis [Thèse de doctorat, École Polytechnique de Montréal]. PolyPublie. https://publications.polymtl.ca/807/

URL de PolyPublie: PolyPublie URL:	https://publications.polymtl.ca/807/
Directeurs de recherche: Advisors:	Aouni Lakis
Programme: Program:	Génie mécanique

UNIVERSITÉ DE MONTRÉAL

DETECTION OF HIDDEN CORROSION BY PULSED EDDY CURRENT USING TIME FREQUENCY ANALYSIS

SEID MOHAMMAD SALEH HOSSEINI

DÉPARTEMENT DE GÉNIE MÉCANIQUE

ÉCOLE POLYTECHNIQUE DE MONTRÉAL

THÈSE PRÉSENTÉE EN VUE DE L'OBTENTION

DU DIPLÔME DE PHILOSOPHIAE DOCTOR

(GÉNIE MÉCANIQUE)

AVRIL 2012

UNIVERSITÉ DE MONTRÉAL

ÉCOLE POLYTECHNIQUE DE MONTRÉAL

Cette thèse intitulée:

DETECTION OF HIDDEN CORROSION BY PULSED EDDY CURRENT USING TIME FREQUENCY ANALYSIS

présentée par : HOSSEINI Seid Mohammad Saleh
en vue de l'obtention de diplôme de : Philosophiae Doctor
a été dûment acceptée par le jury d'examen constitué de :

M. BALAZINSKI Marek, Ph.D., président

M. LAKIS Aouni A., Ph.D., membre et directeur de recherche

M. HOJJATI Mehdi, Ph.D., membre

M. AMAZOUZ Mouloud, Ph.D., membre externe

DEDICATIONS

To my lovely wife, Nioosha

To my mother, my sister and my father; for their emotional supports

ACKNOWLEDGMENT

I wish to thank all those who supported me in the completion of this study and made the way of research smooth for me.

I would like to express my sincere gratitude to my doctoral advisor Prof. Aouni A. Lakis for his patience, guidance and invaluable support throughout the realisation of this research.

My sincere appreciation goes to Prof. Marek Blazinski, Dr. Mehdi Hajjati, Dr. Mouloud Amazouz and Dr. Antoine Saucier for taking part as my dissertation committee.

This project has been made possible by precious support from the collaborative research and development grant of Natural Sciences and Engineering Research Council of Canada (NSERC), Pratt & Whitney Canada, BOMBARDIER Aeronautics and National Research Council of Canada

I Finally I could not have accomplished this without all the supports of my family, especially my lovely wife. To them I tribute a fervent thanks.

RÉSUMÉ

En augmentant le nombre de demandes de voyages par l'intermédiaire des lignes aériennes, on augmente ainsi le nombre d'avions et par conséquent le nombre d'avions vieillissants en service. Dans l'industrie aérospatiale, comme pour d'autres industries de transport, l'existence des défauts dans les véhicules et la capacité de trouver ces défauts peuvent faire la différence entre la vie et la mort.

De ce fait, les méthodes d'essais non destructives sont périodiquement appliquées pour inspecter les composantes d'avions avant qu'elles soient assemblées et également durant toute leur durée de vie. Les composantes d'avions sont conçues pour être aussi légères que possible afin de supporter les charges relativement élevées à leur force matérielle. Cela signifie qu'une petite défaut paille peut causer de grandes ruptures dans le fuselage ou les moteurs de ces avions.

La fatigue et la corrosion sont les deux principales causes des défaillances d'avions en service. Plusieurs méthodes d'essais non destructives sont habituellement appliquées pour inspecter les composantes d'avions lorsqu'elles sont en opération. Ces méthodes sont l'ultrason, les courants de Foucault, le liquide pénétrant, le rayonnement et l'inspection magnétiques des particules. La nature électromagnétique de l'essai des courants de Foucault fournit une grande pénétration des fuselages d'avions et donne de riches informations de l'intérieur de la structure de l'échantillon inspecté. Par conséquent, cette méthode est présentée comme l'une des méthodes d'inspection les plus puissantes dans l'industrie aéronautique. La limitation principale des essais par les courants de Foucault est que cette méthode a besoin d'un inspecteur professionnel et que seulement les matériaux conducteurs peuvent être inspectés par ces essais. Par contre, les tests des courants de Foucault n'ont besoin d'aucun contact physique avec la surface inspectée, ce qui leur donne un grand avantage par rapport aux autres essais non destructifs employés dans l'industrie aéronautique. Deux types d'inspection ont été développés concernant les tests par les courants de Foucault : les tests par les courants de Foucault conventionnels et les tests pulsés. Dans les tests de courant de Foucault conventionnels, la sonde est excitée avec un signal sinusoïdal harmonique aux fréquences uniques ou à fréquences multiples pour étudier les signaux transitoires de courant de Foucault. Contrairement aux essais conventionnels, les essais par les courants de Foucault pulsés appliquent à la place une excitation sous forme d'impulsion carrée ou sinusoïdale et la bobine de la sonde est excitée par des impulsions répétitives à large bande.

Cette thèse rapporte le développement d'une méthode d'inspection automatique avec la méthode de courant de Foucault pulsée pour déterminer l'endroit et les quantités de pailles produites dans les structures en aluminium à double couche et mesurer également la variation d'épaisseur dans un système à une seule couche.

Cette thèse mise au point trois principales parties :

1- l'établissement d'un banc d'essai utilisant les courants de Foucault pulsés avec toutes les composantes pour prendre des signaux d'échantillons défectueux;
2- l'application de nouvelles méthodes de traitement de signaux utilisant les distributions temps-fréquences pour extraire l'information cachée à partir du système utilisant les courants de Foucault pulsés et
3- l'application des méthodes d'intelligence artificielle pour réduire au minimum l'interférence humaine en estimant et en déterminant la distribution de défauts dans les fuselages d'avions.

L'inspection dans l'industrie aérospatiale est une situation très sensible et une méthode non destructive devrait être précise et fiable pour pouvoir l'appliquer dans le contrôle d'avions structures.

Dans la première partie, plusieurs types de pertes de métal dans l'éventail de la profondeur ont été produits afin de simuler la corrosion et les conditions des défauts sur des surfaces de plaques en aluminium. Un banc d'essai utilisant les courants de Foucault pulsés a été établi et programmé pour permettre l'acquisition de signaux précis à partir d'une surface défectueuse et d'une surface non défectueuse. Dans la deuxième partie, des signaux de courants de Foucault pulsés ont été traités par la méthode d'analyse « temps-fréquences ». Les effets internes et externes du bruit tels que la basse quantité de défauts placée loin de la surface de la couche extérieur et intérieur enlèvent la cause réduisant l'efficacité de la représentation du signal dans le domaine de temps et l'analyse en temps-fréquence est mise en application pour améliorer la représentation des signaux et pour indiquer l'information cachée des défauts. Dans cette étape, des signaux pris en utlisant les courants de Foucault pulsés et qui sont représentés par une série de tension-temps (dans le domaine de temps) sont convertis pour représenter les signaux en trois dimensions (temps-fréquence-amplitude).

Plus de dix différentes distributions en temps-fréquences ont été programmées et mises en application. Ces distributions sont la transformée de Fourier à fenêtres glissantes (STFT- comme distribution linéaire en temps-fréquence) et des distributions bilinéaires telles que la distribution de Wigner-Ville, la distribution Wigner-Ville lissée, la distribution de Pseudo-Wigner-Ville, la distribution de la Born-Jordan, la distribution de Rihaczek, la distribution de Choi-Williams, la distribution de Zhao-Atlas-Marks, la distribution de Butterworth et finalement le spectrogramme. La distribution de Rihaczek a été choisie parmi toutes les distributions énoncées ci-dessus pour convertir les signaux du domaine temporel au domaine de temps-fréquence. La distribution de Rihaczek a montré moins d'interférence et moins de termes croisés par rapport aux autres distributions. En plus, utiliser la partie réelle de l'énergie dans la distribution de Rihaczek empêche la nécessité d'abandonner n'importe quelle sorte d'analogie aux phénomènes physiques avec des valeurs négatives. Dans cette thèse, la distribution de Rihaczek a été utilisée pour représenter les signaux qui viennent du système à double couche. Par contre, en cas de mesure de variation d'épaisseur, le spectrogramme a été appliqué pour représenter les signaux en trois dimensions pour le système à une seule couche.

Le dernier point étudié dans cette recherche était de mettre en application la méthode d'extraction de paramètres et la classification pour la détection automatique des défauts. Basée sur le modèle mathématique pour extraire les paramètres à partir des données de représentation en temps-fréquence, l'analyse de composante principale (ACP) a été appliquée pour enlever les données redondantes, réduisant ainsi la taille des données d'une part et d'autre part extraire quelques nouveaux paramètres en tant que spécifications uniques de chaque type de défaut et comme entrée des classificateurs.

L'efficacité des méthodes de classification est habituellement déterminée si la classification est erronée. Deux types de classificateurs discriminatoires et probabilistiques ont eu l'erreur minimum de classification fausse parmi plusieurs classificateurs qui ont été implantés pour ce travail. Ces classificateurs sont l'algorithme des k-moyennes comme méthode discriminatoire et l'algorithme de l'espérance-Maximisation (EM) comme méthode probabilistique.

Dans ce travail, la combinaison de toutes les étapes énoncées ci-dessus fournit un outil d'inspection automatique (matériel et logiciel) de grande précision dans la détection des défauts des fuselages d'avions et structures métalliques multicouches.

ABSTRACT

The increasing demand for air travel has led to an increased number of aircraft in service. A large number of aging aircraft continue to fly. In the aerospace industry, as with other transportation industries, the occurrence of defects in vehicles and the ability to find these defects can make the difference between life and death. For this reason, non-destructive testing methods are periodically applied to inspect aircraft components before they are assembled and also throughout their service life. Components of aircrafts are designed to be as light as possible and also carry very high loads relative to their material strength. This means that a small flaw can cause a major failure in an aircraft fuselage or engine. Fatigue and corrosion are two main causes of failure in aircraft. Several non-destructive testing methods are typically applied to inspect aircraft components while they are in service. These methods are ultrasound, eddy current, liquid penetrate, radiation and magnetic particle inspection. The electromagnetic nature of eddy current testing provides deeper penetration through the aircraft fuselage and brings out rich information describing the interior structure of the inspected sample. Therefore, this method is a powerful inspection method that can be applied in the avionic industry. The main limitations of eddy current testing are that a professional inspector is required to use the method and only conductive materials can be inspected. On the other hand, the main advantage of eddy current testing compared to other non-destructive methods is that it needs no physical contact with the surface. Two types of inspection have been developed in eddy current testing; conventional eddy current and pulsed eddy current. In conventional eddy current testing, a probe is excited with a harmonic sinusoidal signal at a single frequency or multi frequencies to study transient eddy current signals. In contrast to the conventional eddy current method, the pulsed eddy current testing method applies square or sinusoidal shaped pulse excitation and the probe's driving coil is excited by repetitive broadband pulses.

This thesis reports development of an automatic inspection method incorporating pulsed eddy current testing to determine the position and size of flaws buried in an aluminum double-layer structure and also to measure thickness variation in an aluminum single-layer system. Three main aspects are presented; building up a pulsed eddy current setup with all the components to acquire signals from defected samples, applying new signal processing and treatment methods using time-frequency distributions to reveal hidden information from the acquired pulsed eddy

current system and applying artificial intelligence methods to minimize human interference in estimating and determine the defect distribution in aircraft fuselages. Inspection in the aerospace industry is a sensitive case and a non-destructive method must be accurate and reliable for aircraft inspection.

In the first section of this thesis, several types of metal losses with a wide range of depths were fabricated on surfaces of an aluminum plate to simulate corrosion and defect conditions. A complete pulsed eddy current setup was built and programmed to acquire precise signals from defected and non-defected surfaces.

In the second section, pulsed eddy current signals were processed using a time-frequency analysis method. Internal and external noise effects were simulated using small defects placed far from the surface, inter-layer gap and lift off. Noise resources cause a reduction in efficiency of signal representation in the time domain and a time-frequency analysis is therefore implemented to improve representation of signals and reveal more hidden information from defects. In this step the acquired pulsed eddy current signals, which are represented by a voltage-time series (in time domain), are converted to represent signals in three dimensions (time-frequency-amplitude). Over ten different time-frequency distributions were programmed and implemented. These distributions use Short Time Fourier Transforms (STFT) as a linear time-frequency distribution and bilinear time-frequency distributions such as Wigner-Ville distribution, Smooth Wigner-Ville distribution, Pseudo Wigner-Ville distribution, Born-Jordan distribution, Rihaczek distribution, Choi-Williams distribution, Zhao-Atlas-Marks distribution, Butterworth distribution and spectrogram. The Rihaczek distribution was chosen as superior among all the above distributions to convert signals from time domain to time-frequency domain. Two type of bilinear time-frequency distributions are reported in this thesis which are Rihaczek distribution for hidden defect detection in double layer structures and spectrogram for thickness variation detection in single layer. The Rihaczek distribution has shown minimum interference and cross term effects compared to other time-frequency distributions. Additionally, using the real part of the energy in the Rihaczek distribution prevents the need to abandon any sort of analogy to physical phenomena with negative values for energy. In this thesis, the Rihaczek distribution was used to represent signals which come from a double-layer system. In the case of thickness variation measurements, a spectrogram was applied to represent signals from a single-layer system in three dimensions.

The final point studied in this research was to implement and apply a feature extraction method and a classifier for automatic defect detection. Based on a mathematical model for extracting features from time-frequency representation data, principal component analysis (PCA) was implemented and applied to remove redundant data, reduce the size of the data set and also extract some new parameters as a unique specification of each type of synthetic defect and input of classifiers. The efficiency of classification methods is usually determined by misclassification error. Two types of discriminative and probabilistic classifiers had minimum misclassification error among several classifiers which were studied during this project. These classifiers are K-Mean Clustering as a discriminative method and Expectation-Maximization (EM) algorithm as a probabilistic method. To calculate misclassification error in each classifier, several unknown samples were tested to determine the reliability of classification and also amount of misclassification error.

Combination of all the above steps in this work provides an automatic inspection tool (hardware and software) which has high accuracy and reliability for defect detection in aircraft fuselage and metallic multilayer structures.

TABLE OF CONTENT

LIST OF FIGURES

LIST OF ABBREVIATIONS

EM	Algorithme de l'Espérance-Maximisation
STFT	Short Time Fourier Transforms
PCA	Principal Component Analysis
EM	Expectation-Maximization
NDT	Non-Destructive Testing
LPI	Liquid Penetrate Inspection
UT	Ultrasound
ECT	Eddy Current Testing
PEC	Pulsed Eddy Current
EC	Conventional Eddy Current
AC	Alternating Current
PSD	Power Spectral Density
T_{zc}	Arrival Time
V_{pk}	Peak Height
TFD	Time–Frequency Distribution
KL	Karhunen Loeve Transform
A/D	Analog To Digital Converter
FE	Feature Extraction
TOB	Top Of Bottom
BOB	Bottom Of Bottom
BOT	Bottom Of Top

GMR	Giant Magneto Resistive Sensor
NI	National Instrument

INTRODUCTION AND THESIS OBJECTIVE

Background and Problems

Climate conditions are the most significant cause of corrosion, metal loss and flaws between the layers of aircraft fuselage. Due to continual growth in the number of airlines and flights, the number of aging aircrafts in service is increasing and it is vital to develop accurate and reliable inspection methods for defect detection during their service life. Non-destructive testing (NDT) methods are developed to characterize and detect defects in components without removing them from service, or causing damage to the sample during the testing process. The most common non-destructive testing methods currently used in aviation industries are ultrasound (UT), liquid penetrate inspection (LPI), magnetic particle inspection, radiation and eddy current testing (ECT). Each of these non-destructive testing methods has some advantages and limitations based upon its application. Eddy current testing is an electromagnetic inspection method. The main advantage of eddy current testing over other non-destructive testing methods such as magnetic particle inspection and ultrasound is that the eddy current testing is very sensitive to flaws and defects and it does not need to contact the surface physically. On the other hand, eddy current testing is limited in its ability to inspect ferromagnetic materials and these materials need special treatments to address permeability effects. The eddy current technique is a powerful non-destructive testing method. This method can be applied to conductive materials to inspect physical properties such as thickness variation, surface and subsurface defects and coating characterization. It is also used to measure electrical properties such as conductivity and magnetic permeability. Two types of eddy current techniques are used in non-destructive testing, conventional eddy current (EC) and pulsed eddy current (PEC). In contrast to conventional eddy current testing that a probe is excited under single frequency or multi-frequencies, pulsed eddy current testing uses square or sinusoidal pulsed excitation in a wide range of frequencies. Response signals of pulsed eddy current provide good information describing the condition of interior structures. Pulsed eddy current signals are represented by voltage-time series in the Time domain. Several signal processing and signal treatment methods can be applied to bring out additional hidden information from acquired pulsed eddy current signals.

An automatic defect detection method should be fast, reliable and accurate to determine the position and size of defects in a sample test and a real case study. Pulsed eddy current testing is a fast and reliable inspection method. New signal processing methods can be applied to reduce noise effects and improve accuracy of the inspection.

Objective

The principle objective of this research is to develop a fast, reliable and accurate automatic defect detection using the pulsed eddy current testing method as a non-destructive test for targeted practical inspection and maintenance in avionic industry applications, specifically aircraft fuselages. The first objective of this thesis (objective 1) is to fabricate and optimize a new pulsed eddy current testing system to acquire response signals from multilayer and single-layer aluminum structures under various situations. The results of this part are represented in terms of a transient system response in the time domain. Several time-frequency distributions are implemented and applied as new signal processing and signal treatment methods for pulsed eddy current responses. The second objective (objective 2) is to theoretically and experimentally study the effects of Time-Frequency analysis to compare data representation in the time domain and the time-frequency domain. Time-frequency analysis is applied to reduce the noise effects in acquired pulsed eddy current signals and also reveal more hidden information from signals by representation in joint of time and frequency. The third objective (objective 3) is to study and apply feature extraction methods to time-frequency analysis data to provide new patterns by extracting information from the processed data. The final purpose of this study is to develop an automated process for defect detection in aircraft fuselages with minimal human intervention. Typically, artificial intelligence methods are effectively applied. These artificial intelligence methods are used to predict and determine the locations and sizes of unknown hidden defects in a complicated structure by extracting pertinent information from processed data and comparing it with reference patterns. By processing and treatment of acquired data from an unknown sample, new significant and critical points in data set are extracted. New points will compare with reference patterns. Minimum difference between extracted point from unknown sample and each cluster of reference patterns determines closest condition .It defines as a prediction that how much amount of defect is and where it places.

Organization of the thesis

This thesis is organized as follows:

A comprehensive review of the main findings regarding pulsed eddy current testing methods, skin depth theory for pulse excitation and applicable research in the literature is presented in Chapter 1. This section is followed by a literature survey of various time-frequency analysis methods, feature extraction by principal component analysis (PCA) and classification by K-Mean Clustering (discriminative method) and Expectation-Maximization (EM) algorithm (probabilistic method). Chapter 2 summarizes the scientific approach used and explains the coherence between research objectives and the three scientific articles resulting from this work. Chapters 3 to 5 present the three articles which have either been published or been submitted for publication in peer-reviewed scientific journals. Chapter 3 (Article 1) reports on application of Time-Frequency Analysis for automatic hidden corrosion detection in a double-layer aluminum structure using Pulsed Eddy Current. This article mainly focuses on a comparison of common time-domain results of pulsed eddy currents and the application of time-frequency analysis to estimate the location and amount of corrosion and metal losses in a double-layer structure. Chapter 4 (Article 2) deals with metal loss and corrosion detection where defects are placed in overlap conditions. In this article, pulsed eddy current is used as non-destructive testing and time-frequency analysis is applied to represent acquired signals in three dimensions. In Chapter 5 (Article 3), another application of pulsed eddy current and time-frequency analysis method is investigated to determine and estimate thickness variation in single-layer aluminum structure. A new time-frequency analysis distribution is applied during this study. Finally, a general discussion is presented in Chapter 6, while conclusions and recommendations are stated in Chapter 7.

CHAPITRE 1 LITETRATURE REVIEW

Corrosion and cracks are main causes of damage in aircraft fuselages. Many investigations have focused on developing an accurate, reliable and rapid inspection method to predict and determine the locations and sizes of defects in aircraft fuselage where defects are buried between layers in multilayer structures. Pulsed eddy current has been shown capable of reliable and accurate inspection for detection of small-size defects (Sophian, Tian et al. 2001). Before using a pulsed eddy current system for fuselage inspection, it is vital to have a basic understanding of eddy current theory, types of eddy current testing and their specifications and pulsed eddy current testing components. For this reason, eddy current theory is first classified in terms of Faraday and Ampere-Maxwell's law and penetration depth. Following this, the fundamentals of eddy current inspection which may include conventional eddy current, pulsed eddy current and inductance are discussed.

This background information on pulsed eddy current is followed by a review of pulsed eddy current inspection improvements and developments for hidden defect detection, especially in single-layer and double-layer structures. This information is combined with studies on pulsed eddy current inspections which enable optimization of the condition of experiments and inspection through improvements to the new components specially probes improvement or applying signal processing methods. Finally, a literature survey concerning utilization of time-frequency analysis, feature extraction and classification for automatic inspection incorporating pulsed eddy current testing is presented.

1.1 Eddy Current testing

1.1.1 Physical model of Eddy Current testing

In principal, eddy current acts like a transformer. The probe's driving coil and the test sample behave like the primary coil and secondary coil of a transformer respectively. A function generator produces an alternating current (AC) and sends it to the probe's driving coil. According to Ampere's law, a time-varying magnetic field is generated by AC electrical current and is expressed as follows (Sophian, Tian et al. 2002):

$$\nabla \times H = J \quad (1.1)$$

$$J = \sigma E \quad (1.2)$$

where H is the magnetic field intensity, J is current density, E is the electrical field and σ is the conductivity. The probe moves towards the surface of the conductive test sample. The surface is exposed to a time varying magnetic field and according to Faraday's law; flow of electric current is induced on the conductive surface due to variations of the field with time. This is expressed as:

$$\nabla \times E = -B \quad (1.3)$$

$$B = \mu_0 H \quad (1.4)$$

where B is the magnetic field and μ_0 is the magnetic permeability of the vacuum. This electric current is known as eddy current or Foucault current. Eddy current is a circulating flow of electrons inside of materials. This current induces a secondary magnetic field that is known as the eddy current magnetic field. According to the Lenz's law, the direction of the secondary magnetic field is the reverse of the primary magnetic field. Induced eddy current in the conductive material is changed by the presence of metal losses, corrosion, cracks and flaws and consequently the eddy current electromagnetic field changes. A voltage or current in pick-up coil is induced by two types of magnetic fields; eddy current magnetic field and the electromagnetic field from the probe's driving coil. The probe's pick-up coil (differential probe) absorbs the two reverse magnetic fields. The coil's impedance from a non-defected sample is used as a reference signal. Each type of defect is analyzed and inspected by subtracting signals from the defected and non-defected samples. Figure 1.1 shows a schematic of the pulsed eddy current effect and its detection in a metallic structure.

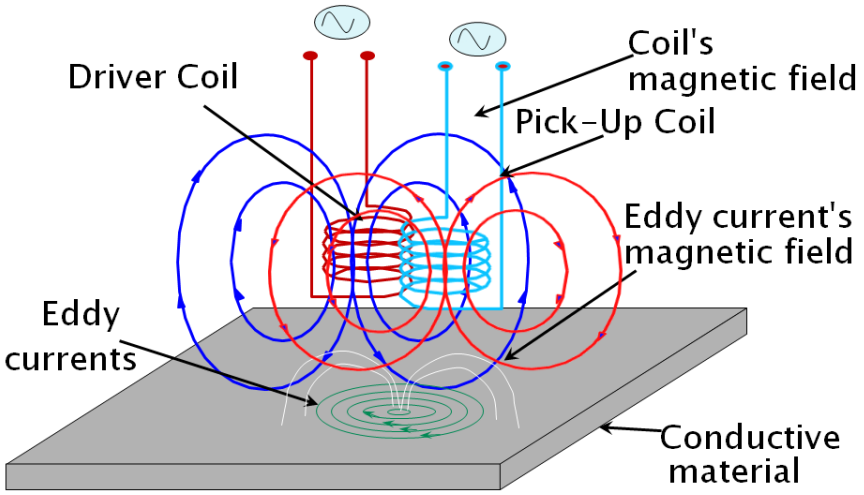

Figure 1.1 a schematic of the pulsed eddy current effect and its detection in a metallic structure.

1.1.2 Penetration depth of transient magnetic field

According to the theory of eddy current, transient magnetic fields penetrate to the bulk of the sample. By increasing the thickness and depth of penetration, the intensity of the magnetic field is reduced. Therefore, the concentration of eddy current decreases with the depth of conductive sample and also the eddy current magnetic field reduces. This means that the eddy current is concentrated on the surface and positions near the surface. For defects located near the surface, inspection and defect detection is done precisely. In contrast, when defects are located in positions far from the surface, penetration of the transient magnetic field drops and the amount of eddy current reduces. Consequently, accuracy and reliability of defect detection is reduced. Effective penetration depth of the transient magnetic field depends on several parameters such as permeability and conductivity of the sample under test, frequency of probe excitation or the circuit time constant.

Penetration depth or skin depth of the transient magnetic field is expressed by the following equations (Krause and Kreutzbruck 2002):

$$\delta = \sqrt{\frac{\tau_c}{\mu\sigma}} \tag{1.5}$$

$$\delta = \sqrt{\frac{2}{\omega\mu\sigma}} = \sqrt{\frac{1}{\pi f \mu\sigma}} = \sqrt{\frac{T}{\pi\mu\sigma}} \tag{1.6}$$

where δ is penetration depth or skin depth of the transient magnetic field, τ_c is the circuit time constant, μ is the magnetic permeability of the conductive test sample, σ is the electrical conductivity of the sample and *f* is the excitation frequency of probe. By increasing the excitation frequency, magnetic permeability and conductivity of the material, induced eddy current in the specimen is reduced and consequently, the magnitude of the eddy current magnetic field is decreased. Defects located far from the surface and optimal penetration depth cannot be detected and inspected precisely.

Due to the factors previously mentioned, the high permeability of ferromagnetic materials such as iron, nickel, cobalt and regular steel results in reduced penetration of transient eddy currents into the bulk of the specimen and defect detection is therefore difficult. On other hand, paramagnetic materials such as aluminum, zinc, stainless steel and titanium with lower magnetic permeability can be inspected effectively using eddy current testing methods; high accuracy defect detection is therefore possible at locations farther from the surface.

1.1.3 Conventional eddy current

Conventional eddy current testing or swept eddy current testing (ECT) is a frequency-domain non-destructive method and that collects eddy current data by probe excitation from a single frequency or multi-frequencies excitation from a hundred hertz to mega hertz. The responses of eddy current testing are displayed on plots of system inductance and resistance called impedance plane diagrams. Variations in sample thickness, permeability, conductivity and also the presence of flaws and corrosion cause changes in amplitude and phase of the acquired eddy current signals. In eddy current testing, impedance of the coil is expressed by:

$$Z_{vacuum}(\omega) = Kj\omega\int_0^{\infty} \frac{P^2(r_1, r_2)}{\alpha^5}\left\{2L + \frac{1}{\alpha}\left[2e^{(-\alpha L)} - 2\right]\right\} d\alpha \tag{1.7}$$

$$K = \frac{\pi\mu_0 N^2}{L^2(r_1 - r_2)^2} \tag{1.8}$$

$$P(r_1, r_2) = \int_{\alpha r_1}^{\alpha r_2} xJ(x)dx \tag{1.9}$$

where r_1 and r_2 are inner and outer diameters of the coil, L is the length of the coil, N is the number of turns in the coil, μ_0 is the permeability of the vacuum, ω is exciting angular frequency and J is the Bessel function. Impedance of the coil above a metallic surface is calculated using the following equation:

$$Z_{metal}(\omega) = Kj\omega \int_0^{\infty} \frac{P^2(r_1, r_2)}{\alpha^5} \left\{ 2L + \frac{1}{\alpha} \left[2e^{(-\alpha L)} - 2 + (e^{(-\alpha l_1)} - e^{(-\alpha l_2)})^2 . \frac{\alpha\mu - \alpha\mu_0}{\alpha\mu + \alpha\mu_0} \right] d\alpha \right. \tag{1.10}$$

where μ is the permeability of the conductive surface. The difference between the coil's reference impedance (without a sample test) and the coil's impedance during an experiment with a metal sample is expressed by:

$$\Delta Z = Kj\omega \int_0^{\infty} \frac{P^2(r_1, r_2)}{\alpha^6} . (e^{(-\alpha l_1)} - e^{(-\alpha l_2)})^2 . \frac{\alpha\mu - \alpha\mu_0}{\alpha\mu + \alpha\mu_0} d\alpha \tag{1.11}$$

Figure 1.2 presents plots of system inductance and resistance during eddy current testing. Figure 1.2(a) shows thickness detection for several points using A-scan detection (point-to-point of metal) for a metallic plate with varying thicknesses. Figure 1.2(b) shows B-scan or line thickness detection from thick to thin state of metal and with a starting point from air.

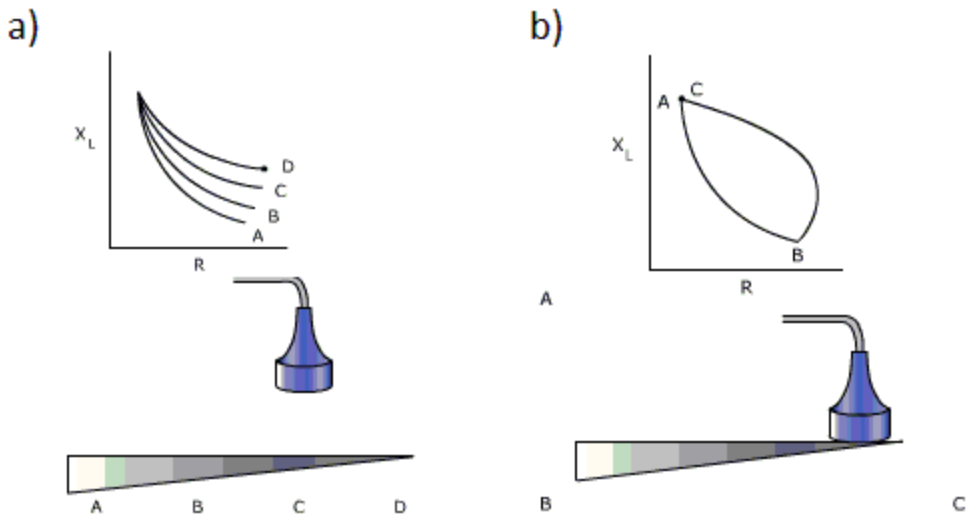

Figure 1.2 plots of system inductance and resistance by eddy current testing (a) thickness detection in A-scan (b) B-scan from thick to thin state of metal with starting point from air

1.1.4 Pulsed eddy current

Pulsed Eddy Current (PEC) is an electromagnetic non-destructive method that provides accurate and reliable measurements when used to inspect aircraft body components for corrosion and cracks. The pulsed eddy current technique is a non-contact inspection method and can be applied on surfaces to detect subsurface cracks, metal losses and estimate the thickness. The pulsed eddy current testing method uses pulsed excitation over a wide range of frequencies. In contrast to conventional eddy currents that use harmonic excitation at a single frequency or several frequencies to study transient eddy current signals, the pulsed eddy current testing method applies square or sinusoidal shaped pulse excitation and the probe's driving coil is excited by repetitive broadband pulses. Pulsed transient excitation over a wide range of frequencies induces scattering eddy currents during sample testing. The broadband nature of Pulsed Eddy Current (PEC) testing allows more penetration than other conventional eddy current methods. Response signals of pulsed eddy current provide good information describing the condition of interior structures. Corrosion, cracks and other defects can be detected by applying signal processing methods on PEC signals. The defects that are closer to the surface excite the pickup coil earlier than defects positioned more deeply. Therefore, a time domain signal can represent the pulsed eddy current response according to depth of defects. The most common features in PEC are peak height (V_{pk}) and arrival time (T_{zc}); the former indicates the size of the defect and the latter generally indicates its depth. Variation of defect's size causes variation of eddy current magnetic field's amplitude that is represented by changing in amount of maximum amplitude of acquired signal from defects place. Additionally the point of crossing the time axis by acquired signal shows place of defect which place how far from surface of sample or surface of probe. These features are not sufficient to discriminate signals due to corrosion because presence of internal and external noise resources. Figure 1.3 shows time-to-peak and time-to-zero of a voltage-time series data for pulsed eddy current response.

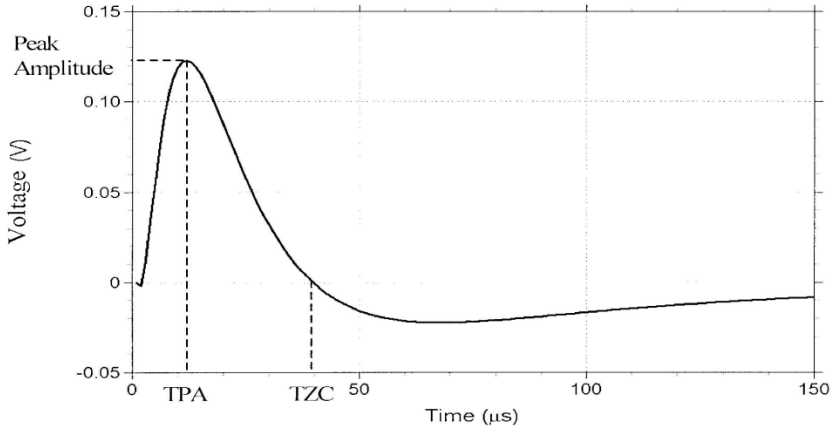

Figure 1.3 Pulsed eddy current response (Giguere, Lepine et al. 2001).

1.2 Signal Treatment

Pulsed Eddy Current inspection is one of the powerful non-destructive techniques that can be applied to assure safe and economic inspection of aircraft components and sub-assemblies. The presence of internal and external noise sources (such as low amounts of defects for internal and interlayer gap and lift off for external noise resources) necessitate use of a signal processing method incorporating mathematical models to improve the performance of the pulsed eddy current inspection (obtained features are not good enough for discriminating corrosion) so that it can detect and measure the size of corrosion and cracks in metallic multilayer components. Advanced signal processing methods are introduced to extract the maximum information contained in the pulsed eddy current signals and also to represent signals in a joint time-frequency analysis to provide better representation of signals. In this thesis, time-frequency analysis methods are discussed in both linear and quadratic representations. In case of hidden defect detection, Rihaczek distribution will be used to process signals and represent them in three dimensions representation. Rihaczek distribution is applied because of minimum amount of crossing effect or interference and also this distribution represents signal in real positive value. In case of thickness variation detection, a spectrogram is used as a bilinear time-frequency representation. Spectrogram shows acquired pulsed eddy current signals in three dimensions.

1.2.1 Linear Time-Frequency Representations

The linearity principle is satisfied by linear time-frequency distributions. The linearity principle is referred to as the superposition principle. This means that the time-frequency representation of a linear combination of several signal components is equal to the same linear combination of the time-frequency representation of each signal component:

$$T\left(ax_1(t)+bx_2(t)\right)=aT\left(x_1(t)\right)+bT\left(x_2(t)\right) \tag{1.12}$$

where *T* denotes any linear transformation, *a* and *b* are scalar constants and $x(t)$'s are the signals. Gabor representation, Wavelet transform and Short-time Fourier transform are three well-known linear time-frequency representations. Fourier transform is a mathematical tool which is used to reveal the frequency domain of signals. For signal *x(t)* in the time domain, Fourier transform *X(f)* is expressed by:

$$X(f)=\int_{-\infty}^{+\infty}x(t)e^{-j2\pi ft}dt \tag{1.13}$$

where *f* is frequency and *t* denotes time.

1.2.1.1 Short Time Fourier Transform

The frequency contents of signals is determined by Fourier transform but any further information about the time at which each frequency component takes place cannot be provided by Fourier transform. To overcome this shortcoming, Fourier transform can be applied to a respectively short portion of the signal (analysis window) around the instantaneous time *t*. Then by ceaselessly moving toward the window along the time axis, a joint time-frequency representation of the signal can be obtained. This transform is called the Short Time Fourier Transform (STFT) and mathematically is expressed by:

$$S(t,f)=\int_{t'}x(t')w(t'-t)e^{-j2\pi ft'}dt' \tag{1.14}$$

where $w(t'-t)$ is the window function or analysis window. The choice of analysis window has a dominant influence on the results of the Short Time Fourier Transform (STFT). At time *t* the frequency components appearing in the representation are in fact the frequency components

of the selected window around that instant. Therefore, in order to have a good time resolution the analysis window must be chosen as short as possible. At the same time, choosing a short analysis window leads to poor frequency resolution.

1.2.2 Quadratic time-frequency distributions

In time-frequency analysis, the estimation of energy distribution or instantaneous power spectra of the signals is provided by bilinear representations which are known as quadratic time-frequency representations. In contrast to linear time-frequency distributions, the linear principle is not satisfied by quadratic distributions. This means that a quadratic representation of signals which combine linearly is expressed as follows:

$$\begin{aligned} &T\left(ax_1(t)+bx_2(t)\right)=a^2T\left(x_1(t),x_1(t)\right) \\ &+b^2T\left(x_2(t),x_2(t)\right)+ab^*T\left(x_1(t),x_2(t)\right) \\ &+a^*bT\left(x_2(t),x_1(t)\right) \end{aligned} \tag{1.15}$$

where T denotes any transformation, a and b are scalar constants, $x(t)$'s denote signals in time, $T(x_1,x_1)$ and $T(x_2,x_2)$ are called auto terms and two other remaining terms are called cross terms or interference terms.

1.2.2.1 Spectrogram

A spectrogram is defined as the squared magnitudes of the short time Fourier transform:

$$Spec=\left|STFT\right|^2 \tag{1.16}$$

Although the spectrogram is nonlinear, the final results of this distribution have no interference terms or cross-term effects. This stems from the fact that nonlinearity is not an instinctive feature of this transform and comes into effect while squaring the magnitude. That together with simplicity, robustness and ease of interpretation, have made the spectrogram a popular tool for many applications (Boashash 2003).

The spectrogram represents an attempt to apply the Fourier transform to a short-time analysis window, within which the signal is expected to be reasonably stationary. The underlying idea is that, by moving the analysis window along the signal, variations of the signal spectrum are

captured as a function of time. However, similarly to STFT, the spectrogram is not the best choice for analyzing rapidly varying signals. If the analysis window is chosen short enough to capture rapid changes in the signal it becomes impossible to resolve frequency components of the signal which are close in frequency. The spectrogram distribution is a Real-valued, time shift invariance and frequency shift invariance distribution.

1.2.2.2 Wigner-Ville distribution

The Wigner-Ville distribution is represented by real values. Shift invariance and marginal condition exist in time and frequency representation of Wigner-Ville distribution. Wigner-Ville scales time and frequency and works based on instantaneous frequency. Wigner-Ville distribution supports finite time and finite frequency. This distribution follows Moyal's formula and Fourier transform and also it has convolution invariance and multiplication invariance.

The Wigner-Ville distribution possesses many desirable mathematical features and is defined as:

$$W(t, f) = \frac{1}{2\pi}\int x^*(t - \frac{1}{2}\tau)x(t + \frac{1}{2}\tau)e^{-j2\pi f\tau}d\tau \qquad (1.17)$$

In contrast to the spectrogram distribution, the Wigner-Ville distribution provides high resolution in time and frequency simultaneously and there is no trade-off between time and frequency resolution. The main limitation of the Wigner-Ville distribution is that its energy distribution is not non-negative and it often contains severe cross terms, or interference terms between components in different (*t*, *f*) regions, potentially leading to confusion and misinterpretation. Additionally, the Wigner-Ville is considered a noise-sensitive time-frequency distribution. In general, if noise exists at a small finite time of the signal, that noise will appear at other times. Also, if the signal is infinite, then it will appear for all times. The other severe drawback is that the Wigner-Ville distribution at a particular time generally reflects properties that the signal has at other times because the Wigner-Ville distribution is highly non-local. Moreover, in general the Wigner-Ville distribution is not zero when the signal is zero, and this causes considerable difficulty in interpretation.

1.2.2.3 Rihaczek distribution

The Rihaczek distribution is represented by complex and positive values. Shift invariance and marginal condition exist in time and frequency representation of Rihaczek distribution. The Rihaczek distribution scales time and frequency. The Rihaczek distribution supports finite time and finite frequency. This distribution follows Moyal's formula and Fourier transform and also it has convolution invariance and multiplication invariance.

In time-frequency analysis, the Rihaczek distribution allows the energy of a complex deterministic signal over a finite range of time and frequency to become infinitesimal. The obtained result is called a complex energy distribution. The interaction energy between a signal **x** restricted to an infinitesimal interval δ_t centered on *t*, where **x** passes through an infinitesimal band pass filter δ_{fil} centered on *f*, can be approximated by the following expression:

$$\delta_t \delta_{fil}[x(t)X^*(f)e^{-j2\pi ft}]. \qquad (1.18)$$

This representation was derived by considering the local energy of the signal that passes through an infinitesimal time window centered at time *t* and an infinitesimal pass band filter centered at frequency *f*. The result is a complex energy density at point (*t*, *f*) from which the definition of the distribution is obtained:

$$RD = \int_{\tau} x(t+\tau)x^*(t)e^{-j2\pi f\tau}d\tau = x(t)X^*(f)e^{-j2\pi ft} \qquad (1.19)$$

The Rihaczek distribution can be interpreted as a complex energy density at point (t, v) with elements of Cohen's class written as $f(f,\tau) = e^{-2j\pi f\tau}$.

The Rihaczek distribution is a bilinear time–frequency distribution (TFD) and is a member of Cohen's class. It is covariant to shifts in time and frequency. The Rihaczek distribution is always zero when the signal is zero. It also perfectly localizes impulses and sine waves.

Many time-frequency analysis methods abandon any sort of analogy to physical phenomena with negative and complex values. The complex energy density in the Rihaczek distribution overcomes the problem of missing phenomena by using only the real part of the energy and trends the energy to the standard and real amount.

1.2.3 Feature Extraction

Time-frequency methods provide very large amounts of data and it is necessary to remove redundant data and reduce the dimensions of the data set. Principal component analysis (PCA) is a method that creates new features and reduces the size of the data set.

1.2.3.1 Principal Component Analysis (PCA)

Principal Component Analysis (PCA) is also known as the Karhunen Loeve (KL) transform or the Hotelling transform. It is based on factorization techniques developed in linear algebra. PCA uses factorization to transform data according to statistical properties to optimize and reduce the amount of redundant data. This data transformation is particularly useful for classification and compression. The main advantage of PCA is generation of independent features.

In PCA processing, the covariance of the input data ($\mathbf{\Sigma_X}$) is calculated:

$$\Sigma_x = E\{(x-\mu_x)(x-\mu_x)^T\}. \qquad (1.20)$$

Eigenvalues λ and Eigenvectors $\mathbf{W}_i$ are identified using covariance of the time-frequency results $\mathbf{\Sigma_X}$.

$$(\lambda I - \Sigma_x) = 0. \qquad (1.21)$$

$$(\lambda I - \Sigma_x) W_i = 0. \qquad (1.22)$$

Where, I is an identity matrix of the same order as Σ_X. Transformation W maps each features vector define as input $\mathbf{C_X}$ into features of output $\mathbf{C_Y}$.Transform features $\mathbf{C_Y}$ are obtained using $\mathbf{C_X . W^T}$. The new features are linearly independent.

The output of time-frequency analysis for each Pulsed Eddy Current signal is an n×n matrix that can be represented by an image. The matrix is expressed as n^2 dimensional vectors. The value of each vector corresponds to the intensity value of each pixel of the time-frequency analysis image. The image contains a large amount of redundant data. Principal Component Analysis (PCA) is applied as feature extraction to reduce the number of parameters and also improve computational efficiency of the classifier.

PCA computes Eigenvalues and Eigenvectors of the covariance matrix. The Eigenvectors are arranged in order of largest Eigenvalues. The first Eigenvector has the direction of the largest variance of the data and it determines the direction of the most significant amount of energy. Principal Component Analysis retains the significant features (Eigenvectors with largest Eigenvalues) and leaves out some less expressive features. PCA reduces the number of parameters without loss of significant information.

1.2.4 K-Means Clustering and Expectation-Maximization Algorithm (EM)

K-means is one of the unsupervised learning algorithms that solves the clustering problem. The K-means algorithm is based on use of the squared Euclidean distance as the measure of dissimilarity between a data point and a prototype vector. K-means separates **n** observations into **K** clusters, for which each observation (data point) belongs to the cluster with the nearest mean. The K-mean algorithm consists of two major parts; (1) review all the data and reassign data to the closest selected centers (centroid), (2) make a loop and recalculate the center points to find the nearest centroids. The K-mean algorithm partitions a set of **n** observations (x_1, x_2, ... ,x_n) into **k** clusters S=[S_1,S_2, … , S_k] to minimize the square error function;

$$\arg\min \sum_{i=1}^{k} \sum_{x_j \in S_i} \left| x_j - \mu_i \right|. \tag{1.23}$$

where; μ_i is the mean of S_i.

The Expectation-Maximization (**EM**) algorithm is a powerful probabilistic classifier method for finding the maximum likelihood solution parameters for unobserved latent variables **S**. A set of **n** observations and a vector of unknown parameters **θ** are used to calculate the maximum likelihood.

$$L(\theta, n) = p(n|\theta) = \sum_{S} p(n, S|\theta). \tag{1.24}$$

EM is an iterative method, alternating between performing an expectation **E** step and a maximization **M** step. The **E** step computes the expectation of the log-likelihood and evaluated responsibilities (posterior probabilities) for the latent variables.

$$Q\left(\theta\middle|\theta^{(t)}\right)=E_{S\middle|n,\theta^{(t)}}\left[\log L\left(\theta;n,S\right)\right]. \tag{1.25}$$

The **M** step (Maximization) re-estimates parameters (means, covariance and coefficients). The expected log-likelihood is achieved in the **E** step.

$$\theta^{(t+1)}=\arg_{\theta}\max Q\left(\theta\middle|\theta^{(t)}\right). \tag{1.26}$$

1.3 Review of the application of pulsed eddy current in defect and thickness detection

A comprehensive review of the literature on the subject of pulsed eddy current testing and pulsed eddy current signal treatment is well beyond the scope of this thesis. Here, the focus is on previous studies on the application of pulsed eddy current for defect detection in metallic plates and also hidden defect detection and thickness detection. A short description is given for each study where its relevancy to works presented in this thesis is provided in the corresponding chapters.

As previously mentioned, time-to-peak and time-to-zero are two main features of pulsed eddy current signals which are used in defect and thickness detection of metallic plates (Lebrun, Jayet et al. 1997; Sophian, Tian et al. 2003). Zhou et al (2010) (Zhou, Tian et al. 2010) applied principal component analysis as a feature extraction method to two main features of a pulsed eddy current response. They sorted acquired responses to find a relationship between thickness variation in a single-layer system and the amplitude and location of points where the pulsed eddy current response curves cross the time axis. They found that by increasing the thickness of the sample, the signal amplitude increases and the location of the peak on the time axis decreases.

Another feature was investigated and used by Tian et al (2005) (Tian and Sophian 2005). They presented a new feature called rising point time. They expressed that rising point time is independent of coil dimensions and it is able to determine the depth of defects regardless of the shape or type of defects. It is applicable to determine lift-off effect in thickness detection in single-layer structures. By using the rising point time as a new feature, measurement of thickness

is faster than using the two general features of pulsed eddy current (time-to-peak and time-to-zero).

Lift-off effect is a noise effect in pulsed eddy current testing. Lift-off reduces accuracy of the inspection (Le Bihan 2002). Several parameters have been studied to remove the effect of lift-off. Giguere et al (2000 & 2001) studied the effect of lift-off in defect detection in a multilayer structure and determined the effect and amount of lift-off in a flawless multilayer sample (Giguere, Lepine et al. 2000; Giguere, Lepine et al. 2001). Mandache et al (2006) (Mandache and Lefebvre 2006) implemented a new algorithm to calculate the amount of lift-off and to remove it from acquired pulsed eddy current signals. By computing the slope of pulsed eddy current signals at different amounts of lift-off, they calibrated and estimated the amount of lift-off. Tian et al (2004) used normalization and also two reference signals to reduce the effect of lift-off in pulsed eddy current inspection (Tian and Sophian 2005). Two reference signals, first from air and a second from a non-defected sample were used. They calculated two types of subtractions; subtraction of the reference signals (which come from air and non defected sample to calculate total amount of eddy current magnetic field) and also subtraction of the defected signals from the reference signal which come from a non-defected sample. The results were then normalized. Another subtraction between two results of subtraction (first between acquired signal from air and non defected sample, second between acquired signal from defected sample and non defected sample) is done and results are normalized. Their results show that by using this method, the lift-off effect can be removed in thickness detection of a single-layer system.

In pulsed eddy current signal acquisition, efficiency of the probe is one the important effects. An efficient and reliable probe provides non-noisy and clear results. Several types of probes have been developed and used in pulsed eddy current inspection. The most well-known probes are the Hall probe, the giant magneto resistive sensor (GMR) and the differential probe (He, Luo et al. 2010; He, Luo et al. 2010). Ewdards et al (2006 & 2008) (Edwards, Sophian et al. 2006; Edwards, Sophian et al. 2008) designed a new dual-probe system containing electromagnetic acoustic transducers (EMATs). Their dual probe was able to detect and measure the size of surface and subsurface defects in a conductive material. They used the dual probe to inspect a single-layer structure with 150 mm thickness. They combined results of two-type inspection to provide a more accurate thickness measurement. Shin et al (2009) (Shin, Choi et al. 2009) used a differential pulsed eddy current probe to measure thickness variation in the presence of lift-off in

a single-layer system. The giant magneto resistive probe is a powerful probe in field of eddy current testing. Kim et al (2010) (Kim, Yang et al. 2010) used this probe to detect cracks at rivet sites in the third layer of an aircraft fuselage. Sophian et al (2002) (Sophian, Tian et al. 2002) designed a new probe with an inductive flat coil and a magnetic field. They used a Hall device probe, which possesses a much wider magnetic field. They used this probe to size defects in a double-layer structure.

Several studies have focused on using new approaches and features for defect detection and defect classification and also thickness variation detection by pulsed eddy current testing in multilayer and single-layer structures. Park et al (2009)(Park, Angani et al. 2009) (Park, Angani et al. 2009) used the frequency domain and calculated the power spectral density (PSD) of pulsed eddy current signals. They calculated RMS value, energy of pulse and PSD of pulsed eddy current signals to describe thickness variation in stainless steel which had been covered by insulation. Safizadeh et al (2001) (Safizadeh, Lepine et al. 2001) applied a time-frequency analysis method as an alternative to improve signal representation using three-dimensional representations. They used the Wigner-Ville distribution as a time-frequency distribution to represent signal in three dimensions. Their results showed that time-frequency analysis can be applied as a powerful tool to reveal hidden information in the time domain and frequency domain. Additionally, by applying the time-frequency distribution for pulsed eddy current signal treatment, external noise effects such as lift-off and interlayer gap can be removed or reduced. Interlayer gap and lift-off provide patterns in images of time-frequency analysis that can be filtered. Finally, they were able to obtain a clear result for multilayer defect detection. In another study, Safizadeh et al (2005) (Safizadeh, Liu et al. 2005) used their procedure for automatic defect detection in multilayer structures. They extracted data from time-frequency results and then used a neural network (NN) model to classify extracted data.

Feature extraction and defect classification are two main parts of each automatic defect detection method and non-destructive testing. In many of the research papers reviewed, principal component analysis (PCA) is the first and main choice for feature extraction. Among the many researchers, Yang et al (2009) (Yang, Tian et al. 2009) used independent component analysis (ICA) as a feature extraction method for classifiers in pulsed eddy current testing. They applied ICA to project the pulsed eddy current signals of different defects in the independent component subspace. They used ICA's results to discriminate defects. Lang et al (2007) (Lang, Agurto et al.

2007) used the Fisher discriminative model as a new model to classify defected and non-defected samples. They extracted new patterns for defected samples and trained the system using a sample case. Then, they compared test results with a training sample. Although their results show good separation and automatic defect detection, we applied their methods and our results did not match theirs because defect distribution in our samples is too close and we have a large number of defects in different locations.

The above discussed studies are the basic studies done in the field of pulsed eddy current testing. Other works are very much in line with the above studies. The main common points among these investigations are that they did not compare close amounts of defects and their distribution in multilayer samples. Instead, they simply discussed one type of metal loss in a single-layer or double-layer system. Also, new feature and signal treatment methods were not discussed during their experiments. These two drawbacks are revisited in this thesis.

CHAPITRE 2 SCIENTIFIC APPROACH AND COHERENCE OF ARTICLES

The principal aim of this work was to develop a fast, reliable and accurate automatic defect detection method based on use of pulsed eddy current testing as a non-destructive test for targeted practical inspection and maintenance of structures used in avionic industries, specially aircraft fuselages and aluminum multilayer structures. To reach this goal, different signal processing and treatment methods were necessary to improve the representation from pulsed eddy current signals. Following this, two-step data mining techniques were implemented to extract significant features from processed and treated data and also to classify each case of synthetic defects separately. Figure 2.1 shows the procedure used in this thesis for automatic defect detection and data mining of pulsed eddy current signals. A new pulsed eddy current testing system was designed, fabricated and optimized to acquire reliable and accurate response from multilayer and single-layer aluminum structures in various situations. Among several time-frequency distributions, the most effective time-frequency analysis method was chosen to process the pulsed eddy current signals. Extracting the features and classification are done to provide a map and new patterns for defect classification and presentation.

This research work was done with the collaboration of Professor Aouni Lakis from École Polytechnique de Montreal. This research was supported by the collaborative research and development grant (No. CRDPJ-335472-05) of Natural Sciences and Engineering Research Council of Canada (NSERC), Pratt & Whitney Canada, Bombardier Aeronautics and National Research Council of Canada (NRC).

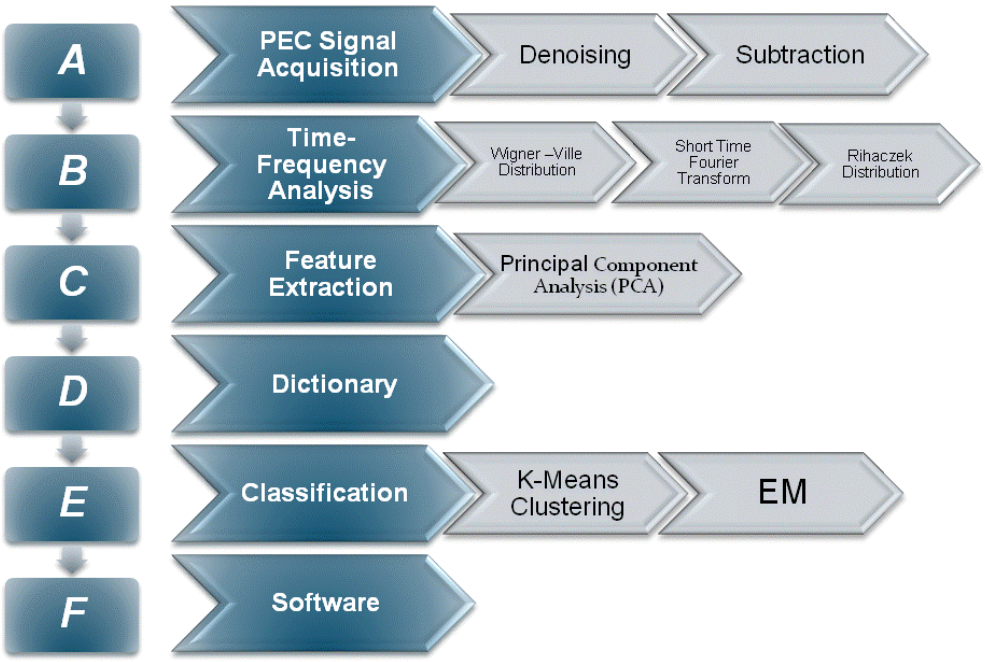

Figure 2.1 Procedure for automatic defect detection and data mining of pulsed eddy current signals

2.1 Article presentation and coherence with research objectives

The main scientific findings and core achievements of this study are presented in Chapters 3 to 5. The work is presented in the form of three peer-reviewed papers written for archival journals (the article in Chapter 3 has already been published). All of these journals focus on non-destructive testing methods, developments and improvements.

In the first two papers, we present application of the time-frequency analysis method for defect detection in double-layer structures where defects are separated and also where defects are placed together in overlapping conditions. In third paper, we extend our development to determine thickness variation in single-layer structures.

CHAPITRE 3 APPLICATION OF TIME-FREQUENCY ANALYSIS FOR AUTOMATIC HIDDEN CORROSION DETECTION IN A MULTILAYER ALUMINUM STRUCTURE USING PULSED EDDY CURRENT[1]

Saleh Hosseini

Section of Applied Mechanics, Department of Mechanical Engineering, École Polytechnique de Montréal, Montréal, Quebec, H3T1J4, Canada.

Aouni A. Lakis

Section of Applied Mechanics, Department of Mechanical Engineering, École Polytechnique de Montréal, Montréal, Quebec, H3T1J4, Canada.

Corresponding author;

Tel.: +1 514 340 4711 (4906)

Fax: +1 514 340 4076

Email: aouni.lakis@polymtl.ca

Abstract

Pulsed Eddy Current (PEC) is a non-destructive testing method used to detect corrosion and cracks in multilayer aluminum structures which are typically found in aircraft applications. Corrosion and metal loss in thin multi-layer structures are complex and variable phenomena that diminish the reliability of pulsed eddy current measurements. In this article, Pulsed Eddy Current signals are processed to improve the accuracy and reliability of these measurements. PEC's results (time domain data) are converted by Time-Frequency Analysis (Rihaczek distribution) to represent data in three dimensions. The Time-Frequency approach generates a large amount of

---

[1] This article was accepted ,5th of dec 2011, in the journal of NDT&E (Nondestructive Testing and Evaluation)

data. Principal component analysis is applied as feature extraction to reduce redundant data to provide new features for classifiers. K-means Clustering and Expectation-Maximization are applied to classify data and automatically determine corrosion distribution in each layer.

Keywords: Multi-layer Aluminum Structures, Pulsed Eddy Current, Time-Frequency Analysis, Feature Extraction, K-Means Clustering, Expectation-Maximization Algorithm.

3.1 Introduction

Climate conditions are the most significant cause of corrosion between the layers of aircraft fuselage. Pulsed Eddy Current (PEC) is one of the new methods that provide accurate and reliable measurements when used to inspect aircraft body components for corrosion and cracks [1-3]. The pulsed eddy current technique is a non-contact inspection method and can be applied on surfaces to detect subsurface cracks, metal losses and estimate the thickness [4, 5]. The Pulsed Eddy Current testing method uses pulsed excitation with a wide range of frequencies. The broadband nature of Pulsed Eddy Current allows more penetration than other conventional eddy current methods [6-8]. Response signals of pulsed eddy current provide good information describing the condition of interior structures [9]. Corrosion, cracks and other defects can be detected by applying signal processing methods on PEC signals. The defects that are closer to the surface excite the pickup coil earlier than defects positioned more deeply [8]. Therefore, a time domain signal can represent the pulsed eddy current response according to depth of defects.

Thickness measurement with high accuracy is the major challenge in the field of pulsed eddy current testing. Many authors have used common results of PEC in the time domain to determine the number and locations of defects in single layer and multilayer systems. Many investigations have succeeded in detecting thickness variations and hidden corrosion by time domain signal processing methods [8, 10, 11]. Many investigations have improved measurement efficiency by changing the properties of the probe and using different types of probes such as the Hall probe [8, 12], giant magneto resistive sensor (GMR) [13-15] and differential probe [6, 16]. Safizadeh et al [17]applied Wigner Ville distribution as a time-frequency analysis method to detect corrosion in a second layer due to an inter-layer gap. Safizadeh et al transformed a response signal into a three-dimensional representation of the signal in time-frequency-amplitude [17, 18].

Pulsed Eddy Currents data is acquired in Time domain. The most common features in PEC are peak height (V_{pk}) and arrival time (T_{pk}); the former indicates the size of the defect and the latter generally indicates its depth [19-21]. Variation of defect's size causes variation of eddy current magnetic field's amplitude that is represented by changing in amount of maximum amplitude of acquired signal from defects place. Additionally the point of crossing the time axis by acquired signal shows place of defect which place how far from surface of sample or surface of probe. These features are not sufficient to discriminate signals due to corrosion because of noise resources [22]. In single layer structures and sub-surface defect detection, Principal Component Analysis can be applied as a signal treatment method to extract more accurate data from peak value, peak time and frequency spectrum analysis [22, 23]. In thin multi-layer systems with variation of metal loss and corrosion, advanced signal processing methods are applied to detect the location and amount of defects on surfaces. The main purpose of this article is to compare common time-domain results of pulsed eddy currents and the application of time-frequency analysis to estimate the location and amount of corrosion and metal losses in a double-layer structure. Defects are simulated on the bottom and top of each layer with layer thicknesses at 3%, 5%, 7%, 10%, 15%, 20% and 25% of metal thickness. Rihaczek distribution is used as the time-frequency method and principal component analysis (PCA) provides a new feature to compress and input classifier data (the time-frequency data). Finally two types of classification methods (discriminative and probabilistic) are applied to classify the results. K-means Clustering and the Expectation-Maximization algorithm (EM) are applied to classify the amount and location of corrosion in each layer separately. The entire step provides a logical automatic method to detect defects in a double-layer system.

3.2 Experiment setup and description of sample

The traditional Pulsed Eddy current system consists of a function generator (which creates a square voltage), a probe (either a reflection probe or dual probe) and an Analog to Digital converter (A/D). The designed system for this experiment has a function generator, reflection probe, preamplifier, digitizer converter card and a computer system with signal processing software.

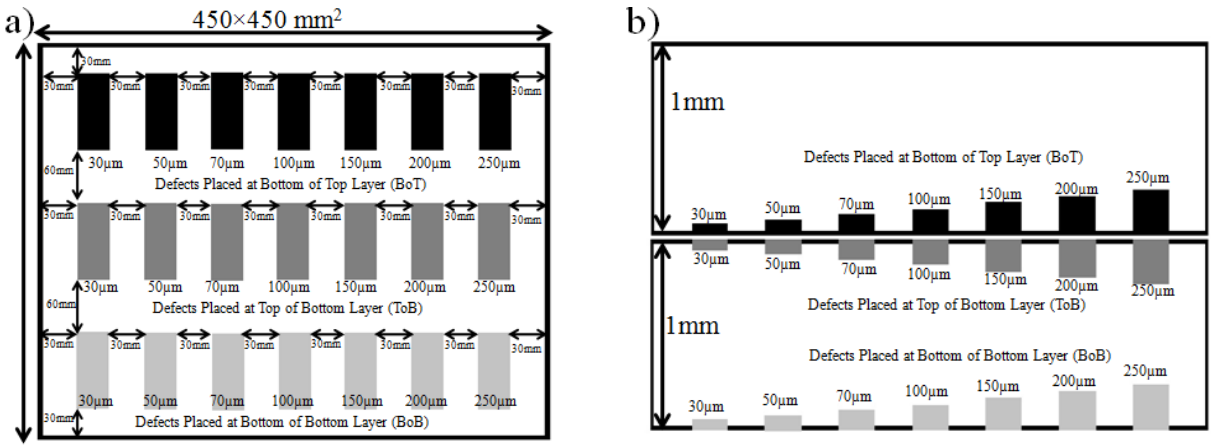

Figure 3.1 Schematic of sampling test. (a) View from above. (b) View from side.

For our experiment, bare aluminum sheets at 1.04 millimeter thickness and 450×450 mm^2 areas, as shown in Figure 3.1(a) and 3.1(b) were used. Figure 3.1(a) and 3.1(b) show schematic of sampling test from above and side. The thicknesses of synthetic defects are 3%, 5%, 7%, 10%, 15%, 20% and 25% of the plate thickness. These synthetic defects were fabricated by laser machining with 1 micrometer tolerance. The depths of the metal losses are 30 µm, 50 µm, 70 µm, 100 µm, 150 µm, 200 µm and 250 µm. Each series of metal losses were placed on top or bottom side of plates. The size of the defects is equal and area of each one is 30×90 mm^2. The reflection probe is excited by a square pulse (1 KHz and 4 volt) by a function generator. A driver coil converts square voltage to an electromagnetic field on the affected conductive surface. A pick-up coil receives the response of the electromagnetic fields from the specimen and the driver coil. It converts this differential response signal into voltage. The first coil has inner and outer diameters of 12 and 15 mm respectively. The second coil has inner and outer diameters of 7 and 11 mm. The pick-up coil sends analogue signals to a preamplifier to amplify the signal and reduce the noise level. The amplifier is a low noise preamplifier and the power of amplifier is 110V and 6 watt. The band pass filter is between 100Hz and 10 KHz and amplifier gain is fixed at 5 times amplifying. NI digitizer (PCI-4070) and LabView software are used to convert the analogue signal to digital and store the signals on a PC. The sampling frequency of the card is 1.6 MegaSample/sec with 23-bit resolution. Figure 3.2 presents the pulsed eddy current system used for the experiments described in this paper.

Figure 3.2 Designed PEC system.

A digitizer converts analogue to digital signals. Digital signals are saved on a PC in text format. Subtraction of each signal that comes from defected surface with different metal loss is then calculated against the reference signal that belongs to a non-defected signal in double-layer condition. Time-Frequency analysis is applied on the subtracted signals and converts the time-domain signal (two dimensions) to three-dimensional signals (time-frequency-amplitude). Principal Component Analysis (PCA) processes the time-frequency analysis results and provides feed of classifiers. K-mean Clustering and Expectation-Maximization algorithms classify the results to create the data bank and dictionary for metal losses in the range of 5% to 25% of plate thickness. Figure 3.3 presents a schematic of the detection process.

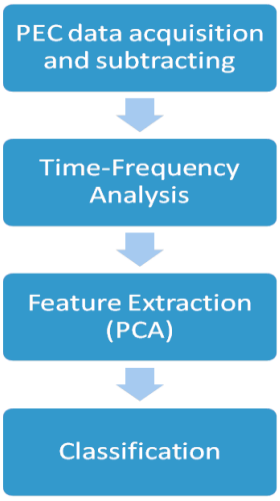

Figure 3.3 Diagram of the detection process.

3.3 Theory

3.3.1 Pulsed Eddy current

A Pulsed Eddy Current system usually consists of four main parts which are; function generator, probes, preamplifiers and an analog-to-digital converter (A/D). The function generator creates a square wave which excites the probe. Probe excitation produces an electromagnetic field that affects the conductive surface and induces a current on the surface called an eddy current. This eddy current generates an electromagnetic field which penetrates the metal bulk. The electromagnetic responses of the eddy current electromagnetic field contain information describing features of inner structures. Its amplitude is related to type of material, metal thickness, defects and cracks that exist in the material. The electromagnetic response is received by another probe. This Pick-Up probe absorbs two types of electromagnetic fields; the electromagnetic field from the driver probe and the eddy current's electromagnetic response. The directions of these fields are inversed. The pick-up probe receives a differential field. Figure 3.4 is a schematic of the pulsed eddy current effect and its detection in a double-layer structure.

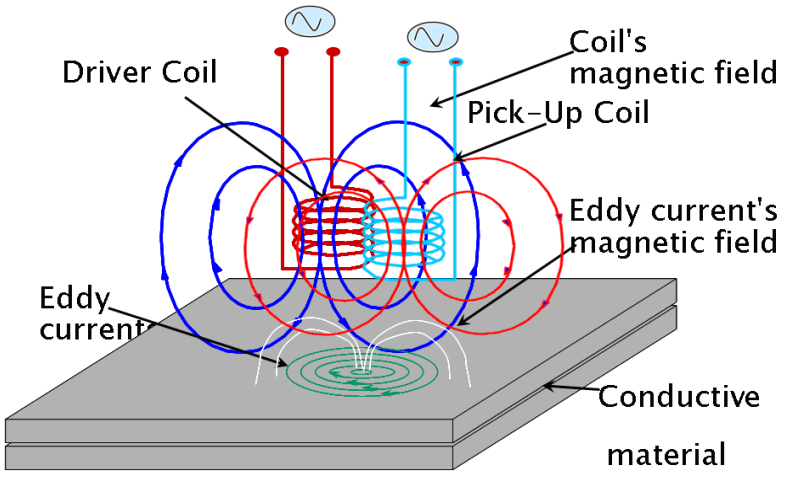

Figure 3.4 Schematic of pulsed eddy current for defect detection in double layer system.

3.3.2 Time-frequency analysis

Common results of the pulsed eddy current technique provide a set of data in the time domain. Noise sources (less amounts of defects, lift-off and interlayer gap), cause close and noisy curves in this domain. It is important to use alternative methods for multilayer structures when

defects and corrosion occur on the surfaces. The frequency contents of signals is determined by Fourier transform but any further information about the time at which each frequency component takes place cannot be provided by Fourier transform. To overcome this shortcoming, Time-Frequency distributions can be applied. Time-Frequency analysis methods provide three-dimensional representations of signals (time, frequency and amplitude) to detect defects with higher accuracy. In this paper, a Rihaczek distribution is applied in a time-frequency analysis method to present the data in three dimensions.

During our studies, different types of time-frequency analysis methods were implemented and applied. The Rihaczek distribution provides best results of three-dimensional representation and also the most clear defect separation during training of classification. Using the real part of energy is the main advantage of the Rihaczek Distribution over other time-frequency analysis methods, due to the fact that many time-frequency analysis approaches such as the Wigner-Ville distribution abandon any sort of analogy to physical phenomena with negative values for energy. In the Rihaczek distribution, the complex energy density overcomes the missing phenomena by using the real part of energy. The presence of cross-terms in time-frequency analysis results reduces the efficiency of signal processing. A Kernel function is applied to the Rihaczek distribution to act as a local filter and also to reduce cross-term effects. Therefore the cross-term effect in Rihaczek distribution images is less than Wigner-Ville distribution images and other time-frequency analysis methods.

3.3.2.1 Rihaczek Distribution

In Time-Frequency Analysis, the Rihaczek distribution allows the energy of a complex deterministic signal over finite range of time and frequency to become infinitesimal. The obtained result is called a complex energy distribution. The interaction energy between a signal **x** restricted to an infinitesimal interval δ_t centered on *t*, where **x** passes through an infinitesimal band pass filter δ_f centered on **v**, can be approximated by the following expression:

$$\delta_t \delta_f [x(t) X^*(v) e^{-j2\pi vt}]. \qquad (3.1)$$

Equation 3.1 leads to the following definition of the quantity of energy density function;

$$R_z(t,v) = x(t)X^*(v)e^{-j2\pi vt} \tag{3.2}$$

The Rihaczek distribution can be interpreted as a complex energy density at point (t,v) with elements of Cohen's class written as $f(v,\tau) = e^{j-2\pi v\tau}$.

The Rihaczek distribution is a bilinear time–frequency distribution (TFD) and is a member of Cohen's class. It is covariant to shifts in time and frequency. In this paper, a Rihaczek distribution is used for discrete-time, non-stationary, harmonizable, zero-mean-time series Pulsed eddy current signals.

Many of Time-Frequency analysis methods abandon any sort of analogue to physical phenomena with negative and complex values. Complex energy density in the Rihaczek distribution overcomes the problem of missing phenomena by using only the real part of the energy and trends the energy to the standard and real amount.

3.3.3 Feature Extraction and Classification

Time-frequency methods provide very large amounts of data and it is necessary to remove redundant data and reduce the dimensions of the data. Principal component analysis (PCA) is a method that creates new features and reduces the size of data.

3.3.3.1 Principal Component Analysis (PCA)

Principal Component Analysis (PCA) is also known as the Karhunen Loeve (KL) transform or the Hotelling transform. It is based on factorization techniques developed in linear algebra. PCA uses factorization to transform data according to statistical properties to optimize and reduce the amount of redundant data. This data transformation is particularly useful for classification and compression. The main advantage of PCA is generation of independent features.

In PCA processing, covariance of input data ($\mathbf{\Sigma_X}$) is calculated:

$$\Sigma_x = E\{(x-\mu_x)(x-\mu_x)^T\}. \tag{3.3}$$

Eigenvalues λ and Eigenvectors $\mathbf{W}_i$ are identified using covariance of the time-frequency results $\mathbf{\Sigma_X}$.

$$(\lambda I - \Sigma_x) = 0\,. \tag{3.4}$$

$$(\lambda I - \Sigma_x) W_i = 0\,. \tag{3.5}$$

Where, I is an identifier matrix of the same order as $\Sigma_{\mathbf{X}}$. Transform features $\mathbf{C_Y}$ are obtained using

$\mathbf{C_X . W^T}$. The new features are linearly independent.

3.3.3.2 K-Means Clustering and Expectation-Maximization Algorithm (EM)

K-means is one of the unsupervised learning algorithms that solves the clustering problem. The K-means algorithm is based on the use of squared Euclidean distance as the measure of dissimilarity between a data point and a prototype vector. K-means separates **n** observations into **K** clusters, for which each observation (data point) belongs to the cluster with the nearest mean. The K-mean algorithm consists of two major parts; (1) review all the data and reassign data to the closest selected centers (centroid), (2) make a loop and recalculate the center points to find the nearest centroids. The K-mean algorithm partitions a set of **n** observations (x_1, x_2, ... ,x_n) into **k** clusters S=[S_1,S_2, … , S_k] to minimize the square error function;

$$\arg\min \sum_{i=1}^{k} \sum_{x_j \in S_i} \left| x_j - \mu_i \right|. \tag{3.6}$$

where; μ_i is the mean of S_i.

The Expectation-Maximization (**EM**) algorithm is a powerful probabilistic classifier method for finding the maximum likelihood solution parameters for unobserved latent variables **S**. A set of **n** observations and a vector of unknown parameters **θ** are used to calculate the maximum likelihood.

$$L(\theta, n) = p(n|\theta) = \sum_{S} p(n, S|\theta)\,. \tag{3.7}$$

EM is an iterative method which alternates between performing an expectation **E** step and a maximization **M** step. The **E** step computes the expectation of the log-likelihood and evaluated responsibilities (posterior probabilities) for the latent variables.

$$Q\left(\theta\middle|\theta^{(t)}\right)=E_{S\middle|n,\theta^{(t)}}\left[\log L\left(\theta;n,S\right)\right]. \tag{3.8}$$

The **M** step (Maximization) re-estimates parameters (means, covariance and coefficients). The expected log-likelihood is achieved in the **E** step.

$$\theta^{(t+1)}=\arg_{\theta}\max Q\left(\theta\middle|\theta^{(t)}\right). \tag{3.9}$$

3.4 Results and Discussion

3.4.1 Time Domain Signals

A 1 KHz pulse was used to excite the probe and the response signals were digitized. Figure 3.5 shows the detected pulse response for defects ranging from 30 to 250 μm respectively for each layer.

The amplitude of the response signals increases as the thickness of the defects increase, i.e., the 30 μm sample has a minimum amplitude whereas the 250 μm defect sample has maximum amplitude. At each location of the defects on the same layers, an increase in the thickness of the defect (metal loss depth) causes a decrease in eddy current field. The directions of electromagnetic fields which are absorbed by pick-up coil are reverse. Amount of electromagnetic field from driver's coil is constant and eddy current electromagnetic field varies by changing the size of defects. Therefore the pick-up coil (probe) receives more electromagnetic field from defect with larger amount of metal losses.

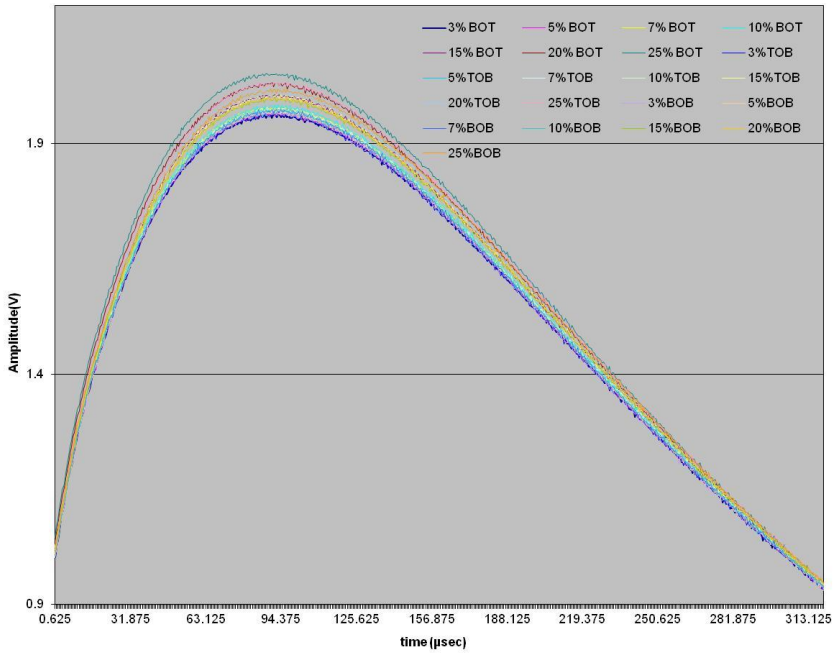

Figure 3.5 Pulsed Eddy Current results from seven different depths (metal-loss defects) placed in three positions.

In Figure 3.5, acquired signals from three positions with different amounts are presented. These signals contain information from surfaces between layers and under layers. The signals are from defects placed on the bottom of the bottom layer (BOB), the top of the bottom layer (TOB) and the bottom of the top layer (BOT) at 30µm, 50µm, 70µm, 100µm, 150µm, 200µm and 250µm depths on each surface. Acquired signals are too closed. The signals are subtracted against reference signal which come from double layer without defects to show the metal losses variations clearly.

Figure 3.6 shows the results of subtraction between the reference signal (double layer without defects) and a defected surface in a different layer ((a) bottom of top layer, (b) top of bottom layer and (c) bottom of bottom layer). It can be observed that the response signals for 3% to 10% are too close.

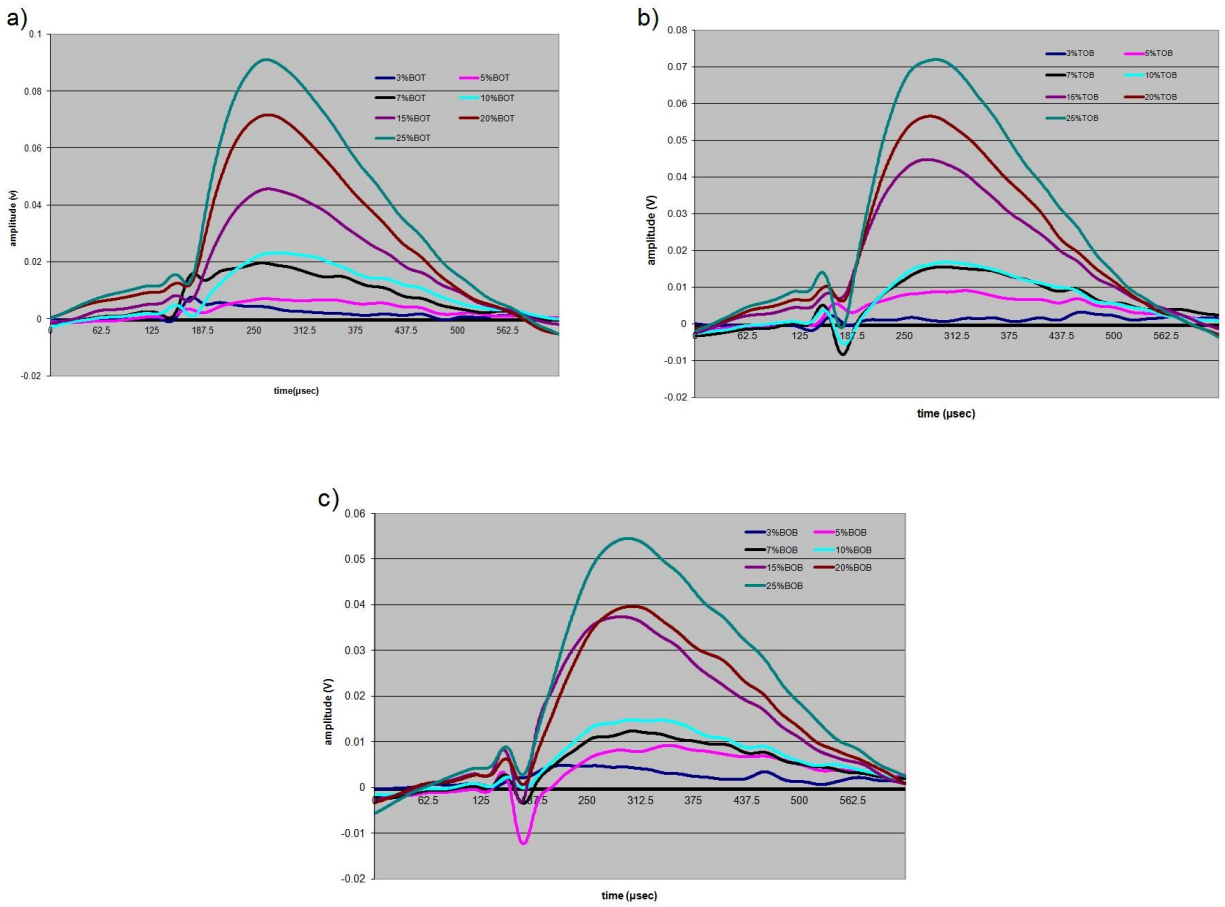

Figure 3.6 Subtraction result of defects with different metal loss. (a) Bottom of Top layer (BOT). (b) Top of Bottom layer (TOB). (c) Bottom of Bottom layer (BOB).

These time-domain signals consist of data from interior layers, but the fact that the curves are so close causes difficulty in extracting reliable information from them. In this case, time-frequency methods are applied to create three dimensions for representation of data.

A-Scan signals in the vertical direction are enhanced from each defected sample case (30μm to 250μm). Results of each sample case were acquired using 5-times detection (in total 105 signals). By repeating the signal acquisition from defected samples, results show that the acquired-subtracted signals from low size defects are not noise and they have repeatative behavior.

3.4.2 Time-Frequency Analysis

The results of Time-Frequency Analysis are the Rihaczek Distribution of Pulsed Eddy Current signals. The output of Time-Frequency Analysis for each Pulsed Eddy Current signal is a n×n matrix and represent by an image. The Time-Frequency Analysis method provides a three-dimensional representation of a signal and allows detection of the size and location of defects in a double-layer system due to close-amount defects and noise resources such as interlayer gap and probe lift-off. Figures 3.7, 3.8 and 3.9 show time-frequency representations of samples with defects located in the bottom-of-bottom layer, top-of-bottom layer and bottom-of-top layer respectively. Deeper defects cause increased penetration of eddy current magnetic fields and the probe receives more eddy current electromagnetic field. This effect causes a decrease in the amplitude of deeper defects.

Figure 3.7 shows the time-frequency analysis output for defected samples placed on the bottom-of-bottom layer (BOB). Defects were 3% to 25% of the thickness, respectively 30 micrometers to 250 micrometers. Figure 3.7(a) shows Rihaczek distribution of defected sample with 3% metal loss and figures 3.7(b), 3.7(c), 3.7(d), 3.7(e), 3.7(f) and 3.7(g) belong to synthetic defects with 5%, 7%, 10%, 15%, 20% and 25% metal losses respectively.

Increasing the depth of metal loss caused a shift in intensity from a narrow to wide state. In cases of more metal loss where depth of defects increase, the intensity magnifies, which shows that the strength of the eddy current magnetic field decreases at the top of the defected surfaces.

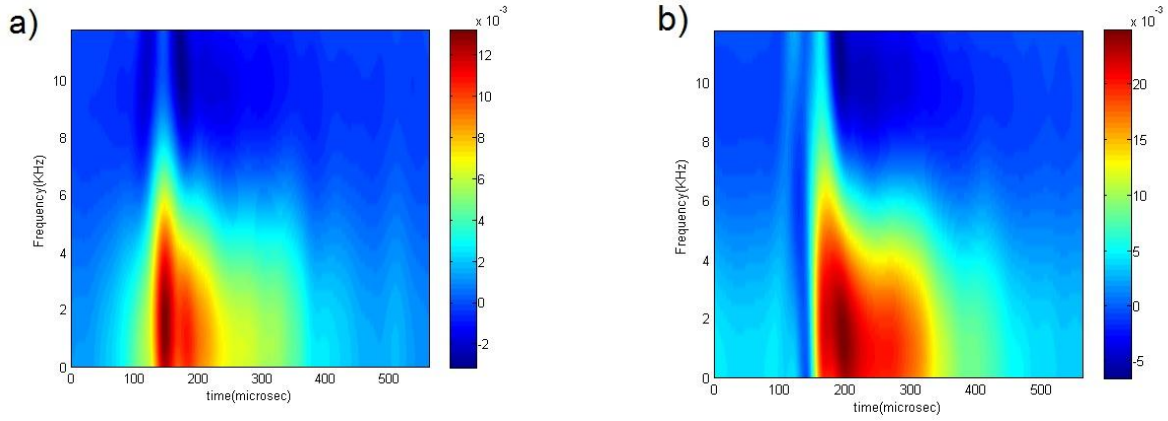

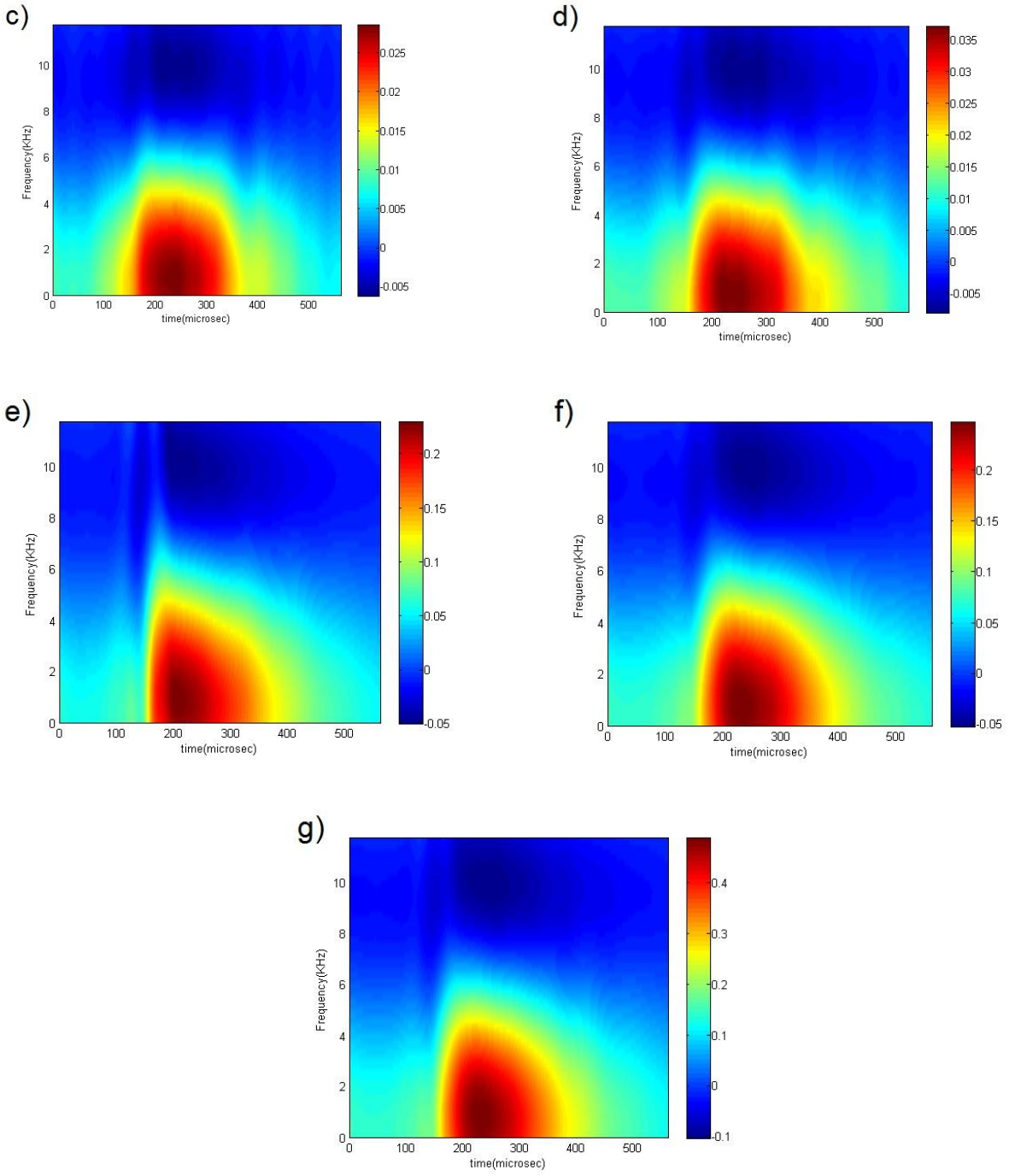

Figure 3.7 Time-Frequency results from defects placed on Bottom of Bottom (BOB) surface. (a) 3% metal loss. (b) 5% metal loss. (c) 7% metal loss. (d) 10% metal loss. (e) 15% metal loss. (f) 20% metal loss. (g) 25% metal loss.

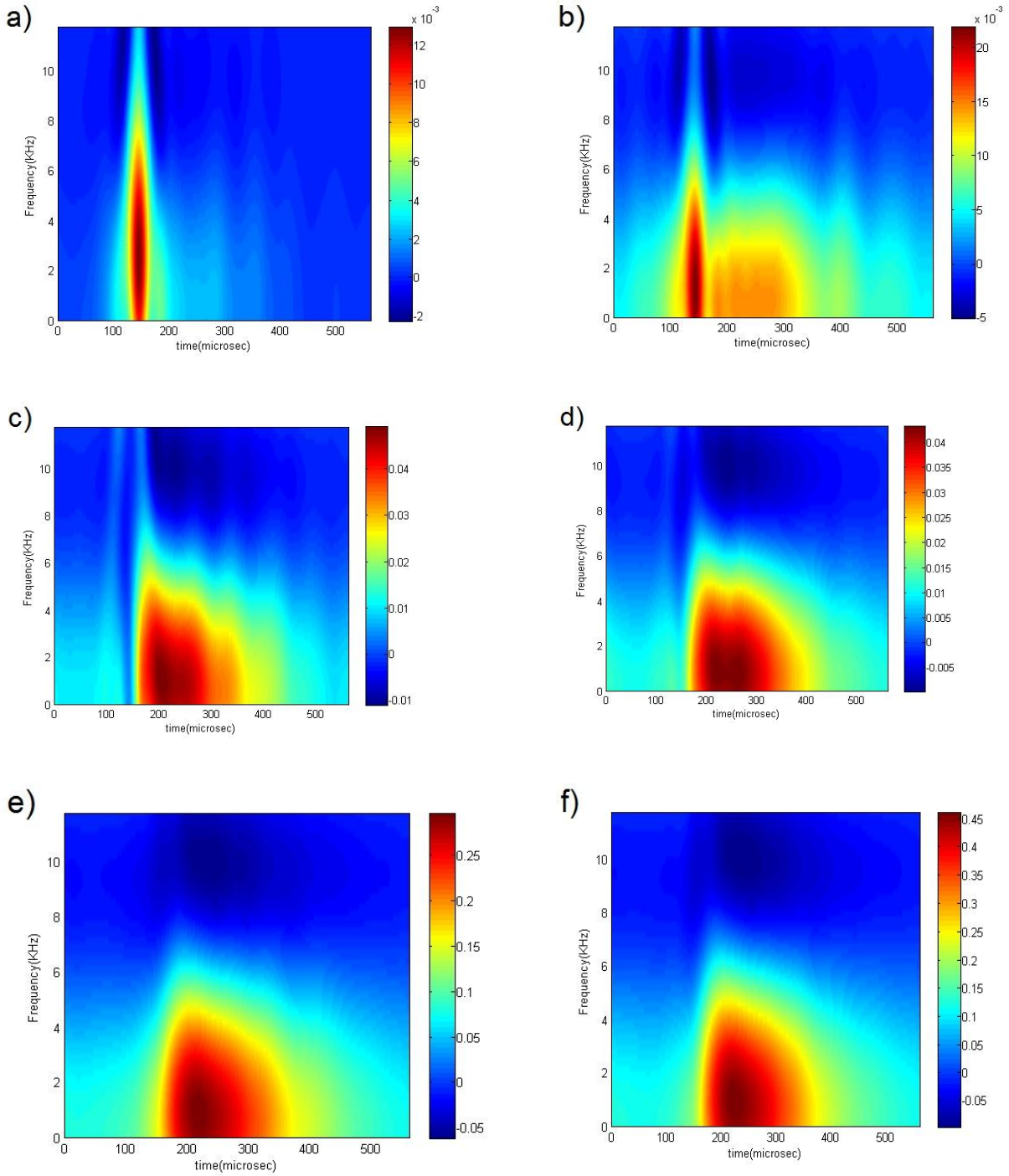
a)
b)
c)
d)
e)
f)
Frequency(KHz)
time(microsec)
x 10^-3

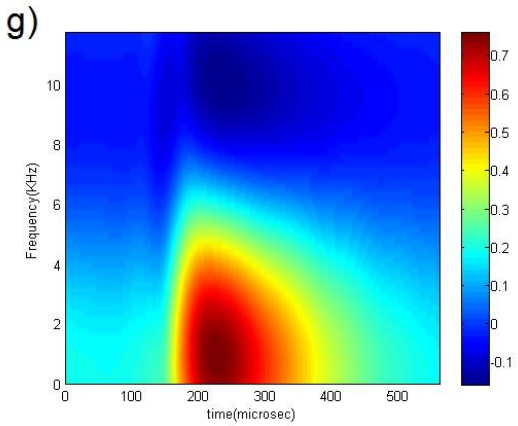

Figure 3.8 Time-Frequency results from defects placed on the Top of Bottom (TOB). (a) 3% metal loss. (b) 5% metal loss. (c) 7% metal loss. (d) 10% metal loss. (e) 15% metal loss. (f) 20% metal loss. (g) 25% metal loss.

Figures 3.8 and 3.9 show the time-frequency output for top-of-bottom and bottom-of-top layers with same-size metal losses in each layer from 3% to 25% of the metal thickness. . Figure 3.8(a) shows Rihaczek distribution of defected sample with 3% metal loss and figures 3.8(b), 3.8(c), 3.8(d), 3.8(e), 3.8(f) and 3.8(g) belong to synthetic defects with 5%, 7%, 10%, 15%, 20% and 25% metal losses respectively. . Figure 3.9(a) shows Rihaczek distribution of defected sample with 3% metal loss and figures 3.9(b), 3.9(c), 3.9(d), 3.9(e), 3.9(f) and 3.9(g) belong to synthetic defects with 5%, 7%, 10%, 15%, 20% and 25% metal losses respectively.

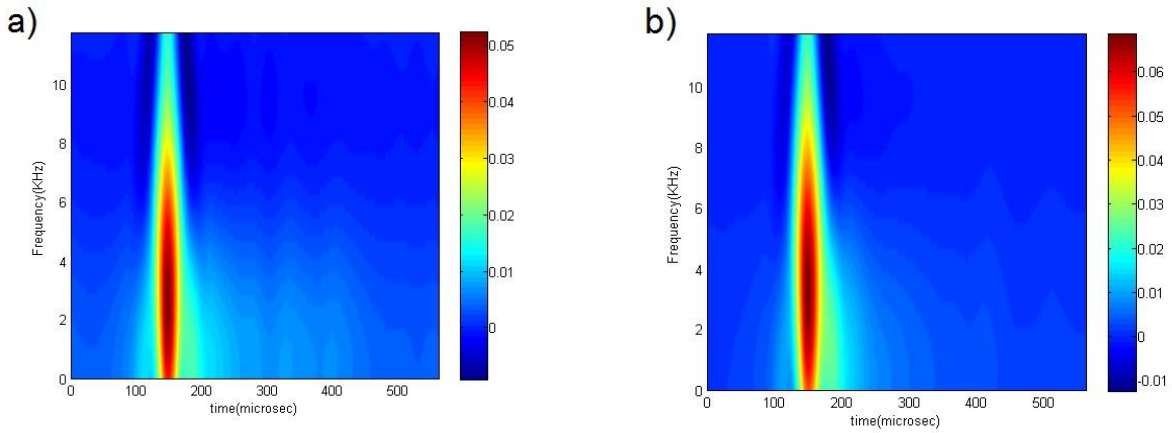

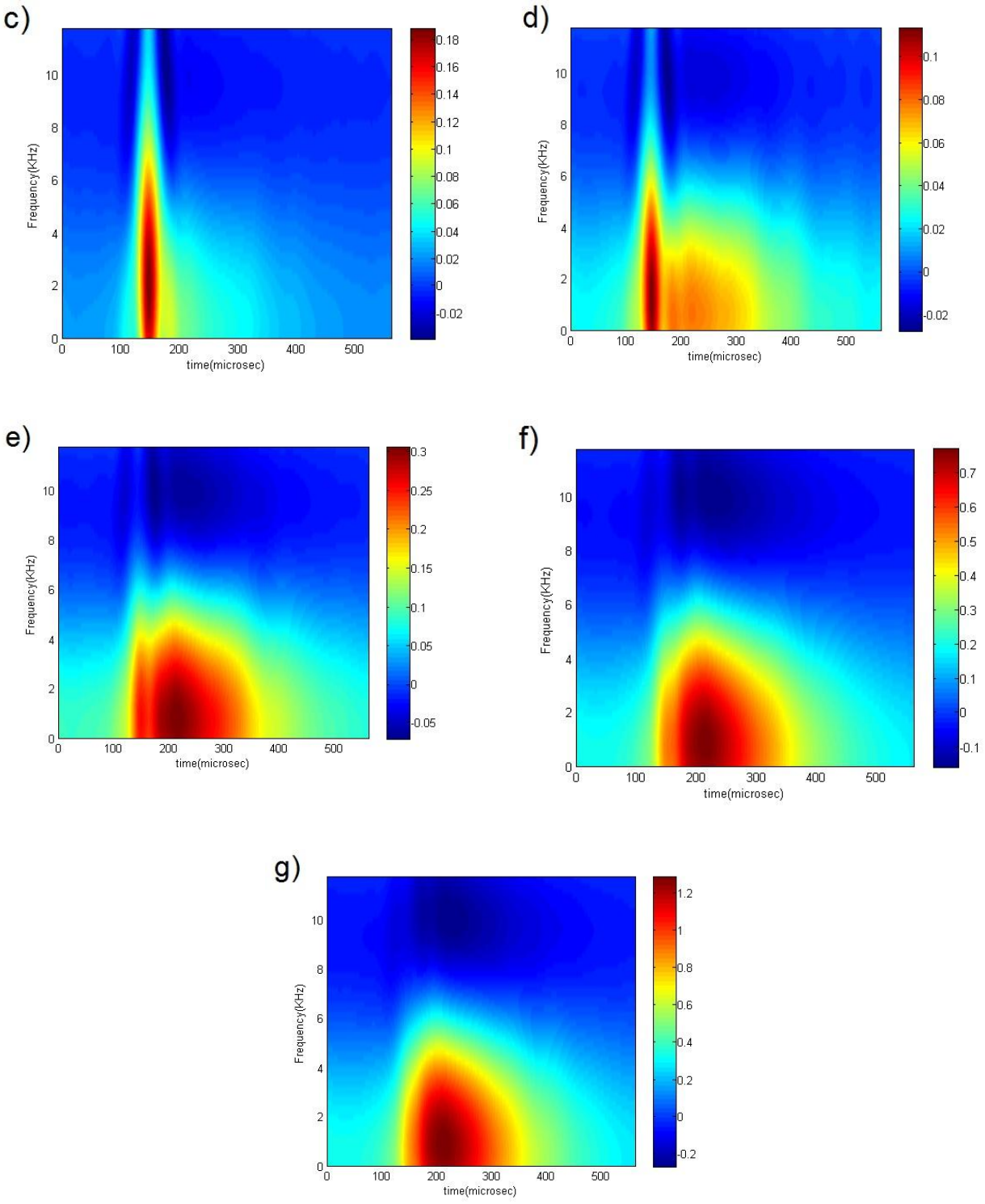

Figure 3.9 Time-Frequency results from defects placed on Bottom of Top (BOT) surface. (a) 3% metal loss. (b) 5% metal loss. (c) 7% metal loss. (d) 10% metal loss. (e) 15% metal loss. (f) 20% metal loss. (g) 25% metal loss.

The comparison between same size metal losses that placed in different depth from surface show some critical key that used in feature extraction and classification which are place of the peaks, shapes of the peaks and maximum amplitude of the peaks. Results of time-frequency analysis show when the defects are closer to surface, they have narrower shape against the same size defects that placed in deeper from surfaces. In other hand, maximum intensity of the defects that are closer to surface is more than the same size defects that placed deeper from surface.

Increasing the thickness of the defect in each surface layer causes an increase in the intensity and size of the response signal. In each defected layer, there is a narrow intensity in the range of 130 μsec and this can be used as a visual specification for defects of less than 5% metal loss. Increasing the depth of defects causes a shift along the time axis. For example, for 5% defects the time of the peak is 130 μsec, but in the case of a 25% defect, a wide peak is observed at 220 μsec. The amplitude and shape (narrow or wide, extended in time axis or both, place of the peak) of the peaks defines the location and size of the defect. They are therefore used as key features during feature extraction and classification.

For each layer, feature extraction and classification were applied to 5 defect ranges: 0-5%, 5-10%, 10-15%, 15-20% and 20-25%.

3.4.3 Feature extraction and classification

The output of Time-Frequency Analysis for each Pulsed Eddy Current signal is an n×n matrix which is represented by an image. The matrix is expressed as n^2 dimensional vectors. The value of each vector corresponds to intensity of each pixel of the Time-Frequency Analysis image. The image contains a large amount of redundant data. Principal Component Analysis (PCA) is applied for feature extraction to reduce the number of parameters and also to improve computational efficiency of the classifier.

PCA computes Eigenvalues and Eigenvectors of the covariance matrix. Eigenvectors are arranged in order of largest Eigenvalues. The first Eigenvector has the direction of largest variance of data and it determines the direction of the most significant amount of energy. Principal Component Analysis retains the significant features (Eigenvectors with largest Eigenvalues) and leaves out some less expressive features. In this way, PCA reduces the number of parameters without loss of significant information.

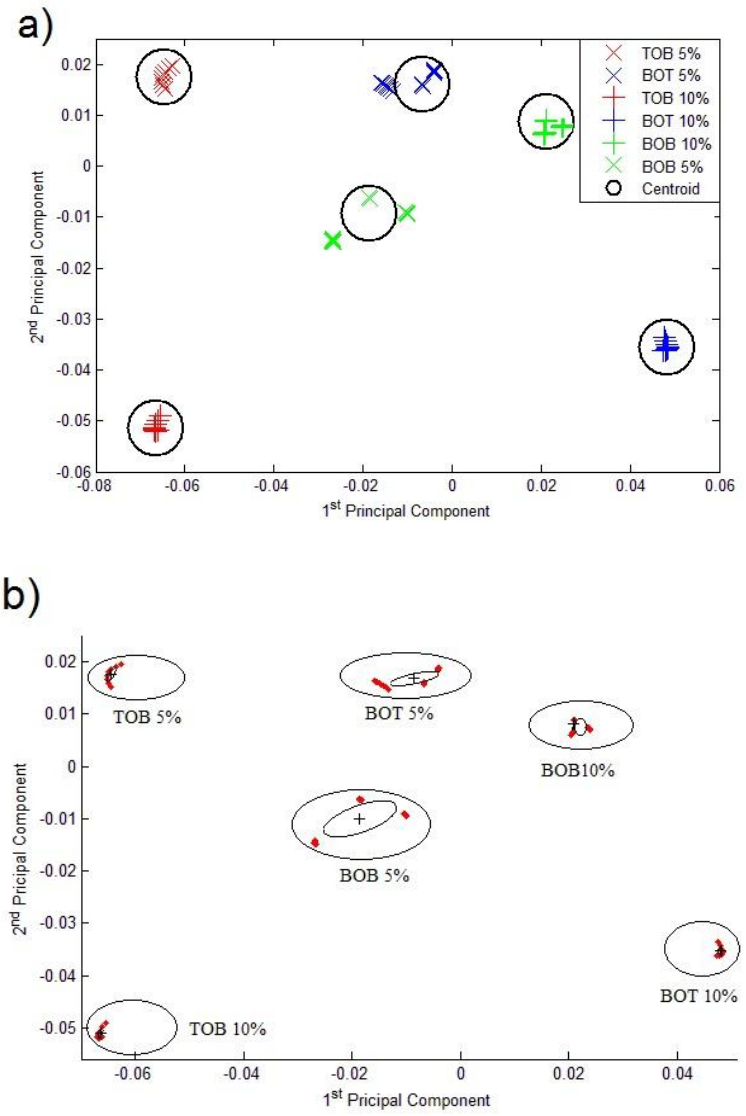

Figure 3.10 Classification of PCA output for defects less than 10% and 10% of thickness metal loss in three different positions (BOB, TOB and BOT). (a) k-mean clustering. (b) EM.

These new features were used as input data for classification. In our research, a group of the 3 largest Eigenvalues was selected for each class. In this study, results of first and second largest eigenvalues are presented by classifiers. Misclassification error is critical factor for each classification method. In this article, K-mean clustering and Expectation-Maximization have minimum misclassification error compared to other methods of classification. The amounts of misclassification error are calculated by inspecting new points and measuring the size of metal losses and then comparing with reference patterns which are used as a map and data base in classifiers. The misclassification errors of K-mean clustering and EM algorithms are calculated

and the values of these errors are 3.11% and 1.78% respectively. The final results of classification using K-means clustering and Expectation- Maximization (EM) based on PCA output data for fewer than 10% and more than 10% are shown in Figures 3.10 and 3.11. In Figure 3.10, PCA output data are classified for samples with defect depths ranging from 30 to 100 micrometers where defects are placed on bottom of bottom (BOB), top of bottom (TOB) and bottom of top layers (BOT). Classification results are represented in 2-D where the first and second principal component have been chosen as the first and second dimensions of the data representation. In Figure 3.10, six separate clusters exist. These clusters belong to less than 5% metal loss and 5-10% metal loss in each layer. Results of 0-5% metal loss and 5-10% metal loss on the bottom of bottom layer are too close but can be separated by classifiers. Figure 3.10(a) and 3.10(b) show a map of classification for K-Means Clustering and EM algorithms respectively. Each circle (Fig. 3.10(a)) belongs to each defected sample (0-5% metal loss or 5-10% metal loss) in three different layers. Defect distribution shows that low-size defects on the deep layer (BOB) are placed in the middle of the diagram. The defects which are placed on BOT and TOB are far from the center of the diagram. These effects depend on time frequency analysis results.

In Figure 3.11, PCA output data are classified for samples with defect depths ranging from over 100 to 250 micrometers where defects are placed on the bottom of bottom (BOB), top of bottom (TOB) and bottom of top layers (BOT). Figure 3.11(a) and 3.11(b) show maps of classification for K-Means Clustering and EM algorithms respectively. The results of the EM algorithm and K-means clustering are similar.

For comparison, it is necessary to calculate the Euclidian distance of each unknown test point with each centroid to define minimum distance. The minimum distance of each unknown sample defines the cluster group in which the defected sample belongs.

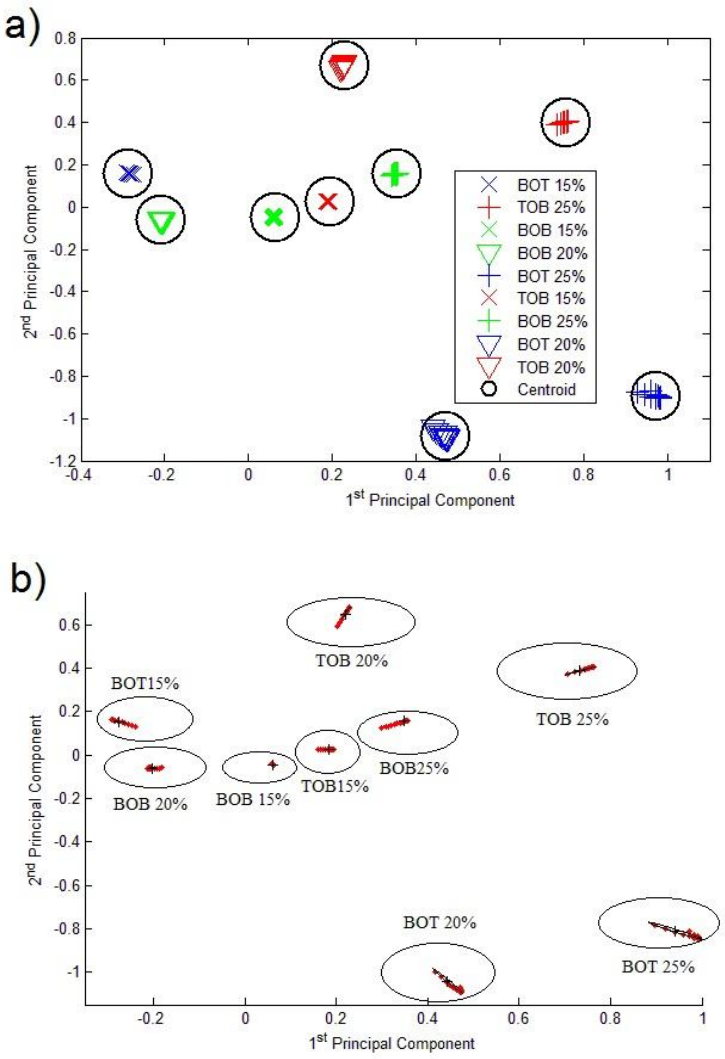

Figure 3.11 Classification of PCA output for defects with more than 10% of thickness metal loss in three different positions (BOB, TOB and BOT). (a) k-mean clustering. (b) EM.

3.5 Conclusion

This paper reports the applicability of the time-frequency analysis method to treat pulsed eddy current data to detect corrosion defects at different depths in different positions in a multi-layer structure. Corrosion is a varied and complex phenomenon and metal loss on surfaces and between layers changes quickly. In many aspects, pulsed eddy current's time domain signals are not able to show variation of metal losses on surfaces and cannot separate them correctly. In our approach, we convert PEC data from time domain to time-frequency domain and analyze the data in an enhanced form to detect defects of different sizes in each layer. Maximum variances of

PCA were selected as features and a classifier was used to separate and classify these new features.

The time-frequency method is a valuable tool to treat PEC data and is capable of detecting defects (such corrosion and cracks) in aluminum multi-layer systems when the size variation of the defect is approximately 30μm. In this study, defects were detected from 30μm and they were classified in range of 50μm. This classification can be improved to detect defects in range of 30μm. This method can be used in aircraft industry applications to detect corrosion and metal loss in double-layer and multi-layer structures. In future studies, other time-frequency analysis methods will be used to compare the precision and reliability of the signal processing method when applied to overlap corrosion and defect detection in an aluminum multi-layer.

Acknowledgment

This research was supported by the collaborative research and development grant (No. CRDPJ-335472-05) of Natural Sciences and Engineering Research Council of Canada (NSERC), Pratt & Whitney Canada, Bombardier Aeronautics and National Research Council of Canada (NRC).

References

[1] Moulder JC, Bieber JA, Ward Iii WW, Rose JH. Scanned pulsed eddy current instrument for nondestructive inspection of aging aircraft. Proceedings of SPIE - The International Society for Optical Engineering 1996;2945:2-13.

[2] Sophian A, Tian GY, Taylor D, Rudlin J. Electromagnetic and eddy current NDT: A review. Insight: Non-Destructive Testing and Condition Monitoring 2001;43:302-6.

[3] Tian GY, Sophian A, Taylor D, Rudlin J. Multiple sensors on pulsed eddy-current detection for 3-D subsurface crack assessment. IEEE Sensors Journal 2005;5:90-6.

[4] Chen T, Tian GY, Sophian A, Que PW. Feature extraction and selection for defect classification of pulsed eddy current NDT. NDT & E International 2008;41:467-76.

[5] He Y, Luo F, Pan M, Hu X, Liu B, et al. Defect edge identification with rectangular pulsed eddy current sensor based on transient response signals. NDT & E International 2010;43:409-15.

[6] He Y, Luo F, Pan M, Weng F, Hu X, et al. Pulsed eddy current technique for defect detection in aircraft riveted structures. NDT & E International 2010;43:176-81.

[7] Shu L, Songling H, Wei Z, Peng Y. Study of pulse eddy current probes detecting cracks extending in all directions. Sensors and Actuators, A: Physical 2008;141:13-9.

[8] Tian GY, Sophian A. Defect classification using a new feature for pulsed eddy current sensors. NDT & E International 2005;38:77-82.

[9] Sophian A, Tian GY, Taylor D, Rudlin J. Design of a pulsed eddy current sensor for detection of defects in aircraft lap-joints. Sensors and Actuators A: Physical 2002;101:92-8.

[10] Li Y, Tian GY, Simm A. Fast analytical modelling for pulsed eddy current evaluation. NDT & E International 2008;41:477-83.

[11] Huang C, Xinjun W, Zhiyuan X, Kang Y. Pulsed eddy current signal processing method for signal denoising in ferromagnetic plate testing. NDT and E International 2010;43:648-53.

[12] Tian GY, Li Y, Mandache C. Study of Lift-Off Invariance for Pulsed Eddy-Current Signals. IEEE Transactions on Magnetics 2009;45:184-91.

[13] Kim J, Yang G, Udpa L, Udpa S. Classification of pulsed eddy current GMR data on aircraft structures. NDT & E International 2010;43:141-4.

[14] Guang Y, Tamburrino A, Udpa L, Udpa SS, Zhiwei Z, et al. Pulsed Eddy-Current Based Giant Magnetoresistive System for the Inspection of Aircraft Structures. Magnetics, IEEE Transactions on 2010;46:910-7.

[15] Fan M, Huang P, Ye B, Hou D, Zhang G, et al. Analytical modeling for transient probe response in pulsed eddy current testing. NDT & E International 2009;42:376-83.

[16] Li S, Huang S, Zhao W. Development of differential probes in pulsed eddy current testing for noise suppression. Sensors and Actuators A (Physical) 2007;135:675-9.

[17] Safizadeh MS, Lepine BA, Forsyth DS, Fahr A. Time-frequency analysis of pulsed eddy current signals. Journal of Nondestructive Evaluation 2001;20:73-86.

[18] Safizadeh MS, Liu Z, Mandache C, Forsyth DS. Automated Pulsed Eddy Current Method for Detection and Classification of Hidden Corrosion. Proc Vth International Workshop, Advances in Signal Processing for Non Destructive Evaluation of Materials,. Quebec City, Canada; 2005, p. 75-84.

[19] Gigu, re S, Lepine BA, Dubois JMS. Pulsed eddy current technology: Characterizing material loss with gap and lift-off variations. Research in Nondestructive Evaluation 2001;13:119-29.

[20] Smith RA, Edgar D, Skramstad J, Buckley J. Enhanced Detection of Deep Corrosion Using Transient Eddy Currents. 7th Joint DoD/FAA/NASA Conference on Aging Aircraft,. New Orleans; 2003.

[21] Tian GY, Sophian A, Taylor D, Rudlin J. Pulsed eddy current system for dynamic inspection of defects. Insight-Non-Destructive Testing and Condition Monitoring 2004;46:256-9.

[22] Sophian A, Tian GY, Taylor D, Rudlin J. A feature extraction technique based on principal component analysis for pulsed Eddy current NDT. NDT and E International 2003;36:37-41.

[23] Zhou D, Tian GY, Zhang B, Morozov M, Wang H. Optimal features combination for pulsed eddy current NDT. Nondestructive Testing and Evaluation 2010;25:133-43.

CHAPITRE 4 OVERLAP METAL LOSS DETECTION USING PULSED EDDY CURRENT AND TIME-FREQUENCY ANALYSIS IN ALUMINUM DOUBLE-LAYER STRUCTURES. [2]

Saleh Hosseini

Section of Applied Mechanics, Department of Mechanical Engineering, École Polytechnique de Montréal, Montréal, Quebec, H3T1J4, Canada.

Aouni A. Lakis

Section of Applied Mechanics, Department of Mechanical Engineering, École Polytechnique de Montréal, Montréal, Quebec, H3T1J4, Canada.

Corresponding author;

Tel.: +1 514 340 4711 (4906)

Fax: +1 514 340 4076

Email: aouni.lakis@polymtl.ca

Abstract

The purpose of this paper is to present a novel approach using Pulsed Eddy Current (PEC) inspection to detect corrosion and metal losses in Aluminum double-layer structures where overlapping defects exist between layers. PEC signals are processed by Rihaczek distribution in a time-frequency analysis method to reveal more hidden data from time domain signals. The Rihaczek Distribution represents PEC signals in three dimensions. Principal component analysis extracts new features from treated data to provide input to a classifier. K-means clustering is applied to classify data and automatically determine metal loss distribution between layers.

Keywords: Multi-layer Aluminum Structures, Defects Overlapping, Pulsed Eddy Current, Rihaczek Distribution, Principal Component analysis, K-Means Clustering.

[2] This article was submitted to the journal of NDT&E

4.1 Introduction

Electromagnetic testing is a highly preferred method amongst all field-ready methods of non-destructive testing used for inspection and defect detection in metallic, layered structures found in avionic applications such as wings and fuselages [1, 2]. For corrosion detection in multi-layer structures, the Pulsed Eddy Current testing method has shown a powerful capacity as a reliable non-destructive testing method in the aircraft industry [3]. In contrast to conventional eddy current that use harmonic excitation at single frequency or several frequencies to study transient eddy current signals, the pulsed eddy current testing method applies square or sinusoidal shaped pulse excitation and the probe's driving coil is excited by repetitive broadband pulses. Transient excitation in a wide range of frequencies induces scattering eddy currents in the sample testing [4]. Consequently, eddy current signals bring out a large amount of information describing parameters such as thickness and electromagnetic properties of the sample under test [5, 6]. The field at the surface of the sample test is measured with a sensor that may be composed of different types of probes such as the Hall probe [7, 8], a giant magneto resistive sensor (GMR) [9, 10] and a differential probe [4, 11]. Pulsed eddy current excitation provides a broadband spectrum of frequencies (up to 100KHz or even more) [6] and possesses many advantages compared to single or multi-frequency testing methods, including higher anti-interference robustness and richer information from the depth of the sample [9]. The defects that are closer to the surface excite the pickup coil earlier than defects positioned more deeply. Therefore, a time domain signal can represent the pulsed eddy current response according to the distance of defects from the surface [8].

Measurement of metal losses with high accuracy and reliability in single-layer and multi-layer structures is a major challenge in the field of pulsed eddy current testing. The Pulsed eddy current signal is represented in the time domain using a series of voltage-time data. Amplitude, time-to-zero crossing and time-to-peak are the most common features in analysis of pulsed eddy current signals in the time domain [12, 13]. These features are used to characterize and detect corrosion and metal losses on surfaces in multi-layer structures. Rising time is another feature that has been applied to detect metal losses in single-layer systems [8]. Time-domain features are not sensitive enough in presence of lower amounts of metal loss and overlap defects exist on surfaces in multi-layer structures. These parameters are also fragile in the presence of noise

sources such as interlayer gaps due to corrosion pillowing and changes in coating thickness as well as variation of probe lift-off [14]. Time-Frequency analysis of pulsed eddy current signals provides three-dimensional representations of signals which can be considered as distributions of signal energy in both time and frequency [15, 16].

In a previous study, application of time-frequency analysis and its advantages for defect and metal loss detection in an aluminum double-layer structure with synthetic defects placed on the bottom and top of each layer with 5% accuracy of metal loss and plate thickness has been discussed. The main purpose of this article is detection and estimation of the location and amount of corrosion and metal losses where overlapping defects exist in a double-layer system. Figure 4.1 presents a schematic of the sample used in both the previous and current study. In this paper, pulsed eddy current signals are processed by the Rihaczek distribution as part of a time-frequency analysis method to reveal hidden information in time-domain signals. Two groups of case studies are considered. In the first case study, the size of the metal loss is 200μm and the defects exist in 5 groups; 200μm metal loss on bottom of top (BOT), 150μm metal loss on BOT and 50μm on top of bottom (TOB), 100μm metal loss on BOT and 100μm on TOB, 50μm metal loss on BOT and 150μm on TOB and 200μm metal loss on TOB. In the second case, the amount of metal loss between layers is 150μm and the defects are in 4 groups; 150μm on BOT, 100μm on BOT and 50μm on TOB, 50μm on BOT and 100μm on TOB and 150μm on TOB. Principal component analysis (PCA) compresses the time-frequency data and provides new features for classifier. K-means Clustering is applied to classify the amount and location of corrosion in each case separately. The entire step provides a logical automatic method to detect defects in a double-layer system.

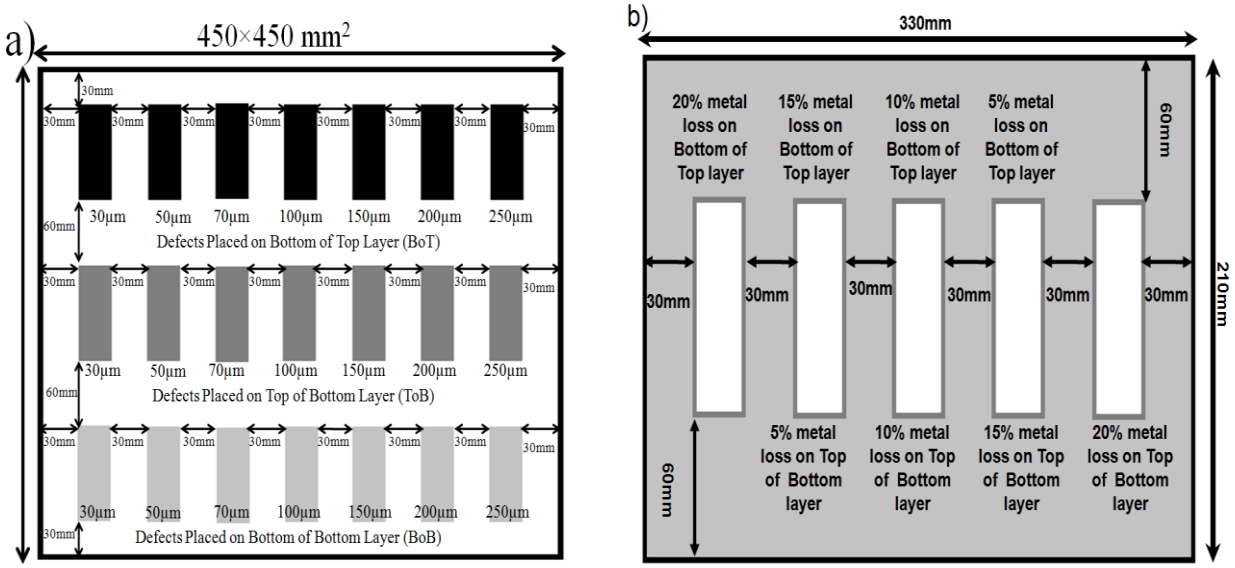

Figure 4.1 Schematic of the sampling under test. (a) Previous study. (b) Current study.

4.2 Experimental setup and specimen

The traditional Pulsed Eddy current system consists of a function generator (which creates a square voltage), a probe (either a reflection probe or dual probe) and an Analog-to-Digital converter (A/D). The designed system for this experiment has a function generator, reflection probe, preamplifier, digitizer converter card and a computer system with signal processing software.

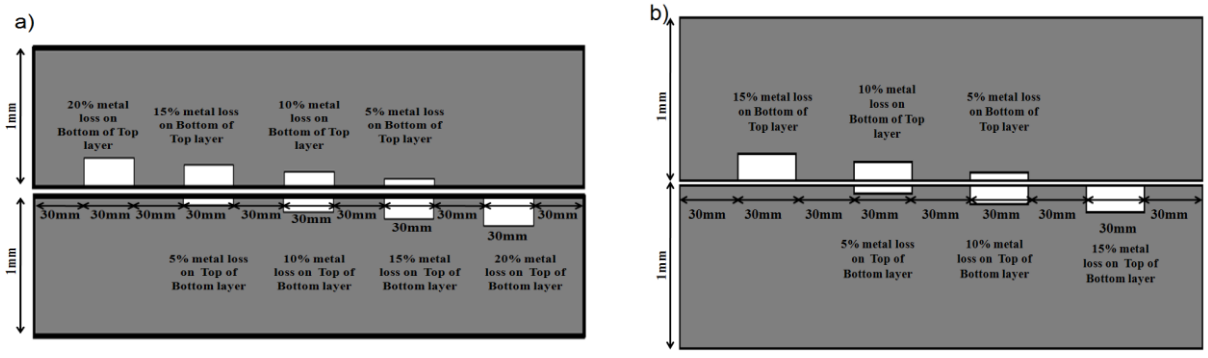

Figure 4.2 Schematic of the sample under test. (a) 200µm. (b) 150µm.

For this experiment, samples as shown in Figure 4.2 are used. The first sample is a double-layer composed of bare aluminum sheets for a total of 2.0 millimeter thickness and 330×210 mm^2

area (Fig. 4.2(a)). The second sample is also double-layer bare aluminum sheets at 2.0 millimeter thickness, this time at 270×210 mm^2 area (Fig. 4.2(b)). The thickness of each aluminum sheet is 1.0 millimeter. The thicknesses of synthetic defects in first sample are 5%, 10%, 15% and 20% of the plate thickness. The thicknesses of synthetic defects in second sample are 5%, 10% and 15% of the plate thickness. These synthetic defects were fabricated by laser machining with 1 micrometer tolerance. Each series of metal losses are placed on the bottom of top layer and top of bottom layer. The size of the defects is equal and the area of each is 30×90 mm^2. In this study, two cases of overlapping defects are simulated. In the first case, the summation of defects is 20% of single sheet thickness or 200μm. Defects are placed on top of each other. Bottom of top and top of bottom layers consist of 4 synthetic metal losses at 50μm, 100μm, 150μm and 200μm in each layer. Synthetic metal losses at 10% of the plate's thickness are placed together and a 15% metal loss is placed on top of a 5% metal loss. Synthetic defects at 20% metal loss in the top and bottom layers are placed on top of surfaces without defects on bottom and top layers respectively. In the second case, total defects in the overlap condition is 15% of single sheet thickness or 150μm. Defects are placed on top of each other. Bottom of top layer and top of bottom layer consist of 3 synthetic metal losses at 50μm, 100μm and 150μm in each layer. Synthetic metal losses at 10% metal loss are placed on top of 5% metal losses in top and bottom layers. Synthetic defects with 15% metal loss in the top and bottom layers are placed on top of surfaces without defects on bottom and top layers respectively.

The function generator excites the probe's driving coil with square pulses at 1 KHz and 4 volts. The probe's driving coil generates electromagnetic fields on the affected conductive surface. The second coil gathers the response of electromagnetic fields from the specimen and driving coil. The first coil has inner and outer diameters of 12 and 15 mm respectively. The second coil has inner and outer diameters of 7 and 11 mm. The response voltage is produced by the second coil and sent to the amplifier. The amplifier is a low-noise preamplifier and the power of the amplifier is 110V and 6 watts. The band pass filter is between 100Hz and 10 KHz and the amplifier's gain is fixed at 5-times amplification. NI digitizer (PCI-4070) and LabView software are used to convert the analogue signal to digital and store the signals on a PC. The sampling frequency of the card is 1.60 MS/sec with 23-bit resolution. Figure 5.3 presents the pulsed eddy current system used for the experiments described in this study.

Figure 4.3 Designed PEC system.

A digitizer converts analogue signals to digital signals. Digital signals are saved on a PC in text format. Each signal from a defected surface with different metal loss is then subtracted from a reference signal that belongs to a non-defected signal in the double-layer condition. Time-Frequency analysis is applied on the subtracted signals and converts the time-domain signal (two dimensions) to three-dimensional signals (time-frequency-amplitude). Principal Component Analysis (PCA) processes the time-frequency analysis results and provides the input to the classifiers. K-mean Clustering classifies the results to create a data bank and dictionary for metal losses in each case. Figure 5.4 presents a schematic of the detection process.

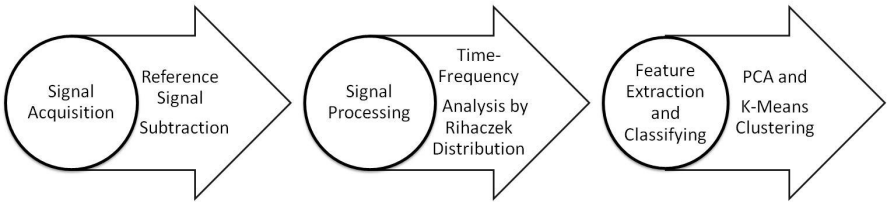

Figure 4.4 Diagram of the detection process.

4.3 Results and Discussion

4.3.1 Time Domain Signals

A 1.8 MHz analogue-to-digital conversion PCI is used for data acquisition. Figure 4.5 shows the voltage-time series detected pulsed eddy current response for overlapping defects with 15%

metal loss and 20% metal loss. The amplitude of the response signals increases as the distance of defects gets closer to the surface because by placing the synthetic defect far from surcease and probe, more eddy current magnetic field in induced in metallic structure and pick up coil absorb fewer amount of magnetic field (two type of magnetic fields are reverse); i.e., the 200μm metal loss on the bottom surface of the top layer has maximum amplitude whereas the 200μm metal loss on the top surface of the bottom layer has minimum amplitude. Therefore, in the case of overlapping defects with equal summation of metal loss, the defect with 150μm metal loss in the bottom of top layer and a 50μm metal loss in the top of bottom layer produces more amplitude than the defects with 50μm metal loss in the bottom of tap layer and 150μm metal loss in the top of bottom layer. For same-size defects in the double-layer system, a closer defect-to-surface distance causes a decrease in eddy current field and therefore the pick-up coil (probe) receives more electromagnetic field.

In Figure 4.5, acquired signals from two cases of overlapping defects with different amounts of metal loss are presented. These signals contain information from surfaces between layers. In Figure 4.5(a), the signals are from the defect with equal summation of metal losses from bottom of top layer (BOT) and top of bottom layer (TOB). The total size of the defects is 200μm. First and last defects have no overlapping condition and they are placed in the bottom of top layer and top of bottom layer respectively. Three types of metal loss are fabricated in the middle of the test sample with 150μm metal loss on BOT and 50μm on TOB, 100μm metal loss on BOT and 100μm on TOB and 50μm metal loss on BOT and 150μm on TOB. In Figure 4.5(b), the signals are from the defect with equal summation of metal losses (150μm) from the bottom of top layer (BOT) and top of bottom layer (TOB). The defects are placed on the surface between layers with 150μm on BOT, 100μm on BOT and 50μm on TOB, 50μm on BOT and 100μm on TOB and 150μm on TOB. The acquired signals match each other too closely. These signals are subtracted from the reference signal which comes from a double layer without defects to clearly show the variations in metal loss.

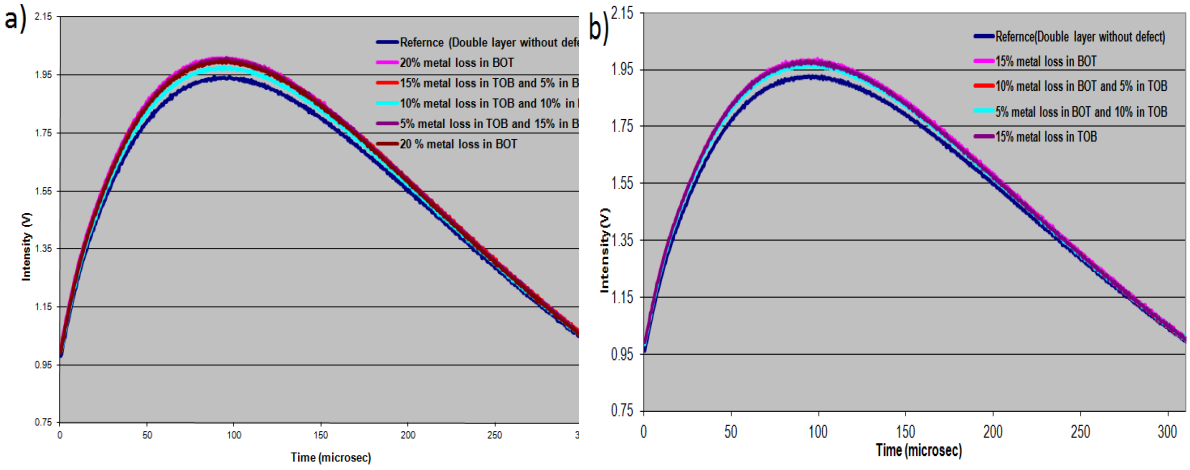

Figure 4.5 Pulsed Eddy Current results. (a) 200µm. (b) 150µm.

Figure 4.6 shows the results of subtraction between the reference signal (double layer without defects) and a defected surface between layers ((a) 200µm metal loss between top and bottom layer, (b) 150µm metal loss between top and bottom layer). It can be observed that the response signals for the two metal loss samples are too close and the rising time and cross time of the signals are almost an exact match. However, these features are clearly shown in time-frequency representation. As the amount of metal loss increases, the amplitude of the signals also increases. Also, as defects are located closer to the surface (same-size metal losses in single defects on surfaces and defects with overlap on surfaces), amplitudes increase. By applying Rihaczek distribution and considering place, shape and maximum amount of amplitude for each types of synthetic defect, these defects will be separated.

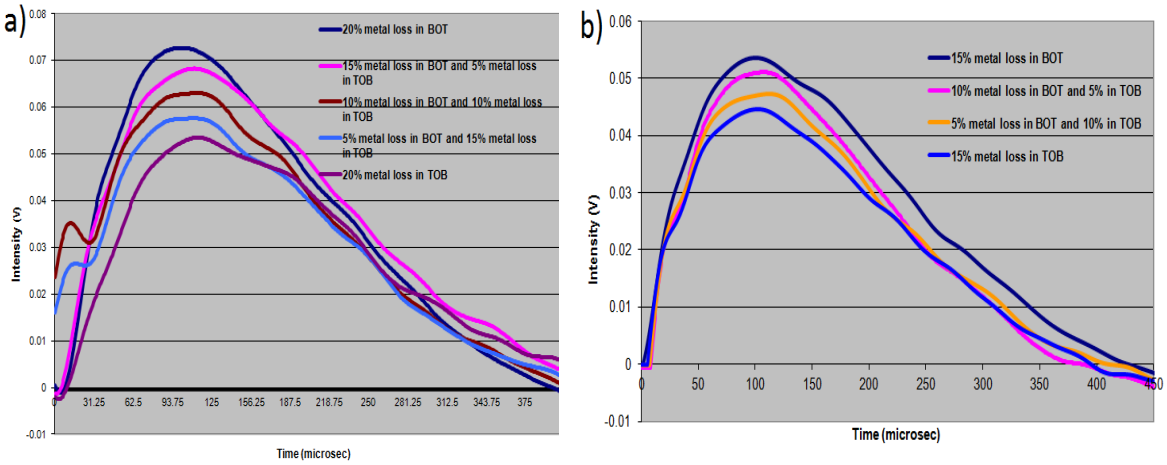

Figure 4.6 Subtraction result of defects in different situations of metal loss (a) 200µm. (b) 150µm.

These time-domain signals produce a voltage-time series consisting of data from between surfaces, but the fact that the features of the curves are so close causes difficulty in extracting reliable information from them. In this case, time-frequency methods are applied to create a three-dimensional representation of data. A-Scan signals in the vertical direction are enhanced from each defected sample case. The results of each sample case were acquired using 5-times detection (a total of 45 signals).

4.3.2 Time-Frequency Analysis

Time-Frequency analysis method is used as an alternative method for multi-layer structures when defects and corrosion occur on the surfaces to detect defects with higher accuracy and also reduce noise effects of the sample such as smaller defects, lift-off and interlayer gap. Several types of distributions of time-frequency have been implemented and applied for signal processing. The presence of cross terms and negative values causes a reduction in the efficiency of time-frequency distributions. In this paper, a Rihaczek distribution is applied as a Time-Frequency analysis method to provide three-dimensional representations of signals (time, frequency and amplitude). The main advantage of Rihaczek distribution over other time-frequency distributions is using the real part of the energy. The Rihaczek distribution prevents the need to abandon any sort of analogy to physical phenomena with negative values for energy. Additionally, a Kernel function is applied to the Rihaczek Distribution to reduce the effect of cross terms. The Rihaczek distribution is calculated using the following equation:

$$R_z(t, f) = x(t)X^*(f)e^{-j2\pi ft} \quad (4.1)$$

Energy density of a signal from Rihaczek distribution is provided by:

$$E = \iint R_z(t, f)\ dt\ df \quad (4.2)$$

The subtracted signals of pulsed eddy current are processed by Rihaczek Distribution in a Time-Frequency Analysis method. The pulsed eddy current signal data is stored in an n×n matrix, which is then represented by an image. Time, frequency and amplitude of the signals are combined to produce these three-dimensional representations that show the size and location of defects between layers in the double-layer system due to close defect variations between surfaces.

Figures 4.7 shows a time-frequency representation of a sample with defects located on top-of-bottom layer and bottom-of-top layer respectively with 200μm metal loss between the top and bottom layer. Defects which are located further down in the sample cause increased penetration of eddy current magnetic fields and the probe receives more eddy current electromagnetic field. This effect causes a decrease in the amplitude of these defects.

Comparison between same-size metal losses placed between layers at different distances below the surface reveals some critical key factors that can be used for feature extraction and classification. According to time-frequency analysis results, defects that are closer to the surface of the sample provide sharp peaks at higher amplitude. Maximum amplitude in defects positioned lower in the sample has a wide distribution in the time and frequency axis compared to defects placed closer to the surface. Therefore, increasing the distance from the surface to defects with same-size metal loss causes a shift in intensity from a narrow to wide state.

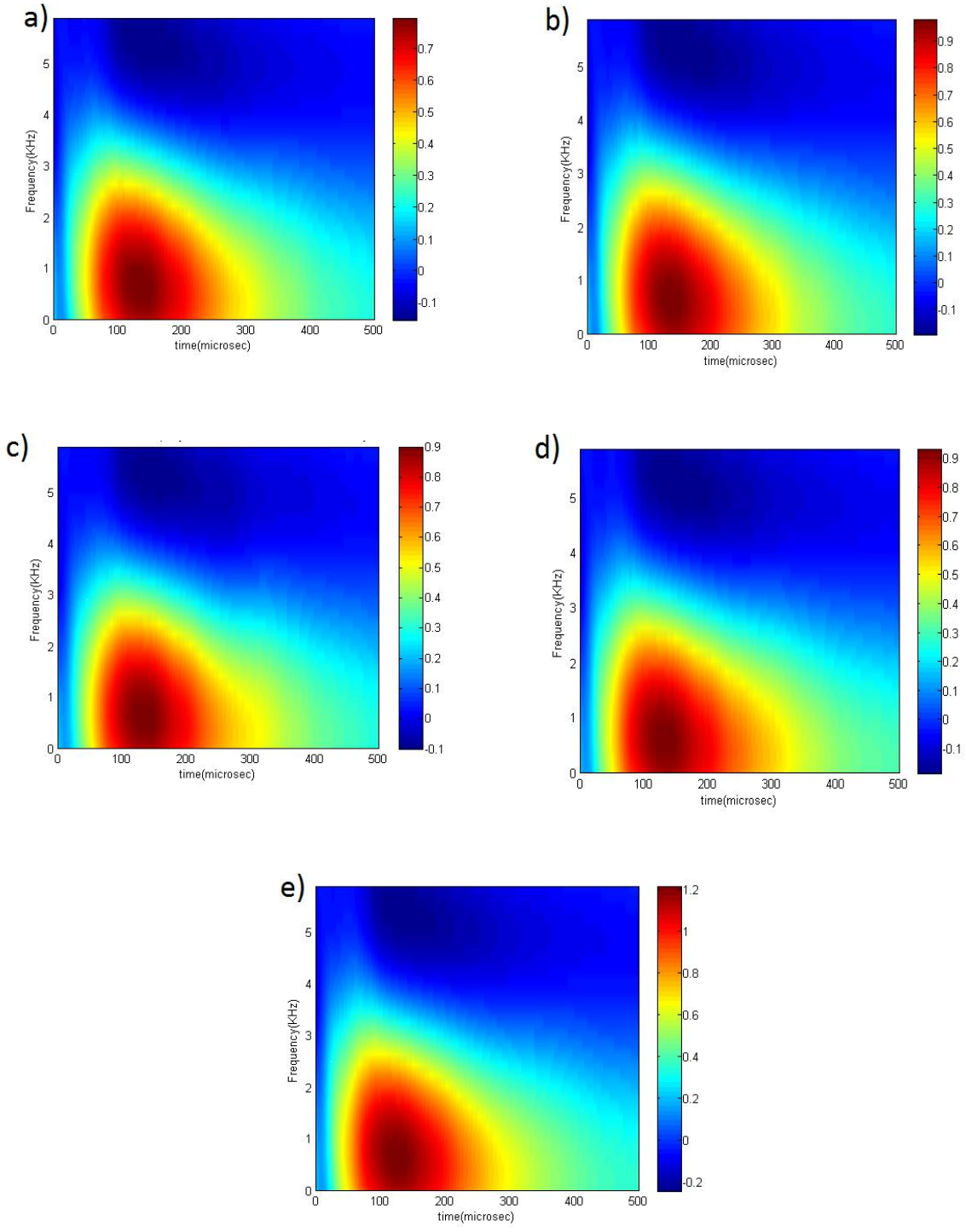

Figure 4.7 Time-Frequency results from 200μm metal loss placed between top and bottom layer. (a) 20% metal loss in Top of Bottom layer. (b) 15% metal loss in Top of Bottom layer and 5% metal loss in Bottom of Top layer. (c) 10% metal loss in Top of Bottom layer and 10% metal loss in Bottom of Top layer. (d) 5% metal loss in Top of Bottom layer and 15% metal loss in Bottom of Top layer. (e) 20% metal loss in Bottom of Top layer.

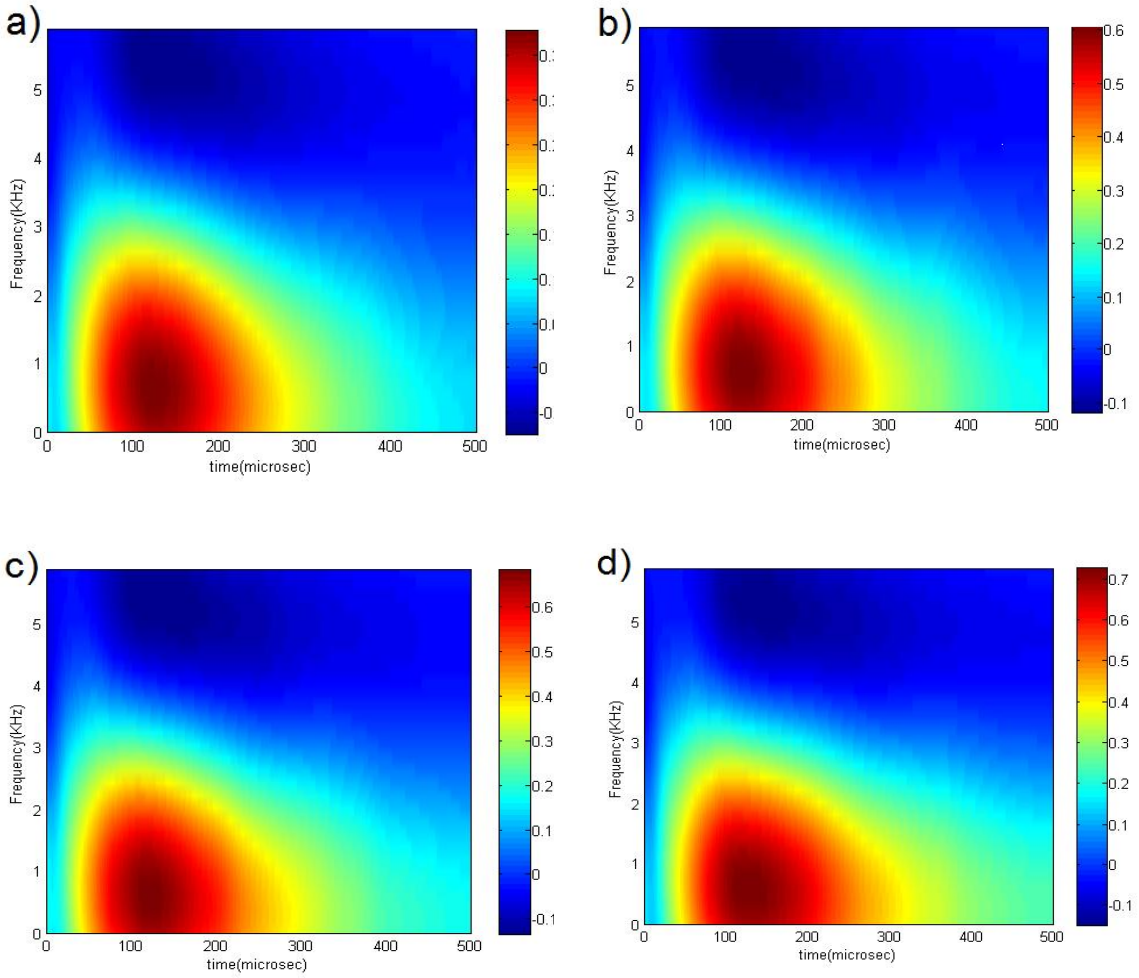

Figure 4.8 Time-Frequency results from 150µm metal loss placed between top and bottom layer. (a) 15% metal loss in Top of Bottom layer. (b) 10% metal loss in Top of Bottom layer and 5% metal loss in Bottom of Top layer. (c) 5% metal loss in Top of Bottom layer and 10% metal loss in Bottom of Top layer. (d) 15% metal loss in Bottom of Top layer.

Figure 4.8 illustrates a Time-frequency representation of sample with defects located between top-of-bottom layer and bottom-of-top layer respectively with 150µm metal loss between top and bottom layer.

Increasing the distance of a defect from the sample surface causes a decrease in the intensity and size of the response signal. In the case of a 15% metal loss there is a peak in the range of 130 µsec. For each case of metal loss with a 150µm synthetic defect, position of the peak in the time axis is constant. By reducing the distance from the metal loss to the surface, the position of the

peak moves towards increasing frequency at constant time. Additionally, defects which are closer to the surface show dense signal amplitude just before the position of the peak. In the case of a defect with 20% metal loss placed between layers, peaks occur in the range of 170 µsec. In this case, the peak moves toward the frequency axis for the same time value. The amplitude, shape and place of peaks define the location and size of the defect. They are therefore used as key features during feature extraction and classification.

For each state of metal loss, feature extraction and classification are applied. For 200µm metal loss between layers, defects are classified in 5 groups (200µm metal loss on BOT, 150µm metal loss on BOT and 50µm on TOB, 100µm metal loss on BOT and 100µm on TOB, 50µm metal loss on BOT and 150µm on TOB and 200µm metal loss on TOB.). For the case of 150µm metal loss between layers, defects are classified in 4 groups (150µm on BOT, 100µm on BOT and 50µm on TOB, 50µm on BOT and 100µm on TOB and 150µm on TOB.)

4.3.3 Feature extraction and classification

The output of Time-Frequency Analysis for each Pulsed Eddy Current signal is an n×n matrix. The matrix is expressed as n^2 dimensional vectors and represented by an image. Each pixel of the Time-Frequency Analysis image corresponds to the value of each vector. The output of time-frequency analysis contains large amounts of data and it is vital to reduce the size of the data without losing critical data. For this purpose, it is essential to apply feature extraction. Feature extraction should reduce the number of parameters and also improve computational efficiency of the classifier. Principal component analysis is applied as a feature extraction method. In principal component analysis (PCA), Eigenvalues and Eigenvectors of the covariance matrix are calculated. Subsequently, Eigenvectors are arranged in order of largest Eigenvalues. Figure 4.9 illustrates the process of PCA schematically.

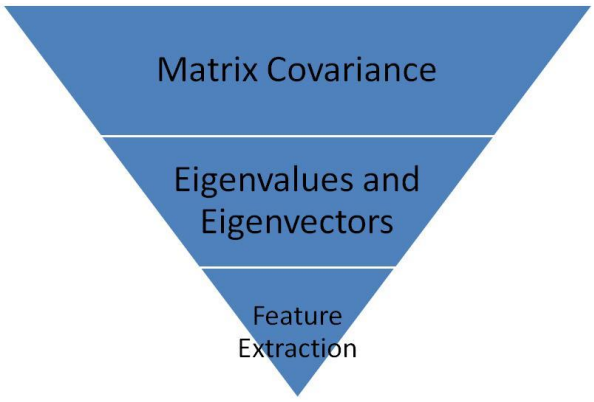

Figure 4.9 schematic of PCA

In the PCA method, the direction of the most significant amount of energy is determined by the direction of largest variance of data, which is the first Eigenvector. Therefore, PCA reduces the number of parameters without loss of information by retaining the significant features (Eigenvectors with largest Eigenvalues) and leaving out some less expressive features. PCA provides new features for each signal and the relative position of each metal loss. These are then fed into the classifier. In this study, a group of the 3 Eigenvectors that correspond to the 3 largest Eigenvalues are selected for each class and position of defects.

Misclassification error is known as the most critical factor for each classifier. In this study, K-means clustering is applied as a classifier, which has minimum misclassification error compared to other methods of classification. The amounts of misclassification error are calculated by inspecting new points and measuring the size of metal losses and then comparing with reference patterns which are used as a map and data base in classifier. The misclassification error of K-means clustering is less than 3% for each case of metal loss.

Figure 4.10 shows the final results of classification using the K-means clustering method based on output of principal component analysis data for defects with 200μm metal loss. In Figure 10(a), PCA output data are classified for samples with 200μm metal loss where defects are placed on surfaces with and without overlapping conditions between bottom of top and top of bottom layers. 5 separate clusters are observed in Figure 4.10(a). These clusters illustrate position and size (metal loss) of defects. The first and second Eigenvectors correspond to first and second maximum Eigenvalues and are chosen as the first and second dimensions of data to represent the classification results. Figure 4.10(b) is a dendrogram of defect clustering for the case of 200μm

metal loss at different positions between layers. A dendrogram is a branch diagram representing hierarchical clustering and classification based on degree of similarity. In Figure 10(b), vertical and horizontal axes indicate similarity of signals and individual signals respectively.

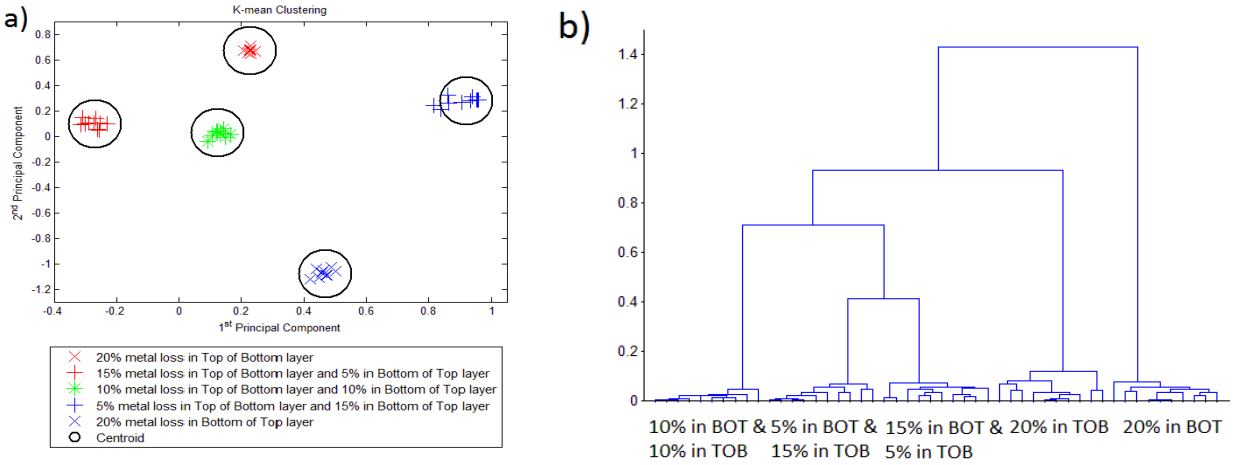

Figure 4.10 Classification of PCA output for 200µm metal loss placed between top and bottom layer. (a) K-Mean Clustering. (b) Dendrogram.

The final results of classification using the K-means clustering method applied to the output of principal component analysis data for defects with 150µm metal loss which are placed on surfaces with overlapping condition is represented in Figure 4.11. Four separate clusters exist in Figure 4.11(a), which illustrates the position and number of defects with 150µm metal loss in different locations. Figure 4.11(b) also represents a tree diagram of clustering for defects with 150µm metal loss on surfaces with and without overlapping condition.

For comparison, it is necessary to calculate the Euclidian distance from each unknown test point to each centroid to define minimum distance. The minimum distance of each unknown sample defines the cluster group in which the defected sample belongs.

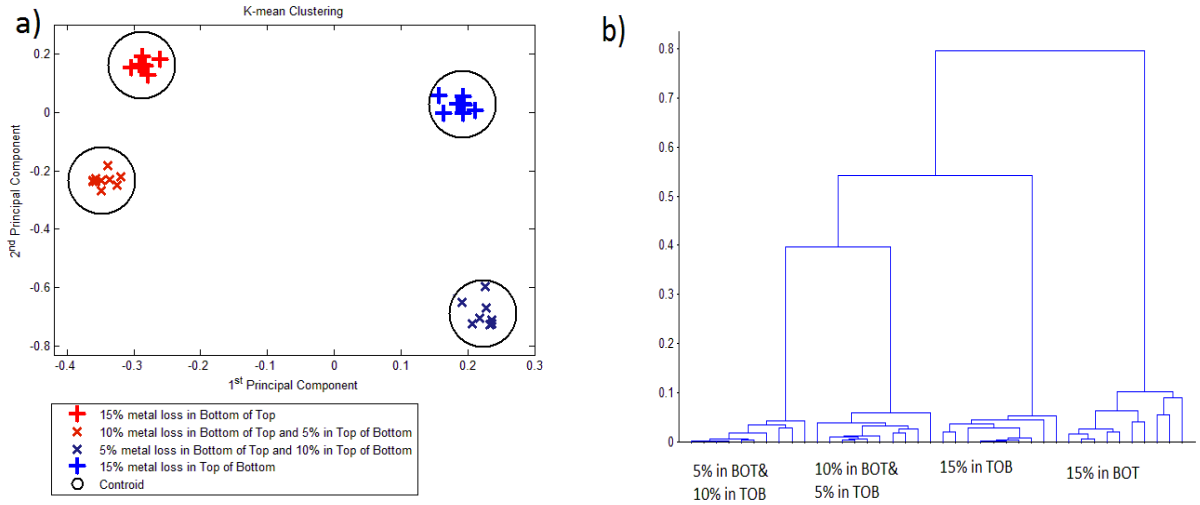

Figure 4.11 Classification of PCA output for 150µm metal loss placed between top and bottom layer. (a) K-Mean Clustering. (b) Dendrogram.

4.4 Conclusion

This paper reports a novel inspection system using a pulsed eddy current testing method to detect defects between layers with and without overlapping condition in a double-layer structure. A Time-Frequency analysis method is applied to treat PEC signals. Time-Frequency analysis is used as an applicable and valuable tool to display the position variation of complex defects where the locations of same-size defects change approximately 50µm between layers with overlapping conditions. Place of the peaks and also amount of maximum amplitude of each peak were considered as critical features which were represented by presence of same size overlap defects. These features were extracted by principal component analysis and were used as feed of classifier. Automatic classification was done by K-means clustering applied to pulsed eddy current signals which have been treated using Rihaczek distribution and principal component analysis. This method can be used in aircraft industry applications to detect corrosion and metal losses in double-layer and multi-layer structures with high accuracy and rapidity. In future studies, more extensive testing with real data will be presented to compare the precision and reliability of this signal processing method when applied to overlap corrosion and defect detection in an aluminum multi-layer.

Acknowledgment

This research was supported by the collaborative research and development grant (No. CRDPJ-335472-05) of Natural Sciences and Engineering Research Council of Canada (NSERC), Pratt & Whitney Canada, Bombardier Aeronautics and National Research Council of Canada (NRC).

References

[1] Smith R, Skramstad JA, Edgar D. Advances in Transient Eddy-Current Imaging for Aerospace Applications. 16th World Conference on NDT, . Montreal, Canada; 2004.

[2] Moulder JC, Bieber JA, Ward Iii WW, Rose JH. Scanned pulsed eddy current instrument for nondestructive inspection of aging aircraft. Proceedings of SPIE - The International Society for Optical Engineering 1996;2945:2-13.

[3] Sophian A, Tian GY, Taylor D, Rudlin J. Electromagnetic and eddy current NDT: A review. Insight: Non-Destructive Testing and Condition Monitoring 2001;43:302-6.

[4] He Y, Luo F, Pan M, Weng F, Hu X, et al. Pulsed eddy current technique for defect detection in aircraft riveted structures. NDT & E International 2010;43:176-81.

[5] Auld BA, Moulder JC. Review of advances in quantitative eddy current nondestructive evaluation. Journal of Nondestructive Evaluation 1999;18:3-36.

[6] Dadic M, Vasic D, Bilas V. A system identification approach to the modelling of pulsed eddy-current systems. NDT & E International 2005;38:107-11.

[7] Tian GY, Li Y, Mandache C. Study of Lift-Off Invariance for Pulsed Eddy-Current Signals. IEEE Transactions on Magnetics 2009;45:184-91.

[8] Tian GY, Sophian A. Defect classification using a new feature for pulsed eddy current sensors. NDT & E International 2005;38:77-82.

[9] Kim J, Yang G, Udpa L, Udpa S. Classification of pulsed eddy current GMR data on aircraft structures. NDT & E International 2010;43:141-4.

[10] Guang Y, Tamburrino A, Udpa L, Udpa SS, Zhiwei Z, et al. Pulsed Eddy-Current Based Giant Magnetoresistive System for the Inspection of Aircraft Structures. Magnetics, IEEE Transactions on 2010;46:910-7.

[11] Li S, Huang S, Zhao W. Development of differential probes in pulsed eddy current testing for noise suppression. Sensors and Actuators A (Physical) 2007;135:675-9.

[12] He Y, Luo F, Pan M, Hu X, Liu B, et al. Defect edge identification with rectangular pulsed eddy current sensor based on transient response signals. NDT & E International 2010;43:409-15.

[13] Fan M, Huang P, Ye B, Hou D, Zhang G, et al. Analytical modeling for transient probe response in pulsed eddy current testing. NDT & E International 2009;42:376-83.

[14] Tian GY, Sophian A. Reduction of lift-off effects for pulsed eddy current NDT. NDT & E International 2005;38:319-24.

[15] Safizadeh MS, Liu Z, Mandache C, Forsyth DS. Automated Pulsed Eddy Current Method for Detection and Classification of Hidden Corrosion. Proc Vth International Workshop, Advances in Signal Processing for Non Destructive Evaluation of Materials,. Quebec City, Canada; 2005, p. 75-84.

[16] Safizadeh MS, Lepine BA, Forsyth DS, Fahr A. Time-frequency analysis of pulsed eddy current signals. Journal of Nondestructive Evaluation 2001;20:73-86.

CHAPITRE 5 TREATMENT OF PULSED EDDY CURRENT SIGNALS USING TIME-FREQUENCY ANALYSIS FOR DETECTION OF THICKNESS VARIATION IN AN ALUMINUM PLATE. [3]

Saleh Hosseini

Section of Applied Mechanics, Department of Mechanical Engineering, École Polytechnique de Montréal, Montréal, Quebec, H3T1J4, Canada.

Aouni A. Lakis

Section of Applied Mechanics, Department of Mechanical Engineering, École Polytechnique de Montréal, Montréal, Quebec, H3T1J4, Canada.

Corresponding author;

Tel.: +1 514 340 4711 (4906)

Fax: +1 514 340 4076

Email: aouni.lakis@polymtl.ca

Abstract

A novel approach for automatic thickness detection using pulsed eddy current is presented in this study. The pulsed eddy current signal response from an aluminum sample with 1 mm thickness containing synthetic defects varying from 50µm to 250 µm is investigated. A spectrogram is used as a time-frequency analysis method for treatment of the pulsed eddy current signals to reveal hidden information through use of three-dimensional representations. Principal component analysis is applied as a feature extraction method to extract features from time-frequency analysis results. These are fed to a classifier. K-Means Clustering is used to classify the data as the final step in this automatic defect detection method.

Keywords: Pulsed Eddy Current (PEC), Time-Frequency Analysis, Spectrogram, Principal Component analysis, K-Means Clustering.

---

[3] This article was submitted to the journal of Applied Physics

5.1 Introduction

Thickness detection, measurement of metal losses and characterization of subsurface defects with high reliability and accuracy are the major challenges in non-destructive testing methods [1, 2]. Use of Pulsed Eddy Current (PEC) as an electromagnetic non-destructive testing method has shown great potential for detecting and characterizing interior corrosion, flaws and metal losses in conductive materials amongst all field-ready methods of non-destructive testing [1, 3, 4]. Pulsed eddy current is a noncontact inspection method and provides reliable and accurate measurements when it is applied for inspection and defect detection in aging components [5, 6]. In contrast to conventional Eddy Current (EC) testing, in which the probe is excited using single frequency or multi-frequencies, pulsed eddy current testing uses square or sinusoidal pulsed excitation over a wide range of frequencies [5, 7, 8].The broadband nature of pulsed eddy current allows more penetration compared to conventional eddy current testing and brings out rich information describing the physical condition of the interior of the structure and the electrical properties of the test sample [1, 9].

A series of voltage-time data represents the pulsed eddy current signals in the time domain. The most common features in pulsed eddy current signals in time-domain analysis are amplitude, time-to-zero crossing and time-to peak [10-12]. Signal processing methods for time-domain data have been used by many authors to improve reliability of inspection and extract more information from pulsed eddy current signals. New features have been presented to identify depth defects regardless of the type or shape of these defects [5]. On other hand, pulsed eddy current probes have been used in many studies to increase the capacity of measurement. Many investigations have focused on measurement efficiency improvement by changing the properties of the probe and applying new types of probes such as giant magneto resistive probes (GMR) [13, 14], Hall sensors [15] and differential probes [7]. The Time-Frequency analysis method is one of the signal processing and data treatment methods that have been used in investigations to improve pulsed eddy current signal representation and reduce noise effects for automatic defect detection [16]. Safizadeh et al. applied Wigner-Ville distribution as a time-frequency analysis method to reduce noise effects of the interlayer gap and provide automatic defect detection in multilayer system [16, 17].

This study compares common time-domain results of pulsed eddy currents and the application of time-frequency analysis to determine the amount of corrosion and metal losses in an Aluminum single layer system. Defects are simulated on the bottom of the layer with thicknesses corresponding to 5%, 10%, 15%, 20% and 25% of the overall layer thickness. Spectrogram distribution is used as the time-frequency method and principal component analysis (PCA) provides a new feature to compress and input classifier data (the time-frequency data). Finally, a discriminative type of classification method is applied to classify the results. K-means Clustering is applied to classify the amount of metal losses on the subsurface separately. The combination of these steps presents a logical automatic method for defect detection in an Aluminum single layer system.

5.2 Experimental Setup and Specimen

5.2.1 Pulsed Eddy Current System Design

The Pulsed Eddy Current system consists of a pulse generator which creates square voltage, the probe (which contains a driving coil and a pick-up coil), a preamplifier that amplifies response signals and an analog to digital converter (A/D). In this study, the probe's driving coil is excited by a square voltage at 1 KHz and 4.5 volt. An electromagnetic field is produced by probe excitation. The conductive surface is affected by the electromagnetic field and eddy current is induced on the metallic surface. The Eddy Current electromagnetic field is generated by eddy current which contains information describing features of the inner structure. The electromagnetic field from the driver probe and the eddy current's electromagnetic response have inverse field directions. These electromagnetic fields are absorbed by the pick-up coil as a differential field. The pick-up coil converts the electromagnetic field to voltage. The probe's driving coil has inner and outer diameters of 12 and 15 mm respectively and probe's pick-up coil has inner and outer diameters of 7 and 11 mm. A low-noise preamplifier amplifies the voltage response at gain 5 and reduces the noise level in the band pass filter between 100 Hz to 10 KHz. NI digitizer (PCI-4070) and Lab View software are used to convert the analogue signal to digital and store the signals on a PC. The sampling frequency of the card is 1.00 MS/sec with 23-bit resolution.

5.2.2 Sample Test and Thickness Variation

A bare aluminum sheet at 1.04 millimeter thickness and 330×210 mm^2 area is used in this study. The thicknesses of synthetic defects are located at 5%, 10%, 15%, 20% and 25% of the plate thickness. Laser machining is used to fabricate a set of synthetic defects on the surface with 1 micrometer tolerance in depth of metal losses. The depths of the metal losses placed on the surface are 30µm, 50µm, 70µm, 100µm, 150µm, 200µm and 250µm. Each series of metal losses are placed on bottom side of plate. The area of the defects is equal at 30×90 mm^2. The sample used for this experiment is shown in Figure 5.1. Figures 5.1(a) and 5.1(b) show a schematic of the test sample from above and the side.

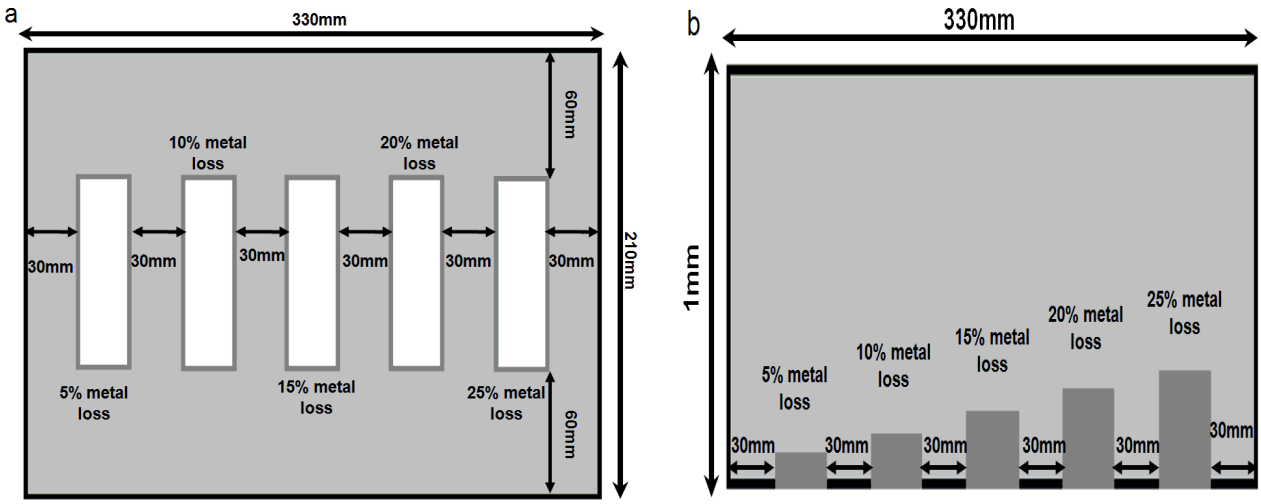

Figure 5.1 schematic of sampling test. (a) From above. (b) From side.

5.2.3 PEC Signals Processing

Signals are acquired from the synthetic defects using an A-scan in the vertical direction. Signal acquisition is performed 5 times for each case of metal losses plus a reference sample without any defect and metal loss (a total of 30 signals). A 1.8 MHz analogue-to-digital converter PCI is used for signal acquisition. Pulsed eddy current provides voltage-time series signals that are represented in the time domain. A reference signal is acquired from a 1 mm thick test sample without defects. The defect signals from the synthetic metal losses are subtracted from the reference signals. Time-frequency analysis is applied on subtracted pulsed eddy current data using the Rihaczek Distribution as a signal processing method. Principal component analysis

(PCA) is applied as feature extraction method to extract new features from the processed pulsed eddy current signals. Principal component analysis is applied to reduce the size of the data and generate infeed for a classifier. Figure 5.2 illustrates a schematic of process levels for inspection and thickness detection of aluminum plates using the pulsed eddy current testing method.

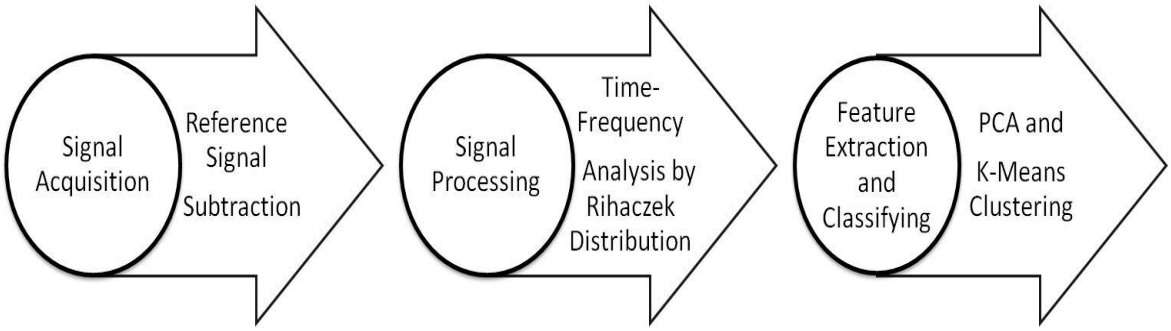

Figure 5.2 Schematic of process levels for inspection

5.3 Results and Discussion

5.3.1 Time-Domain Signals

A 1 KHz pulse excites the probe and the response signal is stored in the PC. Figure 5.3 shows results of the detected pulsed eddy current response for synthetic defects placed on the subsurface at 5%, 10%, 15%, 20% and 25% of plate thickness. By increasing the thickness of the metal losses, the intensity of the eddy current's electromagnetic field reduces. The probe's pick-up coil receives two types of electromagnetic fields; the eddy current electromagnetic field and an electromagnetic field produced by the probe's driving coil. The direction of these electromagnetic fields is inverse. Therefore, the amplitude of the response signals acquired by the probe's pick-up coil is amplified, i.e., the 250 μm metal loss sample has maximum amplitude and intensity whereas the 50 μm and reference signal from no defected sample have minimum amplitude. The pulsed eddy current signals acquired from the subsurface defects are too close. Subtraction between the pulsed eddy current signal from the synthetic metal loss and the reference signal from the non-defected surface is calculated. Figure 5.4 shows results of subtraction between the defect signals and reference signal for synthetic metal losses 50μm,

100µm, 150µm, 200µm and 250µm. As discussed later, increasing the thickness of metal losses causes an increase in the signal amplitude.

Pulsed eddy current signals bring out rich information from the interior of the sample. For automatic inspection, more patterns related to the signal need to be employed to provide reliable automatic fault and thickness detection. Additionally, if a small number of defects are placed close together it is difficult to clarify which defect belongs to which type and amount of metal loss. Time-frequency analysis is a powerful tool that represents signals in three dimensions and reveals more hidden information regarding the signals with more new patterns.

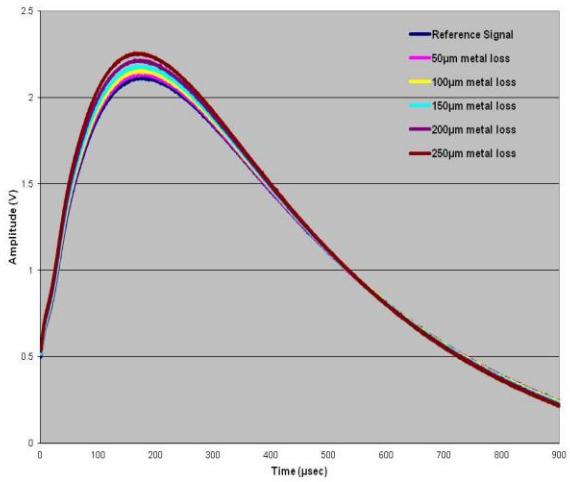

Figure 5.3 Pulsed eddy current response for synthetic defects

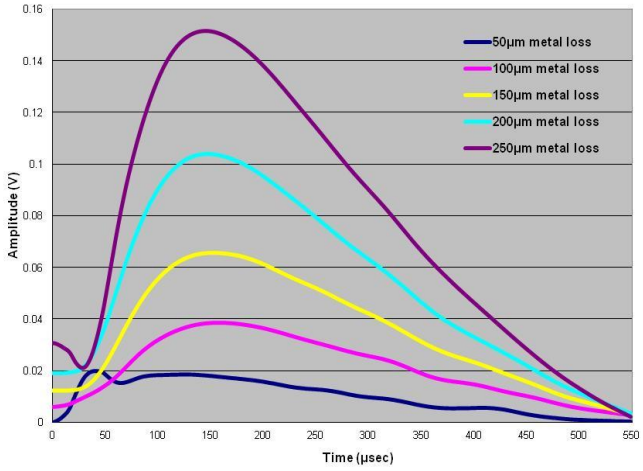

Figure 5.4 Subtraction result of pulsed eddy current response for synthetic defects with different amounts of metal loss

5.3.2 Time-Frequency Representation

The Time-Frequency analysis method is applied as an alternative signal treatment method for defect detection when defects, metal losses and corrosion occur on a subsurface to reduce the noise levels and also improve accuracy and reliability of defect detection. Fourier transform is the most known transform used for presenting the frequency composition of a signal. For a given signal $x(t)$ in the time domain, the Fourier transform $X(f)$ is defined as:

$$X(f) = \int_{-\infty}^{\infty} x(t) e^{-j2\pi ft} dt \tag{5.1}$$

where *f* is frequency and *t* denotes time. The frequency content of the signal is revealed using Fourier transform, although no information is provided about the time at which each frequency component takes place. To tackle this shortcoming, this transform can be applied to a respectively short portion of the signal (analysis window) around the instantaneous time *t*. Then by continuously moving the window along time, a joint time-frequency representation of the signal can be obtained. The resulting transform is called the Short Time Fourier Transform (STFT) and in mathematical terms is written as:

$$S(t, f) = \int_{t'} x(t') w(t' - t) e^{-j2\pi ft'} dt' \tag{5.2}$$

where *w(t'-t)* is the window function or analysis window. A spectrogram is defined as the squared magnitudes of the short time Fourier transform:

$$Spec = |STFT|^2 \tag{5.3}$$

Although the spectrogram is nonlinear, the interference terms do not significantly affect the final results because nonlinearity is not an instinctive feature of this transform and it comes into effect while squaring the magnitude. This, together with simplicity, robustness and ease of interpretation, has made the spectrogram a popular tool for many applications.

The spectrogram is applied as a signal processing step in the time-frequency analysis method for the subtracted pulsed eddy current signals. Time-Frequency analysis provides three dimensional representations of signals and presents time, frequency and amplitude of the signal. The output of Time-Frequency analysis for each case of metal loss is an n×n matrix and is represented by an image. Figure 5.5 shows a time-frequency representation of a single layer sample with synthetic defects located on its subsurface. Thicknesses of the metal losses are 50 μm, 100 μm, 150 μm, 200 μm and 250 μm or 5%, 10%, 15%, 20% and 25% of plate's thickness. Increasing the thickness of synthetic defects located on the subsurface causes an increase in intensity and size of response signals. The result of time-frequency analysis provides some critical factors that can be used in feature extraction for classification and automatic inspection.

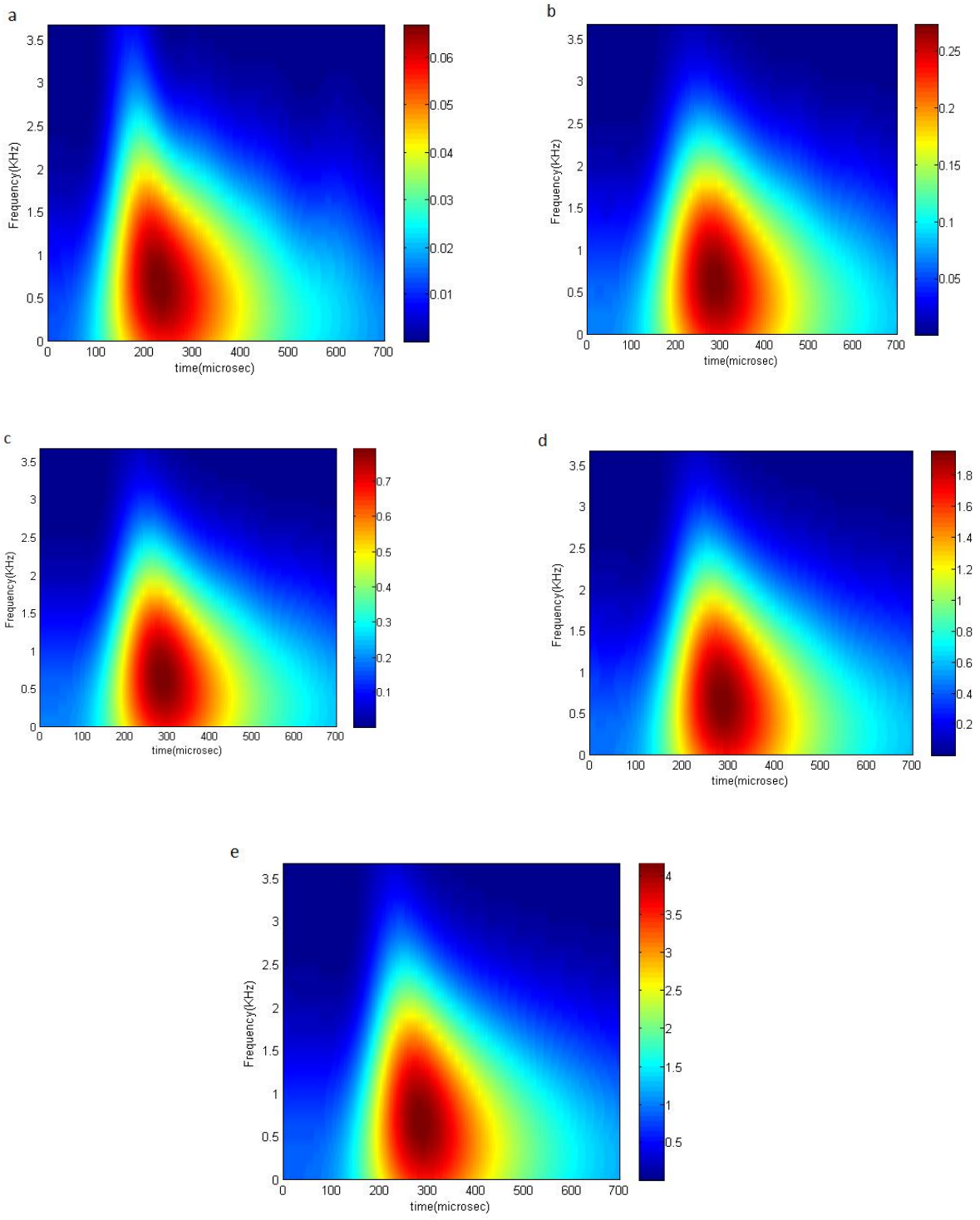

Figure 5.5 Time-frequency representation of synthetic defects located on subsurface. (a) 5% metal loss. (b) 10% metal loss. (c) 15% metal loss. (d) 20% metal loss. (e) 25% metal loss.

5.3.3 Feature Extraction and Classification

Pulsed eddy current signals are processed using the spectrogram method. The result of time-frequency analysis for each pulsed eddy current signal is an n×n matrix and it is represented by images. Each pixel of an image is expressed as a one-dimensional vector and each image has a total of n^2 dimensional vectors. Time-frequency analysis provides large amounts of redundant data. It is vital to reduce the size and number of data to have fast, efficient and reliable classification and automatic defect detection. Principal component analysis (PCA) is a well-known tool that extracts the most significant features of data and also reduces the size of the data set without losing information. As a first step to extract features by principal component analysis, the covariance of the time-frequency data (n×n matrix) is calculated. Then, eigenvalues and eigenvectors of the covariance matrix are calculated respectively. Eigenvectors are arranged in order of largest eigenvalues. The direction of the most significant amount of energy is determined by the largest variance of time-frequency analysis data and is expressed by the first eigenvector. The most significant features (eigenvectors with largest eigenvalues) are retained by principal component analysis and are used to feed the classifier. In this study, a group of 3 eigenvectors corresponding to maximum eigenvalues are selected for each class and size of metal losses. K-means clustering is used as a classifier. Misclassification error of K-Means clustering in this study is less than 1% for each case of synthetic defects.

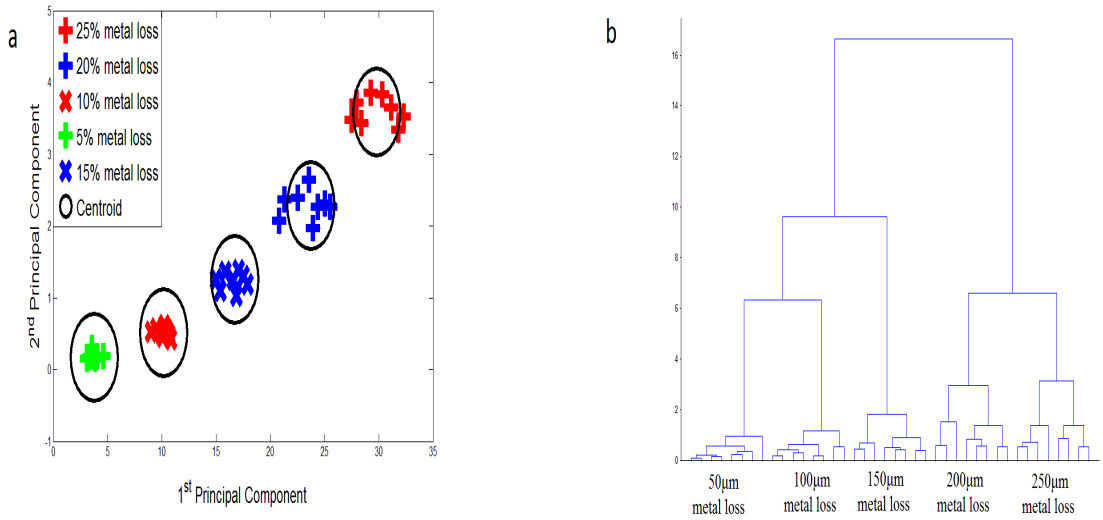

Figure 5.6 Classification of synthetic defects located on subsurface. (a) K-Means Clustering. (b) Hierarchical

Figure 5.6 shows the results of classification using the K-Means Clustering method based on feature extraction of time-frequency data by principal component analysis. Five separated classes correspond to the five different thicknesses of metal loss. Figure 5.6(a) illustrates that by increasing the thickness of metal loss on the surface, classes are placed farther from the center plane. Figure 5.6(b) is dendrogram of metal loss clustering for each defect case. Vertical and horizontal axes indicate the similarity of the signals and individual signals respectively. The location of the defects moves along the horizontal axis from left to right as the thickness of the metal loss increases. In automatic defect detection, Euclidian distance is calculated between the feature extraction results of each unknown test point and each centroid to define a minimum distance. This minimum distance between an unknown test point and centroid is used to associate the unknown test point to a specific type and size of metal loss.

5.4 Conclusion

This study reports a new pulsed eddy current system development for automatic detection of subsurface defects and metal losses. A differential probe detects pulsed eddy current signals from defects with thicknesses ranging from 50μm to 250 μm. A spectrogram is applied on the pulsed eddy current signals as a time-frequency analysis. Place, shape and maximum amount of amplitude are considered as critical features of each types of metal losses .This shows the applicability and capacity of time-frequency analysis in detection of thickness in aluminum plate. Principal component analysis is applied on the output of the spectrograms to extract critical features and new information from the pulsed eddy current signals. Finally, K-means clustering classifies the PCA data. Linear behavior of extracted data by increasing the depth of metal losses shows that this method can be used effectively for automatic defect detection in a single layer system when defects very quickly.

Acknowledgment

This research was supported by the collaborative research and development grant (No. CRDPJ-335472-05) of Natural Sciences and Engineering Research Council of Canada (NSERC), Pratt & Whitney Canada, Bombardier Aeronautics and National Research Council of Canada (NRC).

References

[1] Sophian A, Tian GY, Taylor D, Rudlin J. Design of a pulsed eddy current sensor for detection of defects in aircraft lap-joints. Sensors and Actuators A: Physical 2002;101:92-8.

[2] Sophian A, Tian GY, Taylor D, Rudlin J. Electromagnetic and eddy current NDT: A review. Insight: Non-Destructive Testing and Condition Monitoring 2001;43:302-6.

[3] Moulder JC, Bieber JA, Ward Iii WW, Rose JH. Scanned pulsed eddy current instrument for nondestructive inspection of aging aircraft. Proceedings of SPIE - The International Society for Optical Engineering 1996;2945:2-13.

[4] Smith R, Skramstad JA, Edgar D. Advances in Transient Eddy-Current Imaging for Aerospace Applications. 16th World Conference on NDT, . Montreal, Canada; 2004.

[5] Chen T, Tian GY, Sophian A, Que PW. Feature extraction and selection for defect classification of pulsed eddy current NDT. NDT & E International 2008;41:467-76.

[6] He Y, Luo F, Pan M, Hu X, Liu B, et al. Defect edge identification with rectangular pulsed eddy current sensor based on transient response signals. NDT & E International 2010;43:409-15.

[7] He Y, Luo F, Pan M, Weng F, Hu X, et al. Pulsed eddy current technique for defect detection in aircraft riveted structures. NDT & E International 2010;43:176-81.

[8] Shu L, Songling H, Wei Z, Peng Y. Study of pulse eddy current probes detecting cracks extending in all directions. Sensors and Actuators, A: Physical 2008;141:13-9.

[9] Tian GY, Sophian A, Taylor D, Rudlin J. Multiple sensors on pulsed eddy-current detection for 3-D subsurface crack assessment. IEEE Sensors Journal 2005;5:90-6.

[10] Gigu, re S, Lepine BA, Dubois JMS. Pulsed eddy current technology: Characterizing material loss with gap and lift-off variations. Research in Nondestructive Evaluation 2001;13:119-29.

[11] Smith RA, Edgar D, Skramstad J, Buckley J. Enhanced Detection of Deep Corrosion Using Transient Eddy Currents. 7th Joint DoD/FAA/NASA Conference on Aging Aircraft,. New Orleans; 2003.

[12] Tian GY, Sophian A, Taylor D, Rudlin J. Pulsed eddy current system for dynamic inspection of defects. Insight-Non-Destructive Testing and Condition Monitoring 2004;46:256-9.

[13] Kim J, Yang G, Udpa L, Udpa S. Classification of pulsed eddy current GMR data on aircraft structures. NDT & E International 2010;43:141-4.

[14] Guang Y, Tamburrino A, Udpa L, Udpa SS, Zhiwei Z, et al. Pulsed Eddy-Current Based Giant Magnetoresistive System for the Inspection of Aircraft Structures. Magnetics, IEEE Transactions on 2010;46:910-7.

[15] Tian GY, Sophian A. Defect classification using a new feature for pulsed eddy current sensors. NDT & E International 2005;38:77-82.

[16] Safizadeh MS, Lepine BA, Forsyth DS, Fahr A. Time-frequency analysis of pulsed eddy current signals. Journal of Nondestructive Evaluation 2001;20:73-86.

[17] Safizadeh MS, Liu Z, Mandache C, Forsyth DS. Automated Pulsed Eddy Current Method for Detection and Classification of Hidden Corrosion. Proc Vth International Workshop, Advances in Signal Processing for Non Destructive Evaluation of Materials,. Quebec City, Canada; 2005, p. 75-84.

CHAPITRE 6 GENERAL DISCUSSION

The concept of automatic non-destructive testing for the purpose of corrosion and defect detection in multilayer structures such as aircraft fuselage was investigated. The principal difficulty in this case was clear signal acquisition with minimum noise. Several hardware and software tools exist to improve signal-to-noise ratio and also to reduce the noise level of the acquired signals. The general discussion is divided into three sections. First, pulsed eddy current testing and collecting the response signals from defects of different sizes placed at various locations in two test samples (single-layer and double-layer) is discussed. Secondly, effects and applicability of time-frequency analysis in defect representation in new dimensions are investigated. Finally, extracting the features and defect classification are discussed.

6.1 Pulsed eddy current signal acquisition and time-domain signal representation

The pick-up coil is excited by the electromagnetic field and the response signal is digitized. The amplitude of response signals increases as the thickness of the defects or metal losses increase. For example, a 30μm sample has minimum amplitude whereas a sample with a 250μm defect has maximum amplitude in cases where defects are located on a single layer or the same surface of a plate in double or multi-layer systems. At each location of the defects on the same layers, an increase in the thickness of the defect causes a decrease in eddy current field and therefore the pick-up coil (probe) receives more electromagnetic field.

Due to the electromagnetic nature of eddy current inspection, pulsed eddy current signals contain information from surfaces between layers, under layers and interior structures. The signals come from defects placed on the bottom of the bottom layer (BOB), the top of the bottom layer (TOB) and the bottom of the top layer (BOT). These defect arrays include; defects from 30 to 250 μm deep on each surface (Chapter 3), two cases of defects that overlap between the top-of-bottom layer and bottom-of-top layer and range from 50 to 200 μm deep (Chapter 4) and, metal losses on the bottom of layers ranging from 50 to 250 μm deep (Chapter 5). The acquired signals are too closely spaced and it is difficult to train a machine to detect these defects and separate them precisely. Subtraction from reference signals is the first method used to clarify the signals and defects in time-domain representation. The signals are subtracted from a reference signal

which comes from a double-layer without defects (Chapters 3 & 4) and a non-defected plate (Chapter 5) so that the metal loss variations are clearly shown.

Three main features of pulsed eddy current signals are time-to-peak, time-to-zero crossing and rising time of the pulsed eddy current response. Noise effects, such as signals from small defects and low variation in defect sizes reduces the reliability of time-domain signals and creates the condition that the time-domain features of the pulsed eddy current signals are very close and demonstrate continuous interference. As previously mentioned, the fact that the curves are so close causes difficulty extracting clear information. For this case, time-frequency methods are applied to create three dimensions for representation of data.

6.2 Time-frequency representation of pulsed eddy current signals

The subtracted signals of pulsed eddy current were processed using the time-frequency analysis method. The results of time-frequency analysis are the Rihaczek distribution of pulsed eddy current signals from a double-layer aluminum structure to determine the size and location of defects (Chapters 3 & 4) and a spectrogram of pulsed eddy current signals from a single-layer structure for detection of thickness variation (Chapter 5). The output of time-frequency analysis for each pulsed eddy current signal is an n×n matrix which is represented by an image. The time-frequency analysis method provides a three-dimensional representation of a signal (in time, frequency and amplitude). Time-frequency representation allows detection of the size and location of defects in a double-layer system containing close-sized defects and noise sources such as interlayer gap and probe lift-off and determination of thickness variation in single-layer structures.

Defects located farther from the surface of the structure, penetrating ability of eddy current magnetic fields is increased and also more eddy current magnetic field is induced. Therefore, more eddy current electromagnetic field is received by the probe’s pick-up coil when defects are placed more deeply into the structure. According to the theory of eddy current, this effect causes a decrease in the amplitude of acquired signals from these deeper defects (Chapters 3, 4 & 5).

Increasing the depth of a metal loss caused a shift in intensity from a narrow to wide state. In cases of more metal loss where the depth of defects increase, the intensity magnifies, which shows that the strength of the eddy current magnetic field decreases at the top of the defected

surfaces (Chapters 3 & 5). Increasing the thickness of the defects on the surfaces causes an increase in the intensity and size of the response signal. Increasing the depth of the defects causes a shift in position of the peaks along the time axis.

According to results of time-frequency analysis for same-size defects distributed between layers (Chapter 4); defects that are closer to the surface of the sample provide sharp peaks at higher amplitude. The maximum amplitude from defects positioned lower in the sample has a wide distribution in the time and frequency axes compared to defects placed closer to the surface. Therefore, increasing the distance from the surface to defects with same-size metal loss causes a shift in intensity from a narrow to wide state.

The amplitude and shape (narrow or wide, extended in time axis, frequency axis or both, position of the peak) of the peaks defines the location and size of the defect. They are therefore used as key features during feature extraction and classification.

6.3 Feature Extraction and Classification

The output of time-frequency analysis for each pulsed eddy current signal is an n×n matrix which is represented by an image. This matrix is expressed as n^2 dimensional vectors. The value of each vector corresponds to the intensity of each pixel of the time-frequency analysis image. The image contains a large amount of redundant data. Principal Component Analysis (PCA) is applied for feature extraction to reduce the number of parameters and also to improve computational efficiency of the classifier.

PCA computes Eigenvalues and Eigenvectors of the covariance matrix. The Eigenvectors are arranged in order of largest Eigenvalues. The first Eigenvector has the direction of largest variance of data and it determines the direction of the most significant amount of energy. Principal Component Analysis retains the significant features (Eigenvectors with largest Eigenvalues) and leaves out some less expressive features. In this way, PCA reduces the number of parameters without loss of information.

These new features were used as input data for classification. In our research, for each type of defect a group of the 3 largest Eigenvalues was selected for each class. Misclassification error is a critical factor for each classification method. In this thesis, K-mean clustering and Expectation-Maximization were used because they have minimum misclassification error

compared to other methods of classification. In Chapter 3, the misclassification errors of K-mean clustering and EM algorithms were calculated and the values of these errors were 3.11% and 1.78% respectively. In Chapters 4 and 5, K-means clustering was applied as a classifier, which has minimum misclassification error compared to other methods of classification. The misclassification error of K-means clustering was less than 3% for each case of metal loss in Chapter 4 and less than 1% for each case of synthetic defects in Chapter 5.

CHAPITRE 7 CONCLUSION AND RECOMMENDATIONS

In this dissertation, three studies concerning defect detection for aircraft fuselages using time-frequency analysis as an advanced signal processing method and pulsed eddy current testing as a powerful new inspection method were presented.

In the first study, a novel approach included application of the time-frequency analysis method to treat pulsed eddy current data to detect corrosion defects at different depths and positions in a multi-layer structure. Corrosion is a varied and complex phenomenon and metal loss on surfaces and between layers changes quickly. According to previous studies, pulsed eddy current time domain signals are not able to show variation of metal losses on surfaces and cannot separate them correctly when the defects are closely spaced and distributed in several places on multilayer structures. In our novel approach, pulsed eddy current data from the time domain were converted to time-frequency domain by Rihaczek distribution to analyze the data in an enhanced form. This allowed detection of defects of different sizes in each layer. Maximum variances of PCA were selected as features for the classification method and two types of classifiers with minimum misclassification errors were used to separate and classify these new features. The time-frequency analysis method was a valuable tool to process pulsed eddy current response signals and was also capable of detecting defects (such corrosion and cracks) in aluminum multi-layer systems when the size variation of the defects was approximately 30μm.

In the second study, a novel inspection system using a pulsed eddy current testing method to detect defects between layers with and without overlapping condition in a double-layer structure was presented. Time-Frequency analysis was used as an applicable and valuable tool to display the position variation of complex defects where the locations of same-size defects change approximately 50μm between layers with overlapping conditions. Automatic classification is done by K-means clustering applied to pulsed eddy current signals which have been treated using Rihaczek distribution and principal component analysis.

In the third study, a new development for automatic thickness variation detection using a spectrogram as a time-frequency analysis method which has minimum interference effects for pulsed eddy current signals was investigated. The pulsed eddy current signals acquired using a differential probe ranged from 50 to 250μm of metal losses in a single-layer aluminum plate with 1.04 mm thickness. The spectrogram processed and treated the pulsed eddy current signals to

prepare the input of feature extraction and represent the signals in new dimensions. Principal component analysis was applied on the output of the spectrograms to extract critical features and new information from the pulsed eddy current signals. Finally, K-means clustering classified the PCA data. The results showed that this method can be used for automatic defect detection and thickness variation detection in a single-layer system.

As a recommendation for future works and studies, the following research is suggested:

- In the abovementioned studies, inspection and defect detection methods were performed on double layer structures and single layer systems of aluminum plates. The effectiveness of this inspection method should be further investigated on different paramagnetic conductive materials such as titanium and stainless steel.
- In this study, inspection method and data mining and training were done for synthetic defects on the surfaces of aluminum plates. Similar inspection and defect variation detection should be carried out using data acquisition from real defected aircraft fuselages.
- To improve accuracy of inspection, using different types of probes such as Hall device, Giant magneto resistive and dual probe is strongly recommended. Because by improving the probe, accuracy and signal acquisition will be improved.
- Another probabilistic and discriminative classification method may be implemented to improve accuracy and reliability of classification and defects separation.
- Other types of defects such as fatigue, stress corrosion cracking (SCC) and internal cracks may be inspected using this inspection method. These defects change the microstructure of the testing sample and according to the studies pulsed eddy current inspection is able to probe these defects.

REFERENCES

Abidin, I. Z., C. Mandache, et al. (2009). "Pulsed eddy current testing with variable duty cycle on rivet joints." NDT & E International **42**(7): 599-605.

Abidin, I. Z., C. Mandache, et al. (2009). "Defect depth estimation using pulsed eddy current with varied pulse width excitation." Insight-Non-Destructive Testing and Condition Monitoring **51**(2): 69-72.

Akansu, A. N. and R. A. Haddad (2001). Multiresolution signal decomposition. New York, Academic Press.

Angani, C. S., D. G. Park, et al. (2010). "Differential pulsed eddy current sensor for the detection of wall thinning in an insulated stainless steel pipe." Journal of Applied Physics **107**(9): 09-720.

Angeli, M., P. Burrascano, et al. (1999). "Classification of eddy current NDT data by Probabilistic Neural Networks." Proceedings of the International Joint Conference on Neural Networks **6**: 4012-4014.

Auld, B. A. and J. C. Moulder (1999). "Review of advances in quantitative eddy current nondestructive evaluation." Journal of Nondestructive Evaluation **18**(1): 3-36.

Auld, B. A., F. Muennemann, et al. (1981). "Eddy current probe response to open and closed surface flaws." Journal of Nondestructive Evaluation **2**(1): 1-21.

Babbar, V. K., D. Harlley, et al. (2010). Finite element modeling of pulsed eddy current signals from aluminum plates having defects, USA, American Institute of Physics.

BinFeng, Y., L. FeiLu, et al. (2007). "Research on edge identification of a defect using pulsed eddy current based on principal component analysis." NDT & E International **40**(4): 294-299.

Binfeng, Y., L. Feilu, et al. (2006). "Pulsed eddy current technique used for non-destructive inspection of ageing aircraft." Insight-Non-Destructive Testing and Condition Monitoring **48**(7): 411-414.

Bishop, C. (2006). Continuous Latent Variables. Pattern Recognition and Machine Learning. Cambridge, UK,, Springer**:** 749.

Bishop, C. (2006). Pattern Recognition and Machine Learning. Cambridge, UK, Springer.

Boashash, B. (2003). Time Frequency Signal Analysis and Processing,. Brisbane, Australia, Elsevier.

Chen, D., Q. Ji, et al. (2009). Application of pulsed eddy current in plate thickness evaluation, Xi'an, China, IEEE Computer Society.

Chen, T., G. Y. Tian, et al. (2008). "Feature extraction and selection for defect classification of pulsed eddy current NDT." NDT & E International **41**(6): 467-476.

Cohen, L. (1989). "Time-frequency distributions - A review." Proceedings of the IEEE **77**(7): 941-981.

Cohn, M. J., Y. S. Garud, et al. (1999). "Software and Pulsed Eddy Current Analysis Enhance Detection of Flow Accelerated Corrosion." Power Engineering (Barrington, Illinois) **103**(11): 118-124.

Dadic, M., D. Vasic, et al. (2005). "A system identification approach to the modelling of pulsed eddy-current systems." NDT & E International **38**(2): 107-111.

Dengfeng, C., J. Qichun, et al. (2009). Application of pulsed eddy current in plate thickness evaluation. Industrial Electronics and Applications, 2009. ICIEA 2009. 4th IEEE Conference on.

Dengfeng, C., J. Qichun, et al. (2009). Application of pulsed eddy current and ultrasonic sensors in paint film thickness measuring. Control and Decision Conference, 2009. CCDC '09. Chinese.

Dodd, C. V. and W. E. Deeds (1968). "Analytical solutions to eddy-current probe-coil problems." Journal of Applied Physics **39**(6): 2829-2838.

Duda, H., P. E. Hart, et al. (2001). Pattern Classification. New York, Wiley.

Dunteman, G. H. (1987). Principal Components Analysis (Quantitative Applications in the Social Sciences) SAGE.

Edwards, R. S., A. Sophian, et al. (2008). "Data fusion for defect characterisation using a dual probe system." Sensors and Actuators, A: Physical **144**(1): 222-228.

Edwards, R. S., A. Sophian, et al. (2006). "Dual EMAT and PEC non-contact probe: Applications to defect testing." NDT and E International **39**(1): 45-52.

Elshafiey, I., T. Alkhalifah, et al. (2007). Transfusion of Time-Domain and Frequency-Domain Eddy Current Signals. 4th Middle East NDT Conference and Exhibition. Kingdom of Bahrain.

Fan, M., B. Cao, et al. (2010). "Computation of coil-induced voltage due to a defect-free plate using Stehfest's method for pulsed eddy current evaluation." Insight: Non-Destructive Testing and Condition Monitoring **52**(6): 302-304.

Fan, M., P. Huang, et al. (2009). "Analytical modeling for transient probe response in pulsed eddy current testing." NDT & E International **42**(5): 376-383.

Gigu, S. re, et al. (2001). "Pulsed eddy current technology: Characterizing material loss with gap and lift-off variations." Research in Nondestructive Evaluation **13**(3): 119-129.

Giguere, S., B. A. Lepine, et al. (2000). "Pulsed Eddy Current (PEC) characterization of material loss in multi-layer structures." Canadian Aeronautics and Space Journal **46**(4): 204-208.

Giguere, S., B. A. Lepine, et al. (2001). "Pulsed eddy current technology: Characterizing material loss with gap and lift-off variations." Research in Nondestructive Evaluation **13**(3): 119-129.

Guang, Y., A. Tamburrino, et al. (2010). "Pulsed Eddy-Current Based Giant Magnetoresistive System for the Inspection of Aircraft Structures." Magnetics, IEEE Transactions on **46**(3): 910-917.

He, Y., F. Luo, et al. (2009). "Defect identification and evaluation based on three-dimensional magnetic field measurement of pulsed eddy current." Insight: Non-Destructive Testing and Condition Monitoring **51**(6): 310-314.

He, Y., F. Luo, et al. (2010). "Defect characterisation based on pulsed eddy current imaging technique." Sensors and Actuators A: Physical **In Press, Corrected Proof**.

He, Y., F. Luo, et al. (2010). "Defect classification based on rectangular pulsed eddy current sensor in different directions." Sensors and Actuators A: Physical **157**(1): 26-31.

He, Y., F. Luo, et al. (2010). "Defect edge identification with rectangular pulsed eddy current sensor based on transient response signals." NDT & E International **43**(5): 409-415.

He, Y., F. Luo, et al. (2010). "Pulsed eddy current technique for defect detection in aircraft riveted structures." NDT & E International **43**(2): 176-181.

http://www.ndteng.com/tutorial.html. (2008). "Eddy Current Tutorial."

Huang, C., W. Xinjun, et al. (2010). "Pulsed eddy current signal processing method for signal denoising in ferromagnetic plate testing." NDT and E International **43**(7): 648-653.

Hung-Chi, Y. and T. Cheng-Chi (2002). "Pulsed eddy-current measurement of a conducting coating on a magnetic metal plate." Measurement Science & Technology **13**(8): 1259-1265.

Kamel, G. and M. Zergoug (2005). Characterization of Multilayer Corrosion By Pulsed Eddy Current. 3rd Middle East NDT Conference and Exhibition,. Manama, Bahrain.

Kim, J., G. Yang, et al. (2010). "Classification of pulsed eddy current GMR data on aircraft structures." NDT & E International **43**(2): 141-144.

Krause, H. J. and M. V. Kreutzbruck (2002). Recent developments in SQUID NDE, Elsevier.

Krause, T. W., D. Harlley, et al. (2010). Pulsed eddy current thickness measurement of selective phase corrosion on nickel aluminum bronze valves, USA, American Institute of Physics.

Krause, T. W., C. Mandache, et al. (2008). Diffusion of Pulsed Eddy Currents in Thin Conducting Plates. AIP Conf. Proc., 34th Annual Review of Progress in Quantitative Nondestructive Evaluation,, New York.

Lang, Z. Q., A. Agurto, et al. (2007). "A system identification based approach for pulsed eddy current non-destructive evaluation." Measurement Science and Technology **18**(7): 2083-2091.

Le Bihan, Y. (2002). "Lift-off and tilt effects on eddy current sensor measurements: A 3-D finite element study." EPJ Applied Physics **17**(1): 25-28.

Lebrun, B., Y. Jayet, et al. (1997). "Pulsed eddy current signal analysis: Application to the experimental detection and characterization of deep flaws in highly conductive materials." NDT and E International **30**(3): 163-170.

Lee, C., M. J. Johnson, et al. (2007). Development of a pulsed eddy current system and its characterization, USA, AIP.

Lefebvre, J. H. V. and C. Mandache (2008). "Pulsed eddy current thickness measurement of conductive layers over ferromagnetic substrates." International Journal of Applied Electromagnetics and Mechanics **27**(1-2): 1-8.

Lefebvre, J. H. V., C. Mandache, et al. (2005). Pulsed Eddy Current Empirical Modeling. International Conference of Advances in Signal Processing for Non destructive Evaluation of Maerials, Quebec City, Canada.

Li, S., S. Huang, et al. (2007). "Development of differential probes in pulsed eddy current testing for noise suppression." Sensors and Actuators A (Physical) **135**(2): 675-679.

Li, Y., G. Y. Tian, et al. (2008). "Fast analytical modelling for pulsed eddy current evaluation." NDT & E International **41**(6): 477-483.

Luong, B. and F. Santosa (1998). "Quantitative imaging of corrosion in plates by eddy current methods." SIAM Journal on Applied Mathematics **58**(5): 1509-1531.

Mandache, C. and J. H. V. Lefebvre (2006). "Transient and harmonic eddy currents: Lift-off point of intersection." NDT and E International **39**(1): 57-60.

Mertin, A. (1999). Signal Analysis: Wavelets, Filter Banks, Time-Frequency Transform and Application. Chichester, Wiley.

Morozov, M., G. Y. Tian, et al. (2009). "Comparison of PEC and SFEC NDE techniques." Nondestructive Testing and Evaluation **24**(1-2): 153-164.

Morozov, M., G. Yun Tian, et al. (2010). "The pulsed eddy current response to applied loading of various aluminium alloys." NDT & E International **43**(6): 493-500.

Moulder, J. C., J. A. Bieber, et al. (1996). "Scanned pulsed eddy current instrument for nondestructive inspection of aging aircraft." Proceedings of SPIE - The International Society for Optical Engineering **2945**: 2-13.

Mulligan, C., L. Changqing, et al. (2005). Characterization of magnetron sputtered coatings by pulsed eddy current techniques, USA, AIP.

Munns, I. and P. Crouzen (2006). Pulsed Eddy Current corrosion monitoring in refineries and oil production facilities - experience at Shell. 9th European Conference on NDT,. Berlin, Germany.

Park, D. G., C. S. Angani, et al. (2009). "Evaluation of Pulsed Eddy Current Response and Detection of the Thickness Variation in the Stainless Steel." Magnetics, IEEE Transactions on **45**(10): 3893-3896.

Preda, G., M. Rebican, et al. (2010). Integral formulation and genetic algorithms for defects geometry reconstruction using pulse eddy currents, 445 Hoes Lane / P.O. Box 1331, Piscataway, NJ 08855-1331, United States, Institute of Electrical and Electronics Engineers Inc.

Rao, B. P. C., B. Raj, et al. (2002). "An artificial neural network for eddy current testing of austenitic stainless steel welds." NDT and E International **35**(6): 393-398.

Ruan, J., X. Chen, et al. (1995). "3D transient eddy current calculation by the hybrid FE-BE method using magnetic field intensity H." IEEE Transactions on Magnetics **31**(3 pt 1): 1408-1411.

Rudlin, J. (2006). New Developments in Automated Inspection for Corrosion under Insulation. ECNDT 2006,. Berlin, Germany.

Safizadeh, M. S., B. A. Lepine, et al. (2001). "Time-frequency analysis of pulsed eddy current signals." Journal of Nondestructive Evaluation **20**(2): 73-86.

Safizadeh, M. S., Z. Liu, et al. (2005). Automated Pulsed Eddy Current Method for Detection and Classification of Hidden Corrosion. Proc. Vth International Workshop, Advances in Signal Processing for Non Destructive Evaluation of Materials,. Quebec City, Canada**:** 75-84.

Scottini, R. and H. Quakkelsteijn (2007). Inspection of Coated Subsea Piping and Risers 4th Middle East NDT Conference and Exhibition. Kingdom of Bahrain.

Shin, Y.-K., D.-M. Choi, et al. (2009). "Signal characteristics of differential-pulsed eddy current sensors in the evaluation of plate thickness." NDT & E International **42**(3): 215-221.

Shu, L., H. Songling, et al. (2008). "Study of pulse eddy current probes detecting cracks extending in all directions." Sensors and Actuators, A: Physical **141**(1): 13-19.

Shuai-xia, L., X. Wei, et al. (2010). Simulation of corrosion on detection for pulsed eddy current, Piscataway, NJ, USA, IEEE.

Sicard, R., S. Serhan, et al. (2008). Detection and Imaging of Corrosion and Crack in Multi-Layer Aluminum Aircraft Structures using Pulsed Eddy Currents. Aging Aircraft 2008. Phoenix Convention Center.

Smid, R., A. Docekal, et al. (2005). "Automated classification of eddy current signatures during manual inspection." NDT&E International **38**(6): 462-470.

Smith, R., J. A. Skramstad, et al. (2004). Advances in Transient Eddy-Current Imaging for Aerospace Applications. 16th World Conference on NDT, . Montreal, Canada.

Smith, R. A. and D. Edgar (2006). Progress Towards a Large-area Transient Eddy Current Solution for Second-layer Wing Corrosion 9th Joint FAA/DoD/NASA Aging Aircraft Conference. Hyatt Regency, Atlanta, GA**:** 1-24.

Smith, R. A., D. Edgar, et al. (2003). Enhanced Detection of Deep Corrosion Using Transient Eddy Currents. 7th Joint DoD/FAA/NASA Conference on Aging Aircraft,, New Orleans.

Songling, H., Y. Peng, et al. (2008). "Improved immunity to lift-off effect in pulsed eddy current testing with two-stage differential probes." Russian Journal of Nondestructive Testing **44**(2): 138-144.

Sophian, A., R. S. Edwards, et al. (2005). "Dual-probe methods using pulsed eddy currents and electromagnetic acoustic transducers for NDT inspection." Insight: Non-Destructive Testing and Condition Monitoring **47**(6): 341-345.

Sophian, A., G. Y. Tian, et al. (2001). "Electromagnetic and eddy current NDT: A review." Insight: Non-Destructive Testing and Condition Monitoring **43**(5): 302-306.

Sophian, A., G. Y. Tian, et al. (2002). "Design of a pulsed eddy current sensor for detection of defects in aircraft lap-joints." Sensors and Actuators A: Physical **101**(1-2): 92-98.

Sophian, A., G. Y. Tian, et al. (2003). "A feature extraction technique based on principal component analysis for pulsed Eddy current NDT." NDT and E International **36**(1): 37-41.

Sukhikh, A. V., S. S. Sagalov, et al. (2009). "Use of pulsed Eddy-current testing for flaw detection in irradiated VVER fuel elements." Atomic Energy **107**(2): 148-153.

Tai, C.-C., J. H. Rose, et al. (1996). "Thickness and conductivity of metallic layers from pulsed eddy-current measurements." Review of Scientific Instruments **67**(11): 3965-3972.

Teolis, A. (1998). Computational Signal Processing with Wavelets (Applied and Numerical Harmonic Analysis), , Birkhäuser.

Tetervak, A., T. W. Krause, et al. (2010). Analytical and numerical modeling of pulsed eddy current response to thin conducting plates, USA, American Institute of Physics.

Tian, G. Y., Y. Li, et al. (2009). "Study of Lift-Off Invariance for Pulsed Eddy-Current Signals." IEEE Transactions on Magnetics **45**(1): 184-191.

Tian, G. Y. and A. Sophian (2005). "Defect classification using a new feature for pulsed eddy current sensors." NDT & E International **38**(1): 77-82.

Tian, G. Y. and A. Sophian (2005). "Reduction of lift-off effects for pulsed eddy current NDT." NDT & E International **38**(4): 319-324.

Tian, G. Y. and A. Sophian (2005). "Study of magnetic sensors for pulsed eddy current techniques." Insight-Non-Destructive Testing and Condition Monitoring **47**(5): 277-279.

Tian, G. Y., A. Sophian, et al. (2004). "Pulsed eddy current system for dynamic inspection of defects." Insight-Non-Destructive Testing and Condition Monitoring **46**(5): 256-259.

Tian, G. Y., A. Sophian, et al. (2005). "Multiple sensors on pulsed eddy-current detection for 3-D subsurface crack assessment." IEEE Sensors Journal **5**(1): 90-96.

Vargel, C., M. Jacques, et al. (2004). Corrosion of Aluminium, Elsevier

Vasic, D., V. Bilas, et al. (2003). Pulsed eddy current nondestructive testing of ferromagnetic tubes, Piscataway, NJ, USA, IEEE.

Walnut, D. F. (2002). An Introduction to Wavelet Analysis (Applied and Numerical Harmonic Analysis) Fairfox, America.

Wang, Q., N. Kawagoishi, et al. (2003). "Evaluation of the probability distribution of pitting corrosion fatigue life in aircraft materials." Acta Mechanica Sinica (English Series) **19**(3): 247-252.

Wilson, J., G. Y. Tian, et al. (2010). "Pulsed eddy current thermography: system development and evaluation." Insight-Non-Destructive Testing and Condition Monitoring **52**(2): 87-90.

Yang, B., B. Li, et al. (2010). "Reduction of lift-off effect for pulsed eddy current NDT based on sensor design and frequency spectrum analysis." Nondestructive Testing and Evaluation **25**(1): 77-89.

Yang, B. and X. Li (2010). "Pulsed remote eddy current field array technique for nondestructive inspection of ferromagnetic tube." Nondestructive Testing and Evaluation **25**(1): 3-12.

Yang, G., G. Y. Tian, et al. (2009). "Independent Component Analysisâ€“Based Feature Extraction Technique for Defect Classification Applied for Pulsed Eddy Current NDE." Research in Nondestructive Evaluation **20**(4): 230-245.

Yang, H.-C. and C.-C. Tai (2002). "Pulsed eddy-current measurement of a conducting coating on a magnetic metal plate." Measurement Science and Technology **13**(8): 1259-1265.

Young-Kil, S., C. Dong-Myung, et al. (2010). Performance evaluation of several types of pulsed eddy current probes for detecting wall thickness reduction, USA, American Institute of Physics.

Yunze, H., L. Feilu, et al. (2009). "Defect identification and evaluation based on three-dimensional magnetic field measurement of pulsed eddy current." Insight-Non-Destructive Testing and Condition Monitoring **51**(6): 310-314.

Zainal Abidin, I., G. Yun Tian, et al. (2010). "Quantitative evaluation of angular defects by pulsed eddy current thermography." NDT & E International **43**(7): 537-546.

Zhou, D., G. Y. Tian, et al. (2010). "Simulation based on optimisation of pulsed eddy current probe design." Nondestructive Testing and Evaluation **25**(3): 219-230.

Zhou, D., G. Y. Tian, et al. (2010). "Optimal features combination for pulsed eddy current NDT." Nondestructive Testing and Evaluation **25**(2): 133-143.